Identification of the transcriptional program, establishing adult intestinal stem cells during mouse embryonic development

Dissertation

zur Erlangung des Grades

„Doktor der Naturwissenschaften“

Am Fachbereich Biologie

der Johannes Gutenberg-Universität

in Mainz

Lira Nigmatullina

geb. am 20.11.1988 in Baschkortostan (Russland)

Mainz, 2017

Dekan:

1. Berichterstatter: _____

2. Berichterstatter: _____

Tag der mündlichen Prüfung: 28.09.2017

Table of Contents.

1.1. Summary.

Intestinal stem cellsô (ISCs) identity, mechanisms of their self-renewal and differentiation have been the subject of substantial studies. Lgr5+ ISCs maintain tissue homeostasis and give rise to all cell types comprising the intestinal epithelium. However, mechanisms, responsible for Lgr5+ ISCs appearance during the embryonic gut development, remained unknown.

In vivo cell fate mapping analysis demonstrates that the first Lgr5+ ISC progenies appear at embryonic stage E13.5 as a distinct cell population, which contributes to the ISC pool in adults. Further RNA-sequencing of the embryonic epithelium shows that Lgr5+ cells are Wnt positive and express adult ISC markers, such as *Axin2*, *CD44* and *Ascl2*.

Importantly, this study defined *Id2*, encoding a transcriptional regulator that inhibits the functions of basic HLH-binding proteins, as an essential factor controlling timing and number of Lgr5+ progenitors in the embryonic intestine. In the absence of *Id2*, I observed precocious activation of Wnt signaling and formation of Lgr5+ cells at E9.5, accompanied by dramatic changes in molecular signature of the whole intestinal epithelium. Using a pharmacological inhibitor of Wnt secretion (Wnt C-59) *in vivo* I showed that the expression of ectopic Wnt signaling genes is responsible for the precocious formation of Lgr5+ cell in *Id2* mutants ($Id2^{-/-}$). Lineage tracing analysis of precociously specified Lgr5+ cells revealed their maturation into adult ISCs, however the molecular signature of *Id2*-deficient intestinal epithelium differs significantly from the wild-type. Furthermore, I found that *ex vivo* grown embryonic $Id2^{-/-}$ cells are forming predominantly undifferentiated spheroids, which are positive for cancer markers, such as Trop2, Cnx43 and cytoplasmic EpCam, indicating that *Id2* is important for embryonic intestinal cells differentiation and proliferation.

In summary, I showed that *Id2* loss causes increased number of Lgr5+ cells within the small intestine, leading to impaired differentiation and tumor development.

1.2. Zusammenfassung.

Die Identität der Dünndarmstammzellen (engl.: intestinal stem cells, ISCs), sowie die an ihrer Selbsterneuerung und Differenzierung beteiligten Mechanismen waren und sind das Thema vieler grundlegenden Studien. Lgr5-positive (Lgr5+) ISCs halten die Gewebehomöostase aufrecht und alle Zellarten des Darmepithels entstammen aus diesen. Dennoch sind die Mechanismen, die für die Etablierung der Lgr5+ ISCs während der embryonalen Darmentwicklung verantwortlich sind, bisher unbekannt.

Eine *in vivo* Analyse der Zellabstammung zeigt, dass die ersten Lgr5+ ISC-Vorläufer als eigenständige Zellpopulation im Embryonalstadium E13.5 auftauchen und zum adulten Stammzellenpool beitragen. Eine RNA-Sequenzierung des embryonalen Epithels zeigt weiterhin, dass Lgr5+ Zellen Wnt-positiv sind und adulte ISC-Marker wie z.B. *Axin2*, *CD44* und *Ascl2* exprimieren.

In dieser Arbeit wird Id2, ein Transkriptionsregulator der bHLH-bindende Proteine inhibiert, als ein essentieller Kontrollfaktor für die Anzahl und den Zeitpunkt des Auftretens der Lgr5+ ISC-Vorläufer im Dünndarmepithel identifiziert. Ohne Expression des *Id2*-Gens beobachtete ich die vorzeitige Aktivierung des Wnt-Signalwegs, das Auftauchen Lgr5+ Zellen bereits im Stadium E9.5, sowie drastische Veränderungen der Molekularsignatur im gesamten Darmepithel. Mit Wnt C-59, einem pharmakologischen Inhibitor der Wnt-Sekretion, zeigte ich *in vivo*, dass die ektopische *Wnt*-Expression für die vorzeitige Formation von Lgr5+ Zellen in *Id2*-Knockouts ($Id2^{-/-}$) verantwortlich ist. Die Abstammungsanalyse von vorzeitigen Lgr5+ Zellen zeigte ihre Entwicklung zu adulten ISCs, jedoch unterscheiden sich hierbei die Molekularsignaturen signifikant zwischen Wildtyp und $Id2^{-/-}$ Darmepithel. Weiterhin stellte ich fest, dass embryonale $Id2^{-/-}$ Zellen in *ex vivo* Kultur vor allem zu undifferenzierten Spheroiden, die positiv für Krebszellmarker wie z.B. Trop2, Cnx43 und zytoplasmatisches EpCam sind, heranwachsen. Dies weist darauf hin, dass *Id2* wichtig für die Embryonalproliferation und -differenzierung im Darmepithel ist.

Insgesamt zeigt meine Arbeit, dass der Verlust der *Id2*-Expression eine Erhöhung der Lgr5+ Zellzahl im Dünndarm bewirkt, die Zelldifferenzierung beeinträchtigt und zur Tumorentwicklung beiträgt.

2. Index of abbreviations.

3D ï 3 dimensional

APC - adenomatous polyposis coli

Ascl2- homologous to the *Drosophila* Achaete-scute complex gene

BMP - bone morphogenic protein

bp ï base pairs

cDNA ï reversely transcribed DNA

DE - differentially expressed (genes)

DIG ï Digoxigenin

EpCam ï Epithelial cell adhesion molecule

ERT - estrogen hormone-binding domain

FACS - Fluorescence activated cell sorting

FSC-A ï Forward-scatter area

GFP ï Green Fluorescent protein

Id2 - inhibitor of DNA binding 2

IF ï immunofluorescent staining

IHC- immunohistochemistry

ISCs - intestinal stem cells

ISH ï in situ hybridization

Lgr5 - leucine rich repeat containing G protein-coupled receptor 5

Lrig1 - leucine-rich repeats and immunoglobulin like domains 1

NICD ï Notch intracellular domain

ON ï overnight

PCR ï polymerase chain reaction

Prom1 ï Prominin 1 (CD133)

RNA-seq ï RNA-sequencing

R-spo ï R-spondin1

RT- room temperature

Shh ï Sonic hedgehog

TA - transit- amplifying cells

Tcf4 - T-cell factor 4

3. Introduction.

3.1. Adult intestinal stem cells and their niche.

The small intestine is an organ, responsible for digestion and absorption of nutrients. Necessitated by the constant exposure to physical, chemical, and biological insults from food, the intestinal epithelium has to constantly replace damaged or dead cells throughout the life of the animal (Barker et al., 2012). The process of continues cell replacement is called tissue homeostasis and is critical for the maintenance of adult tissues. The small intestine homeostasis is maintained by the presence of intestinal stem cells (Guiu and Jensen, 2015). Stem cells could be functionally defined by their two major properties: ability to self-renew and to differentiate into the cell lineages of their tissue of origin (Blanpain, 2007), while any dysregulation in this balance could lead to severe abnormalities, including chronic inflammation and cancer.

Intestinal epithelium constitutes an excellent model system to study stem cells due to its simple repetitive architecture and high self-renewing capacity (Clevers, 2013). Indeed, the adult intestinal epithelium is the most rapidly proliferating tissue in mammals. The small intestine is organized into a numerous amount of villi-crypt units (Fig. 1A) and the entire monolayer of epithelium is replaced every 4-5 days. This process is driven by a pool of self-renewing intestinal stem cells (ISCs) located in crypt compartment ((Blanpain, 2007), Fig. 1B). These ISCs give rise to the fastly proliferating transit-amplifying (TA) cells that ultimately develop into terminally differentiated intestinal cells. Five cell types are generated by ISCs: mucus-secreting goblet cells, hormone-releasing enteroendocrine cells, antimicrobial Paneth cells, and chemo-sensing and opioid-secreting tuft cells (Barker, 2014; Gerbe, 2011), Fig. 1B). The differentiated cells migrate upwards, functioning in the villus and undergo apoptosis when they reach the villus-tip. One exception to this migration is the Paneth cells, that reside at the bottom of the crypts and believed to keep ñstemnessò in crypt compartment (Fig.1B).

ISCs are suggested to function within restricted tissue microenvironment known as stem niche. This niche generates signals that regulate the maintenance of ISCs and regulate their function, controlling the crucial choice/balance between self-renewal and the initiation of differentiation (Donati and Watt, 2015). Moreover, this niche is made of and influenced not only by proliferating and differentiating epithelial cells, but by surrounding mesenchyme as well. Separated from the epithelial cells by the basement membrane, the mesenchymal cells (i.e, blood vessels, lymphocytes, and fibroblasts/myofibroblasts) together with the extracellular matrix, provide the epithelial-mesenchymal crosstalk, necessary to maintain the stem cell niche (Umar, 2010).

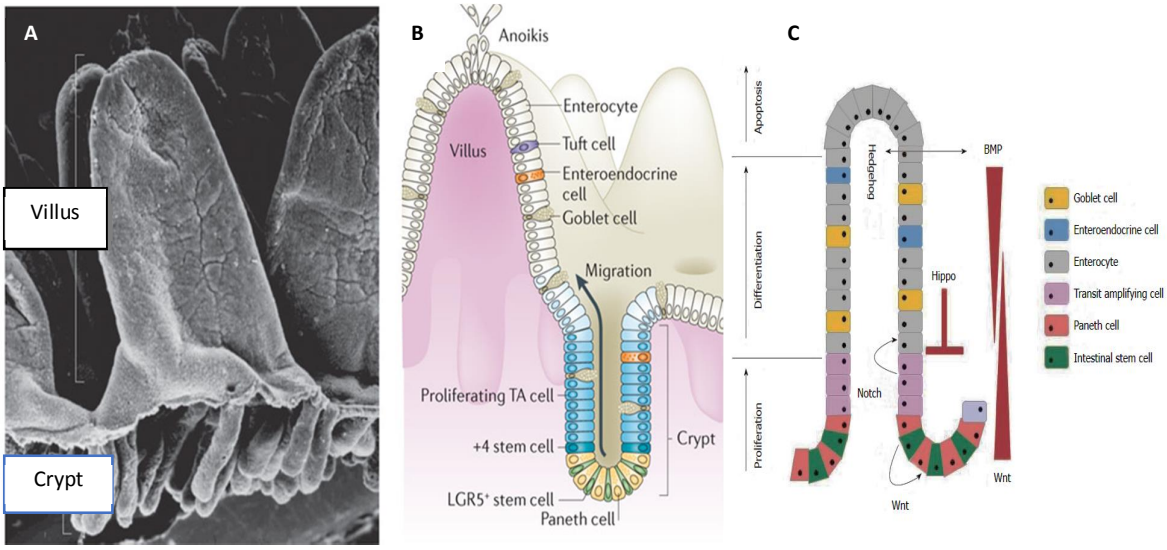

Figure 1. The organization of the intestinal epithelium. A. Villus-crypt units; B. Intestinal stem cells and their progenies. C. Signaling pathways essential for ISCs stemness along crypt-villi axis. *The figures are adapted from Barker N., 2014 and Jeon, 2013.*

Obviously, the proper tissue structure and cell composition of the small intestine is orchestrated by a complex interplay between the major signaling pathways. Many studies have been performed in order to understand which niche signals are essential in this regard. Experiments using transgenic and knock-out animal models showed that different signaling pathways, such as Wnt, bone morphogenic protein (BMP), Notch, Hedgehog, EGF, YAP/TAZ etc. play an important role in the regulation of intestinal epithelial renewal, particularly ISCs function (reviewed by (Jeon et al., 2013), Fig. 1C).

3.2. Wnt signaling pathway and markers of ISCs.

The intestinal epithelium represents the best described example of Wnt signaling importance for the proper balance between stem cell self-renewal, differentiation and oncogenic transformation. WNT genes encode a large family of secreted glycoproteins that have crucial roles in controlling the fate and proliferation of epithelial cells (Grigorieff, 2005). Often canonical Wnt signaling is named as Wnt/ß-catenin pathway, because Wnt-stimulated signals modulate ß-catenin-dependent transcriptional activation. When Wnt ligands are absent, cytoplasmic ß-catenin protein undergoes constant proteosomal degradation by the action of the Axin complex, which is composed of the scaffolding protein Axin, the tumor suppressor *adenomatous polyposis coli* gene product (APC), casein kinase 1 (CK1), and glycogen synthase kinase 3 (GSK3). This destruction process prevents ß-catenin from reaching the nucleus, and Wnt target genes are therefore repressed by the DNA-bound T cell

factor/lymphoid enhancer factor (TCF/LEF) family of proteins. When stabilized, ϐ-catenin is translocated into the nucleus and in cooperation with TCF-associated proteins activates transcription of the Tcf/ϐ-catenin target genes (Fig. 2C).

When Wnt ligands were firstly characterized and linked to cancer progression, it encouraged the scientists to study further mutations of Wnts. However, sequences of Wnt coding genes in tumors were not altered, indicating that most likely downstream mechanisms of Wnt signaling are responsible for cancerogenesis (Nusse and Varmus, 2012). The first functional evidence for Wnt signaling came from studies on colon cancer diseases, where the tumor suppressor gene APC was found mutated in a large number of familial and sporadic cases of colorectal cancer (Groden, 1991), (Kinzler, 1991), (Powell, 1992). The same mutation was shown in a mouse strain called Min (Multiple intestinal neoplasia, (Su, 1992)) and nowadays APC ^{min} mouse became a classical model strain to study intestinal tumor *in vivo*.

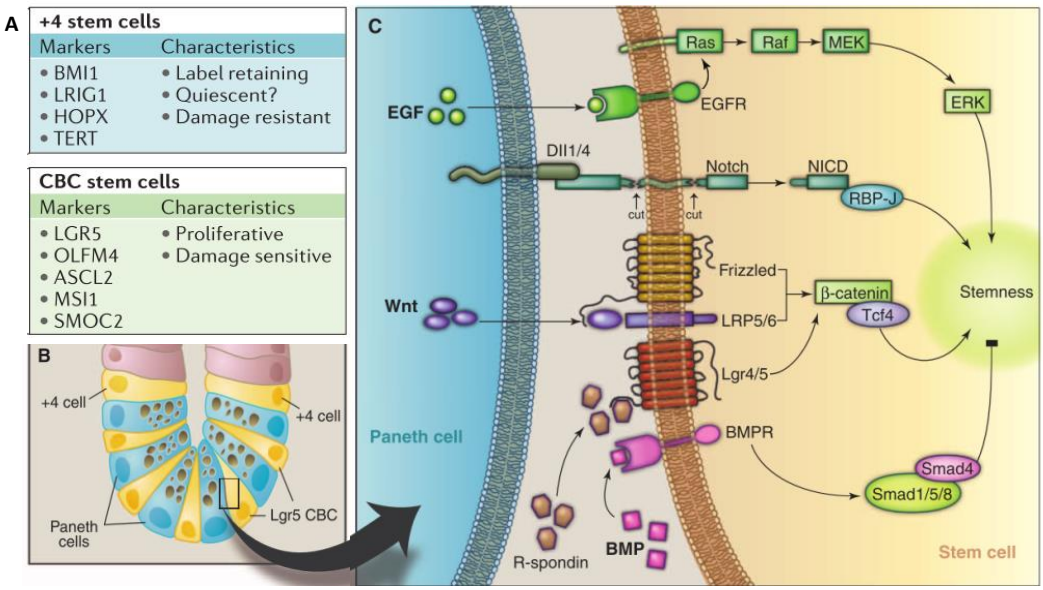

Figure 1. Biological interaction of intestinal stem cells and their niche. A. Molecular signature of quiescent +4 stem cells and Lgr5+ stem cells (from Barker, 2014). **B.** Scheme of the intestinal stem cell niche. Lgr5+ cells are interspersed between granular Paneth cells, which provide factors for stem cell maintenance. **C.** Three signals (EGF, Notch, and Wnt) are essential for intestinal epithelial stemness, whereas BMP is a negatively regulator. For full Wnt activation in the intestinal epithelium, R-spondinï Lgr4/5 signal interaction is required (*from Sato, 2013*).

Furthermore, many other studies strengthen the fact that Wnt signaling causes tumorigenesis, because imbalance in Wnt activity impairs maintenance of ISCs in crypts. Thus, removal of Wnt transcriptional factor *Tcf4* (Korinek, 1998), *c-Myc* (Muncan, 2006), b-catenin (Fevr, 2007) or Wnt inhibition by Dkk1 (Kuhnert, 2004) (Pinto, 2003b) abrogates epithelium proliferation, that leads to

loss of ISCs and abnormal cell differentiation. In opposite, when Wnt signaling is constantly activated either by APC loss (Sansom, 2004) or activated b-catenin (Romagnolo, 1999), stem cell compartment expands and causes neoplastic regions formation.

Importantly, in 2002 the lab of Hans Clevers first showed that the transcription program of APC-driven colorectal cancer cells has the same genetic profile as proliferating cells in normal healthy crypts (van de Wetering, 2002). Genetic screen revealed around 80 genes, regulated by Wnt signaling activity. Many of those were expressed in TA cells or Paneth cells as well, so the researchers had to test each Wnt pathway candidate by *in situ* hybridization in order to find specific genes for ISCs. One of the Wnt target genes called *Lgr5*/*Gpr49*, which encodes for an orphan G-protein-coupled receptor, was found to be specifically expressed in ISCs, that are localized between the Paneth cells in the small intestine (van de Wetering, 2002),(Barker et al., 2007), Fig 2B.)

Generation of *Lgr5-eGFP-CreERT2* knock-in mouse strain and further *in vivo* lineage tracing experiment have shown that *Lgr5* is a gene exclusively expressed not only in the small intestine, but also in colon, stomach and hair follicles in mice (Barker et al., 2007). Based on this marker, the adult ISCs were isolated and characterized on a molecular level (Munoz et al., 2012). Furthermore, it has been shown that *Ascl2 (*homologous to the *Drosophila* Achaete-scute complex gene) transcription factor is the master regulatory gene for $Lgr5^{+}$ ISCs maintenance. It binds to the *Lgr5* gene promoter and is itself a Wnt target gene. Expression of *Ascl2* gene in non-stem cells caused crypts to form, whereas deleting the gene in the small intestine caused the stem cell population to disappear (van der Flier et al., 2009). Taken together, *Ascl2*, *Tcf4* and b-catenin are the core gene products, establishing the stem cell state (Schuijers et al., 2015). Other Wnt/ɓ-catenin target genes with expression pattern restricted to the very bottom of the crypt in the stem cell zone (Lgr5+ ISCs stem ñsignatureò genes) are *Tcf4* transcription factor, *Rnf43, Olfm4*, *CD44*, *Kcnq1, Smoc2, Sox9* etc. ((van der Flier et al., 2009); (Munoz et al., 2012), Fig. 2 A). Many of those genes have been also confirmed by *in vivo* genetic studies. Thus, results from Musashi-1 (Potten, 2003), Prominin 1 (Snippert et al., 2009) or lineage tracing of Smoc2-EGFP-ires-CreERT2 (Munoz et al., 2012), showed the similar *Lgr5*-specific expression pattern. However, knockout of latter listed genes, including *Lgr5* itself, does not reveal significant abnormalities in intestinal homeostasis.

Perhaps unexpectedly, studies on Lgr5+ ISCs ablation *in vivo* (Tian et al., 2011); (van Es et al., 2012), (Tetteh et al., 2016) showed very interesting results: upon the acute loss of stem cells, TA cells and differentiated enterocytes readily revert into Lgr5+ ISCs. The ability of the small intestine to survive without stem cell pool may probably relate to epigenetic plasticity of differentiated progenitors (Barker et al., 2012). Alternatively, such phenomenon could be explained by the presence of so-called +4 quiescent stem cells, located upper from the crypt bottom (counted as 0, figure 2A-B). Although +4 stem cells share some of Lgr5+ ISCs signature, they express a unique set of genes, such as *Bmi1*

(Sangiorgi and Capecchi, 2008), *Tert* (Takeda et al., 2011); *Hopx* (Montgomery et al., 2011) and *Lrig1* (Powell et al., 2012) and are activated upon cell damage.

In the small intestine, Paneth cells are believed to provide Wnt ligands to neighboring Lgr5+ cells and maintain Wnt stem cell program. However, ISCs could function even after complete loss of Paneth cells (Durand et al., 2012). Recent data from Stzepourginski et al., (Stzepourginski et al., 2017) report that CD34+ mesenchymal cells, localized around crypts, might maintain ISCs by Wnt2b and R-spo1 expression.

Summarizing, current evidence indicates that the Wnt cascade is the dominant force in controlling cell fate along the crypt-villus axis: the strongest Wnt signaling is detected at the crypt base (where some cells display nuclear ϐ-catenin localization) and gradually decreases toward the luminal side of villi. However, many aspects of how Wnt pathway is functioning in ISCs, are remain uncovered.

3.3. Notch signaling in the adult small intestine.

The Notch pathway in the intestine mediates cell-to-cell signaling and plays an important role in the maintenance of ISCs as well as their commitment towards the absorptive/secretory lineage. The proliferative zone of intestinal crypts contains essential Notch pathway components, such as trans-membrane receptors Notch1 and Notch2, trans-membrane ligands delta-like 1/4 (Dll1, Dll4) and Jag-1, and downstream effector Hes-1. Dll1/4 expressing Paneth cells activate signaling by Notch ligands on neighboring ISCs (Fig 2C., (van Es et al., 2012)). Dll1/4 ligandï Notch receptor interaction leads to receptor cleavage by proteases, including ADAM (A Distegrin And Metalloprotease) and ɔ-secretase, and release of Notch intracellular domain (NICD). Subsequently, NICD translocates to the nucleus and associates with the transcription factor RBP-J, inducing in stem cells transcription of downstream target genes, such as *Hes1*, *myc, Cyclin D* (Fig. 2C).

The functional role of Notch cascade activity has been shown by genetic depletion of its components, including the crucial Notch DNA-binding protein RBP-J (van Es, 2005), both Notch1 and Notch2 receptors (Riccio et al., 2008) or both Dll-1 and 4 ligands (Pellegrinet et al., 2011), which results in the loss of cellular proliferation in the intestinal crypts. Moreover, experiments with pharmacologic ɔ-secretase inhibitor, blocking the release of NICD (Milano et al., 2004); (van Es, 2005)), or with antibodies against both Notch1 and 2 receptors (Wu et al., 2010) showed the similar phenotype (Fig.3A). Histological examination of the small intestine revealed a complete conversion of crypt progenitors into goblet cells causing secretory cells hyperplasia (Fig. 3B), as well as loss of $Ki67^{+}$ dividing cells, indicating loss of the proliferative crypt compartment (Fig. 3A). Mice with inactivated Notch signaling suffered from poor grooming, rapid loss of weight and died within 4-6

days (Pellegrinet et al., 2011). Another evidence for Notch activity in ISCs came from lineage-tracing experiments using specific reporter mice to follow the progeny of ISCs that expressed Notch1. Eight months after Notch activation, entire crypt-villi axis was labeled, demonstrating that the Notch pathway is active in ISCs that give rise to all progeny in the intestine (Pellegrinet et al., 2011).

In contrast, when constitutively activated in the entire epithelium, Notch signaling leads to expansion of the intestinal stem/progenitor pool and blocks secretory cells differentiation (Fre et al., 2005). These studies revealed binary functions of Notch in gut homeostasis: on one hand, Notch is required to promote stem cell self-renewal in the intestinal crypts, and on the other - Notch signals direct the differentiation fate of intestinal progenitors at commitment between secretory and absorptive lineages. Activation of Notch in Apc^{Min} tumor mouse results in a remarkable increase (minimum 20-fold) in the number of adenomas developed, causing lethality after 4 moth after birth (Fre, 2009), showing that Notch signaling is involved in intestinal tumor formation. Indeed, in humans Notch signal activation has been observed in most adenomas, suggesting that Notch signaling enhances Apc-driven tumor initiation.

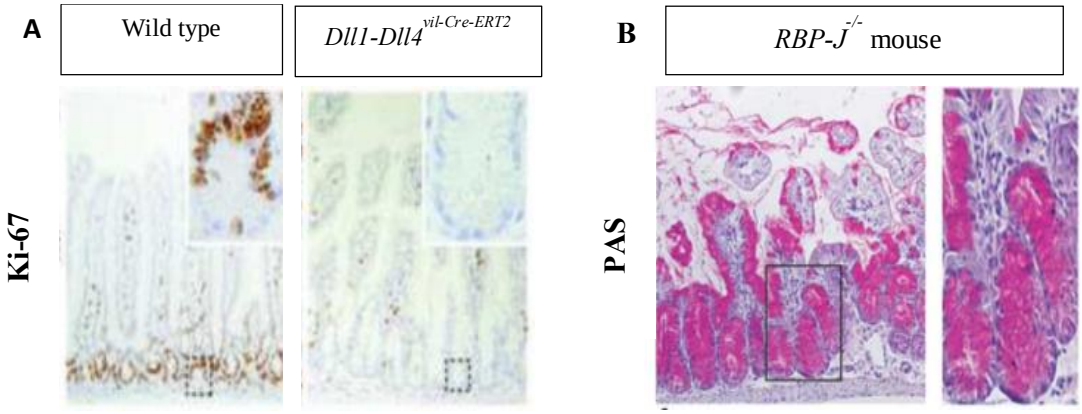

Figure 3. Complete conversion of crypt progenitors into post-mitotic goblet cells. A. Proliferative Ki-67+ crypt compartment of *Dll1-Dll4* mutant mouse is totally absent (*Pellegrinet, 2011*), because all cells differentiated into PAS+ goblet cells, as also shown on **B)**, using *RBP-J*$^{-/-}$ mouse (*van Es, 2005*).

In the small intestine the key regulator, responsible for secretory fate commitment is Atoh1 (or Math1) - a bHLH transcriptional activator that drives differentiation of goblet, entero-endocrine and Paneth cells (Yang, 2001). Proper Notch signaling is required not only for proliferation of intestinal progenitor cells, but also to suppress their Atoh1-dependent differentiation. Atoh1 mutant mice lack most secretory cells and are only colonized by enterocytes (van Es et al., 2010). In contrast, deletion of the Notch pathway components or inhibition of NICD release causes elevated Atoh1 expression and premature conversion of proliferative crypt cells into post mitotic secretory goblet cells (VanDussen

and Samuelson, 2010); (VanDussen, 2012). Furthermore, conditional deletion of Atoh1 rescues the Notch-loss of function phenotype (Kim et al., 2014); (Tian et al., 2015), described above.

Conversely, absorptive lineage commitment is established through Notch-dependent repression of Atoh1, which is directly mediated by the Notch-activated transcription factor Hes1. Interestingly, human CRCs are typically devoid of Goblet secretary cells and express very low levels of HATH1 (the human orthologue of Atoh1), (Leow, 2004) suggesting that Notch receptor signaling might be activated in most human intestinal tumors. This suggests that under normal conditions Notch signaling is required to maintain stem cells in an uncommitted state until Atoh1 is activated (van Es et al., 2012). Recently published data confirm the crosstalk between Nocth and Wnt signaling in ISCs, where in the absence of Atoh1 the small intestine increases the production of Wnts (Tian et al., 2015).

Thus, Dll1/4 expressing Paneth cells trigger signaling by Notch ligands on neighboring ISCs and keep them from secretory lineage. In other words, each day ISCs lose contact to Dll1/4 Paneth cells, while some of those cells downregulate Notch to undergo secretory fate (van Es et al., 2012).

3.4. BMP signaling in the adult gut homeostasis.

The initial role for BMP signaling in intestinal homeostasis has been also discovered from gastrointestinal cancer studies, such as juvenile intestinal polyposis and Cowden disease (Howe, 1998) (He et al., 2004). Mutations in BMP related intracellular signal transducing Smad4, or in the gene, encoding the BMP receptor type IA, have been found in patients with juvenile polyposis (Howe, 2001).

According to the current model, ligands BMP2 and BMP4 bind to their type I or II receptors - Bmpr1a and Bmpr1b. The hallmark of active BMP signaling is phosphorylation of Smad transcription factors with their further translocation from cytoplasm into the nucleus. Activity of BMP signaling could be inhibited by its antagonist, Noggin, encoded by *Nog* gene (He, 2004; Fig.2C).

In the adult mouse intestine, it has been shown, that BMP4 was strongly expressed in intravillus mesenchyme ((Karlsson, 2000); (Haramis, 2004); (He et al., 2004)), whereas Bmpr1a was highly expressed specifically in ISCs, but not in the cells in the proliferative zone (TA-cells). The presence of active BMP signaling was confirmed by phosphorylated Smad 1/5/8 proteins in both villi and ISCs. To investigate the role of BMP in regulating intestinal homeostasis, numerous studies on transgenic mice has been performed. Thus, the mouse model, expressing the BMP inhibitor Noggin under control of *Villin* gene promoter, was generated. This promoter is used to drive specific expression throughout the intestinal epithelium. Indeed, transgenic Noggin was present in epithelial

cells and effectively caused the loss of phosphorylated Smad 1/5/8 factors in the gut (Haramis, 2004). Transient expression of Noggin led to the severe phenotype in adult animals: the branching villi in the intestinal epithelium, combined with the enlarged cysts, which resembled the characteristic feature of the intestinal polyps (Haramis, 2004), Fig. 4A-B). Another study with conditional inactivation of *Bmpr1a* gene in mice showed overgrowth of intestinal tissue with an increased number of crypts and fused villi (He et al., 2004). In *Bmpr1a* mutant intestine the proliferating cells were expanded, as a result of ~5-fold increase in the number of ISCs and visible polyps formation (He, 2004, Fig.4C). The consequence of BMP signaling inhibition was also nicely shown in studies on *Fabp1/Noggin* transgenic mouse, where enlarged small intestine of 14-week old mice showed intestinal hyperplasia with abnormally shaped villi. Disorganized tissue contained also stromal hyperplasia, as well as regions with rudimentary villi or proliferative crypts (Batts et al., 2006, Fig. 4D).

Noggin binds to and inactivates the BMP4 protein, resulting in a blockade of the BMP/Smad signaling pathway, which helps ISCs maintain their proliferative status (He 2004). Taken together, BMP receptors, activated by BMP signals, lead to complexes between Smad proteins to repress stemness genes in the nucleus (Sato and Clevers, 2013).

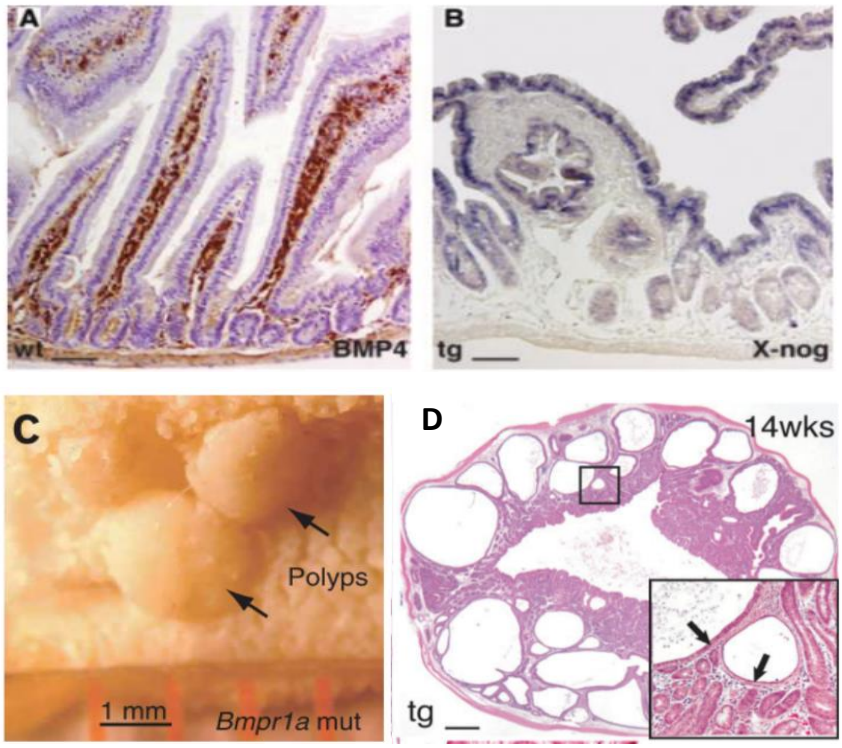

Figure 4. Villus epithelial cells in the mouse intestine are sensitive to mesenchymal BMP signaling. A.Expression of BMP4 protein is detected in the intravillus mesenchyme of adult wild-type (wt) mice. **B.** Transgenic expression of Xenopus noggin (X-nog) inhibits BMP signaling. *In situ* hybridization showed that the X-nog mRNA is expressed by intestinal epithelial cells, which leads to neoplastic regions formation (*Haramis, 2004*). **C, D**. *Bmpr1a* mutation in the gut strongly alters villi and mesenchymal stroma shapes (*He, 2004; Batts, 2006, resp.*) and causes multiple polyps in epithelium.

3.5. Embryonic gut development in mammals.

In the process of embryonic development, the mammalian small intestine emerges from a simple tubal structure, resulting in the subsequent formation of a three-dimensional complex organ. The mature gut is composed of the three germ layers - endoderm (which forms the epithelial lining), mesoderm (which forms the smooth muscle layers), and ectoderm (which includes the enteric nervous system) (De Santa Barbara, 2003).

Until embryonic day 9 (E9.0) the endoderm undergoes extensive folding to form the complete embryonic gut tube. The entire process of gut tube formation is completed within 2 days after the end of gastrulation in mice (Wells, 2014). From this time, the epithelium condenses and at E13.5 the gut tube is composed of a single-layered pseudostratified epithelium (Fig.5A). At E14.5, the thickened epithelium begins a drastic remodeling process to form intestinal villi and becomes compartmentalized

into differentiating villus and proliferating intervillus epithelium (Fig. 5B-C). Intervillus units will subsequently develop into crypts, harboring ISCs inside (Fig.3D). However, this process doesnôt occur fast: the neonatal intestine is characterized by still low levels of epithelial cell proliferation, the absence of crypts and crypt-based Paneth cells. In mice, the formation of intestinal crypts takes place late during the second week after birth, eventually initiates increased proliferation and rapid epithelial cell renewal along with the generation of Ŭ-defensin-producing Paneth cells (Renz, 2011, Fig. 5D).

Distinct epithelial cell types were found by morphological and molecular markers after villus-intervillus epithelial re-organization at E15.5 (Fig. 3C). At this stage, the following cell types can be identified: enterocytes, Goblet cells and enteroendocrine cells. These epithelial cell types are derived from multipotent stem cells in the adult intestine, but whether distinct stem cells exist in the embryo is unclear. Currently the most intriguing question is to identify specific markers and molecular mechanisms, that define cellular heterogeneity within the developing epithelium prior to villi formation at E14.5-E15.5, when actively proliferative fetal progenitors of ISCs become restricted to intervillus pockets.

As in the adult small intestine, during embryonic gut development several signaling pathways and transcription factors, regulating mesenchymalï epithelial interactions, are very important for its proper specification in space and time (Le Guen et al., 2015). However, the entire process, controlling emergence of so-called adult state, with functionally mature intestinal stem cells, from its fetal progenitors during gut development remains uncovered. Despite our knowledge about pathways, maintaining stemness in crypts, there is limited understanding of transcriptional networks, required for establishing Lgr5+ adult ISCs in embryonic epithelium, in particular, the role of Wnt/ƀ-catenin activity in this molecular switch.

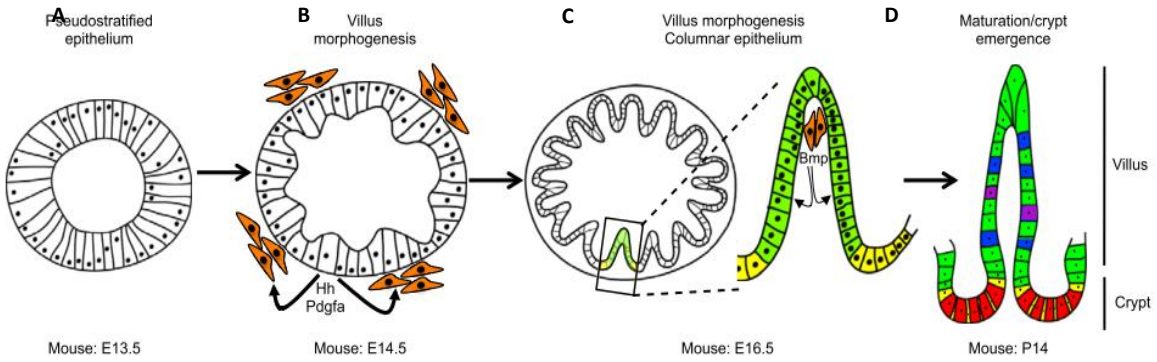

Figure 1. Mouse intestinal development. A. At E13.5 the mouse gut represents a tube with pseudostratified epithelium. **B.** At E14.5 mesenchymal clusters (orange), responding to Hh and Pdgf-a signaling, appear during villus morphogenesis. **C.** Reorganization of intestinal epithelium into villi-intervilli compartments, driven by villi-associated BMP signals from underlying mesenchyme. **D.** The embryonic intervillus gives rise to crypts by postnatal day 14. The mature crypt harbors Lgr5+ ISCs and Paneth cells (*from Wells, 2014*).

3.6. Crosstalk between signaling pathways in the embryonic gut.

First evidence supporting a role for the Wnt pathway in fetal intestines came from mice in which the b-catenin transcriptional binding partner Tcf4 (encoded by *Tcf7l2*) was disrupted: *Tcf4*$^{-/-}$ embryonic intervillus epithelium lost their proliferation capacity, which caused impaired villi formation and neonatal lethality. However, epithelial homeostasis appeared normal before E16.5, showing that the initial specification of intestinal stem cell progenitors requires Wnt/ɓ-catenin (Korinek, 1998). Further *in vivo* studies have implicated Wnt signals in establishment of crypt compartment. Thus, van Noort and colleagues (van Noort, 2002) showed the presence of nuclear b-catenin in intervillus epithelium at E16.5, confirming the activation of Tcf/ɓ-catenin in stem cell progenitors. Loss of b-catenin abolished crypt appearance both in fetal and adult epithelium (Chin et al., 2016); (Ireland et al., 2004) respectively); as well as overexpression of Wnt inhibitor Dkk1 induced crypt loss and morphological alterations in the small intestine (Pinto, 2003a, Pinto, 2003b); (Kuhnert, 2004). Altogether, Wnt signaling seems to regulate a master switch between proliferation and differentiation, establishing crypt-villi axis in gut epithelium (van de Wetering, 2002).

During embryonic gut development, Wnt signaling crosstalk with other pathways, regulating mesenchymalï epithelial interactions, is very important for the proper specification of crypt compartment - the eventual place of ISCs (Madison, 2005); (Le Guen, 2015).

The Hedgehog (Hh) pathway has been shown to play essential role in small intestinal morphogenesis. Sonic (Shh) and Indian (Ihh) hedgehog proteins, expressed ubiquitously in early gut

epithelium, become concentrated in cells of the intervillus region after E16.5 (Fig. 5B), but surprisingly display the opposite phenotypes (Ramalho-Santos, 2000);(Crosnier et al., 2006)). *Ihh-/-* mice die before birth, showing depletion of crypt compartment due to reduced proliferation in the intervillus region, whereas *Shh-/-* mice developed intestinal transformation of the stomach epithelium, or metaplasia (Ramalho-Santos, 2000). Furthermore, complete or partial blockage of the Hh activity by overexpression of its inhibitor, caused a complete loss of villi with increased activation of the Wnt pathway (Madison, 2005)). These studies clearly demonstrate that Hh signaling is required for establishing the proliferative compartment in intervillus base by modulating the Wnt activity.

Perhaps surprisingly, although stem cell proliferation and differentiation are supposed to be crucial for homeostatic maintenance of the villi, the initial formation of the villi at E15-16.5 does not appear as a stem-cell-dependent process (Korinek, 1998); (Shyer et al., 2015)). As a crypt-villi axis in the adult small intestine, maintenance of villi-intervilli axis is rather orchestrated by activity of several signaling cascades.

Thus, analysis of Notch pathway in the developing fetal intestine of *Atoh*$^{-/-}$ mutant mice at E14.5 and E18.5 revealed normal villus architecture; however, all differentiated cells were only absorptive enterocytes, whereas Goblet cells, entero-endocrine cells and Paneth cell precursors, expressing cryptidin-1, were totally absent (Yang, 2001). An opposite phenotype has been observed in *Hes1*-deficient intestines with increased number of mucose-secreting and enteroendocrine cells at the expense of enterocytes (Jensen, 2000). These results indicated the role of Notch signaling target genes in directing of TA cells towards absorptive or secretory populations. Of note, *Hes1* is expressed not only in fetal intestinal epithelium but also in the adjacent mesenchyme, just beneath the nascent epithelium, indicating Notch pathway activity in developing mammalian gut, driven by mesenchyme-epithelium crosstalk (Kim et al., 2011). Furthermore, when Notch function was ablated specifically in fetal mesenchyme, newborn mice died by 1 week of age. In these mice, intestinal length was significantly reduced after birth and caused malnutrition. This shortening reflected a developmental defect because the intestines at E14, E16 and newborn Notch-deficient mutants were 20-30% shorter on average (Kim, 2011).

The possible role of BMP signaling activity in developing intestinal tract has been described in the work of Karlsson et al. (2000), where the authors studied epithelial-mesenchymal crosstalk prior to villus formation at E15.5. It has been shown that the generation of the villus epithelial folds coincides with the formation of mesenchymal clusters that express PDGFR-Ű, BMP-2 and BMP-4 ligands (Fig. 6A-B). These clusters remain beneath the villus tip during its invagination into the gut lumen (Karlsson, 2000).

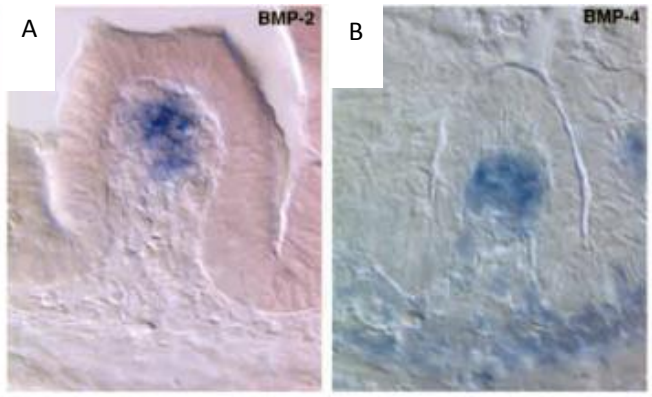

Figure 6. Embryonic intestine reorganization, taking place at E15.5, is driven by BMP signaling. Mesenchyme expresses *BMP2* (**A**) and *BMP4* (**B**) under the villus tips (*Haramis, 2004*), that are formed by ñvillus clustersò.

Further studies confirmed mesenchymal expression of *Bmp4*, *Bmp5* and *Bmp7* (Haramis, 2004); (Walton et al., 2016) in nascent villi, but not in the mesenchyme underlying the epithelial pockets, which are the pre-cursors of the crypts. To test the effect of BMP signaling on villi emergence, the embryonic intestine was harvested at E13.5, prior to cluster formation and cultured *ex vivo* in the presence of Bmp-soaked beads. In control albumin-treated bead the clusters formed as expected, whereas BMP-beads showed inhibited mesenchymal cluster formation and subsequent villus emergence in the region surrounding the bead (Walton, 2016). Moreover, it has been demonstrated that only mesenchymal Bmp signaling has a functional role in intestinal development, because the epithelial knockout of *Bmpr1a* in *Shh*-driven mouse didnôt show any tissue abnormalities (Mao et al., 2010), however the loss of *Bmpr1*a in mesenchyme results in enlarged clusters and merged villi (Walton, 2016). Together, these data demonstrate that in the developing intestine the patterning of mesenchymal clusters is determined by the level of Bmp signal transduction in the mesenchymal compartment.

Nowadays it became clear that in embryos, even when structured crypts are absent, boundaries of transcriptional activities between villi and intervilli are established during epithelium reorganization at E14-E16.

3.7. Lgr5+ progenitors in the embryonic gut.

Despite our knowledge about adult ISCs markers and signaling pathways, it has remained unclear when and how embryonic endodermal cells undergo specification into Lgr5+ stem cells.

The very first fetal precursors of adult ISCs are believed to originate after E15.0-E16.0 when gut epithelium undergoes dramatic reorganization to villi-intervillus units and actively proliferating cells are restricted to intervillus compartment. *Lgr5*-expressing cells have been detected at E15.5 stage in intervillus region and become exclusively localized in a forming crypt compartment harboring Lgr5+ adult ISCs (Garcia et al., 2009); (Kim, 2012); (Kinzel et al., 2014). Fig.5C). Moreover, expression of other ISC markers, such as *CD44* (Kim et al., 2007), *Axin2* (Garcia et al., 2009) and *Olfm4* (Kinzel, 2014) in intervillus pockets further indicated the appearance of embryonic precursors of adult ISCs late during embryogenesis. Altogether these studies confirm the presence of Wnt/b-catenin activity in crypt progenitors, as it has been demonstrated *in vivo* (Korinek, 1998); (Chin et al., 2016).

However, according to the recent studies from Shyer and colleagues (Shyer, 2015), *Lgr5*-expressing cells are found throughout the epithelium already in the embryonic day 12.5 (E12.5) small intestine, just prior to villus formation. Over the following days of development, *Lgr5* expression, as well as CD44, is lost in the forming villus tip and is progressively restricted to the space between villi as they form. Furthermore, authors suggest that the entire mechanism of Wnt activity in crypt progenitors is regulated by Shh in the subadjacent mesenchyme, that subsequently triggers villus clusters gene expression (*Bmp4, Pdgfa*) at the tips of the villi. Bmp signaling clusters block Wnt activity, thus repressing expression of *Lgr5* gene in villi.

Interestingly, Lgr5 knockout in embryonic intestine didnôt show dramatic phenotype on ISC formation: at E18.5 both proliferation rate and cytodifferentiation are not affected (Garcia, 2009). However, Lgr5-deficient mice had precocious Paneth cell formation already at E17.5 (instead of P14 in WT animals) and upregulation of ISC markers such as *Ascl2*, *Axin2*, *Rnf43*. This data shows that Lgr5 itself could be a negative regulator of expanded Wnt signaling activity, preventing premature Paneth cell differentiation (Garcia, 2009).

The potential negative regulators of *Lgr5*+ ISCs identity in embryos are supposed to be the genes, inhibiting trio of *Ascl2* transcription factor, ß-catenin, and *Tcf4* transcription factor. When *Ascl2* is expressed, it leads to activation of Tcf/b-catenin pathway and proliferation of intestinal epithelium. One of the candidate genes, that might regulate stemness capacity of the cell by binding basic HLH Ascl2 transcription factor, is *Id2* (Russell et al., 2004).

Id2 belongs to an Id family of HLH proteins identified and named for its dual role as both, inhibitors of the differentiation process and inhibitors of DNA binding. Id proteins are inhibitors of the bHLH class of transcription factors. While *Id1* and *Id3* were shown to be expressed at embryonic mesenchyme and adult epithelium, only *Id2* gene is expressed in epithelial cells in embryonic intestine from E10.5 until E18.5, then its level dramatically drops down. Importantly, it has been found before, that loss of *Id2* (*Id2*$^{-/-}$) in the mouse intestinal epithelium prevents exit from cell cycle and proper differentiation of enterocyte precursor cells during embryogenesis. *Id2-null* intestinal epithelial progenitors at E18.5 fail to undergo terminal differentiation whereas retaining a hyperproliferative state. The consequent proliferative activity and loss of differentiation of the intestinal epithelium leads to tumor formation in postnatal life (Russell et al., 2004).

Two opposing models, the late *Lgr5*+ cells formation (Kim, 2007, Garcia, 2009, Kinzel, 2014) and early ubiquitous *Lgr5* expression model (Shyer, 2015), describe the appearance of intestinal stem cells during gut development. Answering this controversy will require knowledge about whether Lgr5 is expressed in the embryonic small intestinal epithelium and to characterize the identity of Lgr5+ progenies *in vivo*.

3.8. Approaches for stem cell progenitorôs identification.

3.8.1. Clonogenic cell capacity *ex vivo*.

In 2009, Sato and colleagues reported a successful method, devised for growing the long-term three-dimensional culture of adult intestinal epithelium as organoids (Sato et al., 2009). An organoid could be defined as an in vitro 3D cellular cluster derived exclusively from primary tissue, ESCs or iPSCs, capable of self-renewal and self-organization, and exhibiting similar organ functionality as the tissue of origin (Fatehullah et al., 2016). Intestinal organoid cultures were derived from single Lgr5+ stem cells embedded in Matrigel and the growing medium contained EGF, Noggin, and R-spondin-1 (Fig.7A, 7C). In such 3D conditions ISCs gave rise to all the major cell types of the adult intestinal epithelium, including Paneth cells (Sato et al., 2009). Stem cell proliferation first created cystic spheroids, which then formed crypt-like buddings that within 2 weeks further developed into ómini-gutsôô with distinct crypt-villus compartmentalization as seen *in vivo* (Kretzschmar and Clevers, 2016), Fig. 7B)

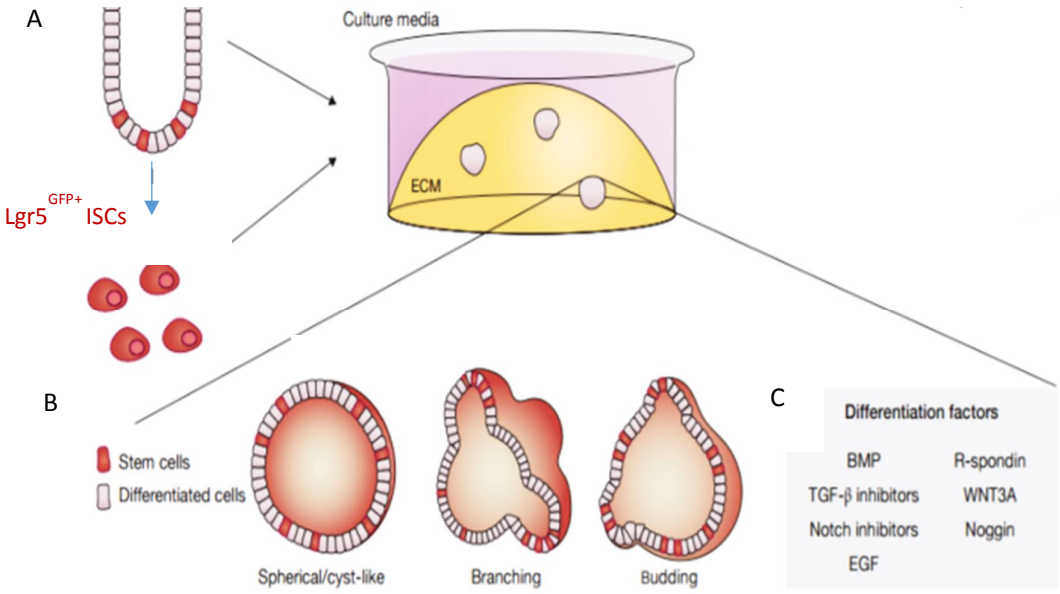

Figure 7. 3D ex vivo intestinal cell culture. A. Organoids could be derived from the whole intestinal crypts, as well as from FACS-sorted Lgr5+ ISCs. **B.** Stem cells are maintained in a Matrigel drop and give rise to differentiated intestinal cell lineages, forming spheroids or budding organoids. **C.** By adding the growth factors, promoting either cell differentiation or proliferation, ISCs progeniesô cell fate could be controlled. *Adapted from Fatehullah, 2016.*

When I started my PhD project, only organoids, derived either from the adult gut (Sato, 2009), or from human iPSCs (Spence et al., 2011) were described. By adapting these culture conditions for mouse embryonic material, I established the method to maintain primary isolated cells *ex vivo*. However, at this time two other research groups (Fordham et al., 2013); (Mustata et al., 2013)) independently reported the similar results.

These two groups examined the *in vitro* growth of intestinal epithelial cells isolated from different stages in embryonic and postnatal mouse development. Mustata et. al. showed that embryonic cells, isolated from early stages (E14-E15), formed not organoids, but so called spheroids, or hollow spheres (Fig. 8A, 8D). Intestinal spheroids were suggested to be composed of stem cells and lack budding and branching structures enriched for differentiated cells in organoids (Mustata et al., 2013, Fig. 8D). The early fetal spheroids didnôt require Wnt signaling ligands for their growth as well as did not express the adult stem cell marker Lgr5. Moreover, genes *Cnx43* and *Trop2*, found highly upregulated in spheroids compared to differentiated organoids, were proposed as stem cell markers for early gut embryogenesis. Similarly, in the work of Fordham et al. (2013) the existence of a rapidly proliferating population of intestinal progenitors that forms prior to the establishment of ISCs was demonstrated. This unknown cell population, present in the fetal intestine from E14.5, grow *in vitro* as cystic Foetal Enterospheres (FEnS) and subsequently during postnatal development, FEnS are replaced by organoids (Fig. 8B, 8E). In fact, at P15 only organoids will be formed (Fig. 8C, 8F). Moreover, transplantation of FEnS showed that those spheroids can mature *in vivo* and contribute to regeneration of damaged gut epithelium in mouse (Fordham, 2013). However, the cellular composition inside embryonic spheroids, origin of ISCs progenitors as well as transcriptional programs, establishing ISCs, remain uncharacterized.

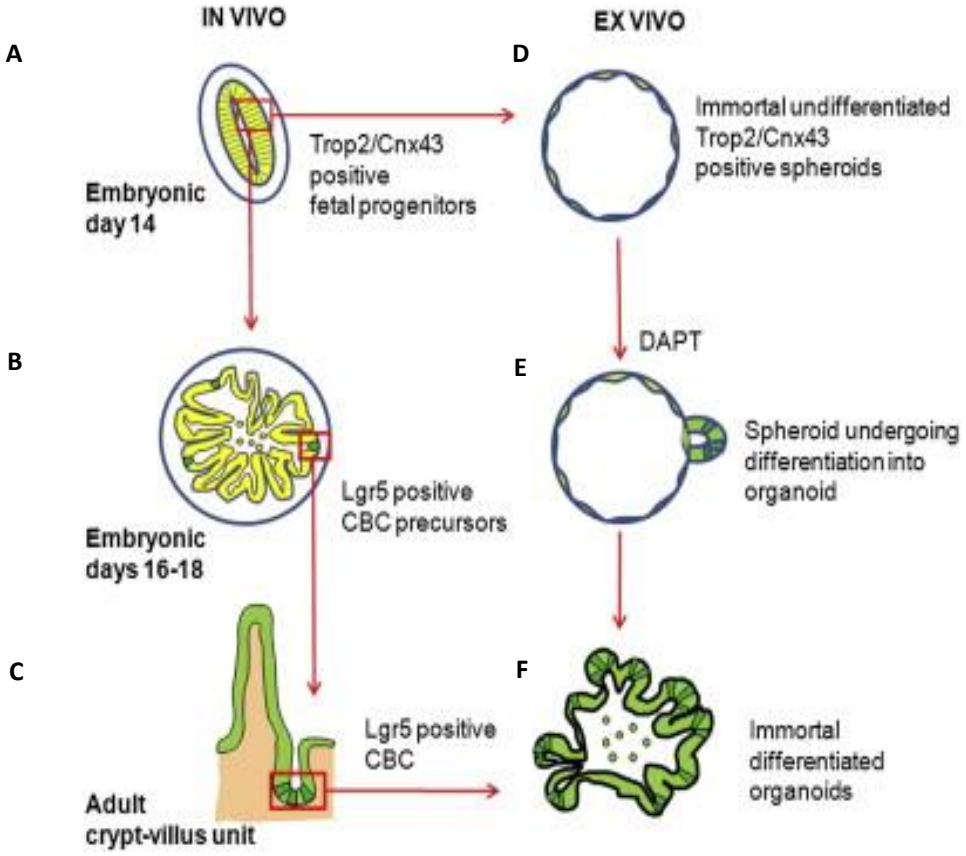

Figure 8. Ex vivo embryonic intestinal cell culture as a tool to understand development of the small intestine and ISCs *in vivo*. A-F. At E14.5 embryonic epithelium is composed of undifferentiated *Trop2+Cnx43+* cells (**A**), that are growing in a form of spheroids *ex vivo* (**D**). During epithelial reorganization into differentiated villi and Lgr5+ ISCs in intervilli (**B**), spheroids in culture undergo transformation into organoids (**E**). In postnatal stage, when villi-crypt axis is well established in mice (**C**), intestinal cell culture converts completely into budding organoids, thus representing adult ISCs program (**F**). *From the graphical abstract of Mustata, 2013.*

As discussed earlier, multi-lineage contributions and tissue-tissue interactions are critical for the development a functional intestine. Thatôs why although intestinal organoids have been called as ñmini-gutsò, in fact they lack the mesenchymal, stromal, immune and neural cells that make the whole functioning gut *in vivo* (Fatehullah, 2016) and represent only a part of such a complexed organ as the small intestine.

Nevertheless, nowadays 3D *ex vivo* organoid system is a commonly used tool not only for propagation of stem cells and their embryonic progenitors, but also a material for lentiviral transduction, Crispr/Cas9 mediated genome editing, transplantation and intestinal disease models.

3.8.2. Lineage tracing.

One of approaches to study embryonic cell population progenies fate through development is lineage tracing. This technique identifies precursors of mature cell types *in vivo* and describes the cell fate steps they undergo in temporal order. In mice, the most popular labelling technique is based on a drug-inducible Cre recombinase together with a reporter system. By placing a drug-inducible Cre recombinase (for example, Creï estrogen receptor ï ERT) under the control of a gene-specific promoter, its transient activation by drug administration (for example, tamoxifen) leads to the excision of a stop cassette and the permanent expression of a reporter construct in targeted cells and their progeny. The use of different cell-specific driven promoters and adjustment of the drug dose allow different cell subpopulations to be labelled (Blanpain and Simons, 2013).

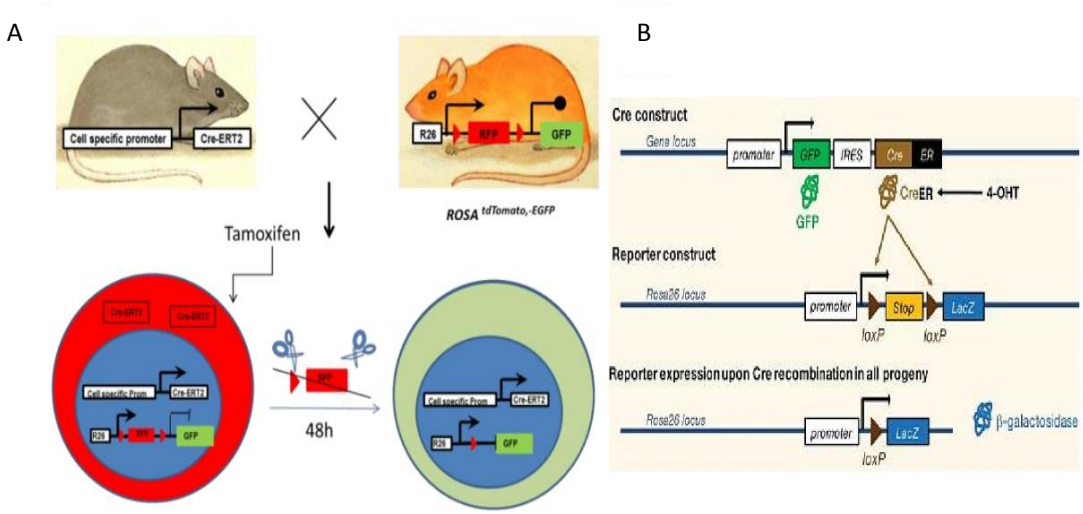

Figure 9. Tamoxifen inducible Cre^{ERT2} mouse system for cell lineage tracing *in vivo*. A. Schematic representation of cell labelling by fluorescent signal. Cre recombinase is fused to a tamoxifen-inducible mutated estrogen receptor (CreERT2). Cre recombinase is expressed under the control of a tissue- or (stem) cell-specific promoter. In those cells, Cre can recombine loxP sites in the ubiquitously expressed reporter Rosa$^{tdTomato/eGFP}$ construct to remove the STOP cassette. After Tamoxifen treatment, Cre recombinase is active and removes the STOP. Afterwards all progenies of Cre^{+} cells will express GFP forever, as well as all their progenies. **B.** Schematic representation of the labelling by X-Gal. Cre recombines at loxP sites to remove the STOP cassette, enabling LacZ expression. All progenies of those Cre^{+}/Rosa^{LacZ+} stem cells express LacZ as a permanent genetic mark. In this scheme, a genetic construction of Lgr5-CreRT mouse is illustrated. Barker et al. (2007) made a mouse strain, in which CreERT2 was expressed in conjunction with a reporter GFP to visualize the areas of *Lgr5*^{CreRT2} gene expression. *Adapted from Kretzschmar, 2012.*

In our group, we have several reporter mouse strains to label Cre-expressing cell populations. One of them is *Rosa*$^{(tdTomato;-eGFP)}$ mouse line (Mao, 2001, Fig.9A). All tissues and cells in *Rosa*$^{(tdTomato;-eGFP)}$ mouse have strong red fluorescence due to expression of loxP-flanked Tomato gene under the ubiquitous Rosa promotor. When bred to Cre recombinase expressing mouse, the resulting offspring have Tomato deleted in the Cre expressing cells/tissues, allowing expression of eGFP cassette located just downstream. Upon tamoxifen administration only cells, expressing Cre, and their progenies will become GFP+ forever.

Another reporter system based on *Rosa*^{LacZ} mouse strain allows us to visualize the labelled cells without fluorescence. In this case loxP-flanked stop cassette under the ubiquitous promotor Rosa makes LacZ gene expression to be silent (Sorriano, 1999; Fig.9B). In a *Cre*-expressing mouse, cell-specific Cre recombinase cuts out the stop cassete and all the progenies become LacZ-positive. Labelled cells can be visualized by blue signal from X-gal staining.

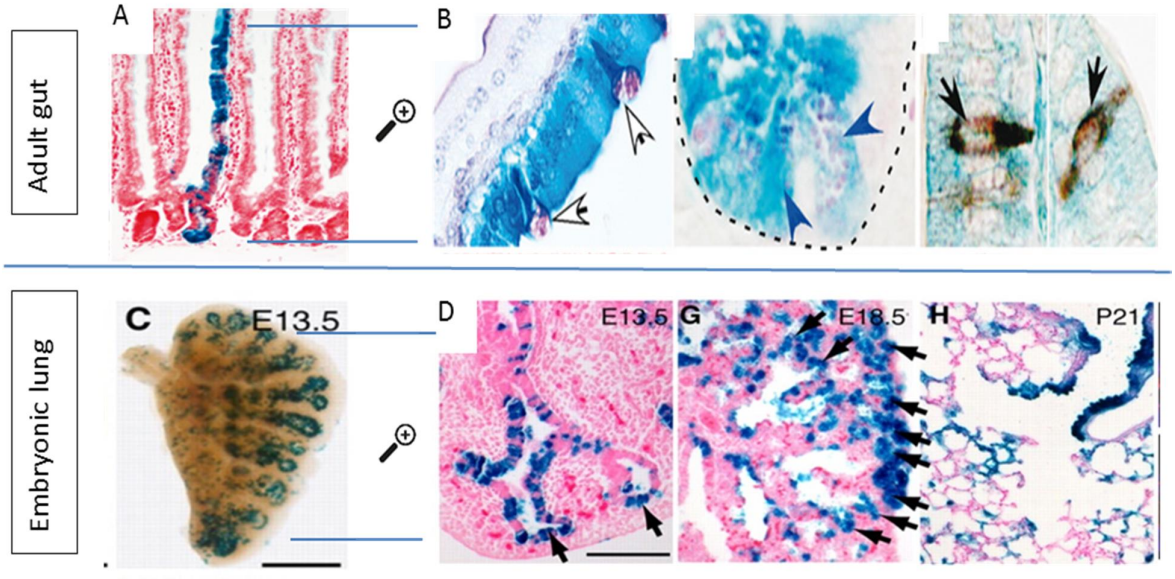

Figure 10. Lineage tracing allows the identification and tracking of the progeny of a specific type of cell population. A. Whole-mount analysis of Tamoxifen-induced LacZ expression in small intestine of Lgr5-EGFP-Ires-CreERT2 knock-in mice crossed with Rosa26-LacZ reporter. Lgr5+LacZ+ ISCs progenies differentiated to all intestinal cell types, including secretory cells ((**B**), arrows). **C.** Lineage tracing on Id2^{CreRT}/Rosa^{LacZ} mice demonstrates that embryonic Id2+ cells, labelled at E11.5, are multipotent and contribute to progenies of all lineages in lung development. However, when labelled later, embryonic Id2+ cells progenies are found only in alveolar part of the lung (**D**). *Adapted from Barker, 2007; Rawlings, 2009.*

One of the most successful studies using lineage tracing as a tool to track stem cells was performed by the Clevers lab. Cassette, expressing *EGFP– ires–CreERT2* transgene was inserted into the murine *Lgr5* locus (Fig. 9B). Then Lgr5-eGFP-CreRT2 mice were crossed to $Rosa26^{LacZ}$ reporter mice, described above, and the resulting double mutant strains were treated with tamoxifen to activate Cre specifically in a small number of *Lgr5*-expressing stem cells in intestinal crypts. Labelled clones formed cohesive ribbons of blue LacZ+ cells emanating from the crypt and terminating on villi (Fig.10A). GFP+ and LacZ+ stem cells remained localized, while villi were only Lacz+ and differentiated into all intestinal lineages, confirming that they were progenies of the Lgr5-expressing stem cells (Barker, 2007; Fig. 10B).

This strategy to identify stem cell populations in adults has been applied in developmental biology as well. One of the examples using lineage tracing to track stem cells during mouse lung organogenesis is that by Brigid Hogan lab. It has been shown that the distal tip cells in developing lung have a high proliferation due to activities of the Wnt, Bmp and Fgf signaling pathways and upregulation of several genes, including *N-myc*, *Id2*, *Sox9*, *Foxp1* and *Foxp2* (Rawlins et al., 2009). Based on the specific expression pattern of *Id2* in tip epithelial cells, authors have generated a new *CreERT2* knock-in allele to follow the fate of these cells at different stages during lung development. Tracing the progenitors of the E11.5 tip epithelium showed that *Id2*-expressing cells contributed to both the bronchioles and alveoli and importantly, was partially observed at postnatal stages (Fig. 10C, Rawlins et al., 2009). Another example for stem cell fate studies on embryos is the work of Fuchs and colleagues (Nowak et al., 2008)). They placed Cre under the control of *Sox9*, an epidermal marker, specifically expressed in hair follicle bulge stem cells. By using this mouse strain to trace the origin of bulge stem cells and their progeny during epidermal morphogenesis, they demonstrated that Sox9-positive cells can give rise to all epidermal lineages (Nowak et al., 2008).

To summarize, although genetic knockout studies, gene expression profiling and colony formation assays contribute to our understanding of stem cell program regulation, the mechanisms, driving stem cells and their progenitors cell fate determination, requires dynamic information, which can be obtained only by *in vivo* from lineage-tracing studies, followed by microscopy imaging.

4. Aims of the PhD study.

Nowadays adult ISCs, their signaling pathways and molecular markers, such as *Lgr5*, *Ascl2, Olfm4* are well described. However, the process, responsible for ISCs appearance in gut development, remains unknown. The controversy over the existence of *Lgr5*-expressing cells in early gut development arises many important questions such as:

- When exactly endodermal embryonic cells are determined to differentiate into adult ISCs?
- Which transcriptional programs establish ISCs pool in early gut development?
- How many embryonic cell types will give rise to adult ISCs?

The aim of my study is to investigate the role of Wnt signaling in early gut formation and the molecular mechanisms, establishing Lgr5+ ISCs appearance. To address this question, I would like to characterize embryonic gut epithelium on molecular level and identify specific markers that define heterogeneous cell populations within the developing epithelium. The major goal of my work is to understand the functions of cell populations and co-expressed genes prior to ISCs formation. This will provide an information about embryonic states, facilitate fate mapping, and let us to modulate specific molecular pathways both *ex vivo* and *in vivo*.

To reach the goal I am using mouse genetics, cellular and computational biology approaches. Since one of the markers of adult ISCs is *Lgr5* gene, I will test whether embryonic intestinal cells express *Lgr5* at early stages of gut embryogenesis. Our RNA *in situ* analysis on E13.5 small intestine showed a subset of epithelial cells expressing *Lgr5*. The hypothesis of early Lgr5+ precursors in embryonic intestinal epithelium will be further strengthened by $Lgr5^{eGFP\text{-}CreRT2}$ mouse lineage tracing experiments.

5. Results.[♣]

5.1. FACS sorting approach.

To study molecular mechanisms, driving formation of ISCs in the developing gut, I decided to work with mouse embryos at stage E13.5 ï 2 days prior to differentiation of the small intestine from a simple tube to villi-intervilli units. Although at E13.5 the small intestine is still very short, it could be visually distinguished from embryonic stomach and colon and thereby could be manually dissected out (Fig. 11A). Of note, limited embryos number and a very small initial amount of embryonic intestinal cells that I will work with, demands high accuracy in dissection, optimization of conditions for embryonic cells isolation and careful preparation of cell suspension. I started my project by establishing conditions to isolate alive embryonic cells from mouse embryos.

Briefly, embryonic intestinal cells at E13.5 were collected by dissecting of pregnant mice, followed by isolation of embryonic guts, tissue digestion by collagenase treatment and FACS sorting (Fig. 11B-E). Staining with fluorophore-conjugated antibodies against Epithelial cell adhesion molecule (EpCam), hematopoietic cell marker CD45+ and T-cell marker CD31+ allowed to separate epithelial cells and excluded contamination with cells from mesenchymal tissue. To set correct gates, I have used a negative selection, based on low forward scatter (FSC) and high side scatter (SSC) plots together with $DAPI^{+}$ dead cells. This gating strategy enabled us to collect only viable single cell suspension, which was free of debris, dead cells or clumps of undigested doublet cells. Fig. 11E. is illustrating the successful FACS-sorting strategy to work with a pure population of EpCam+ embryonic epithelial cells. Specificity of EpCam antibody was also validated by numerous immunostainings against this antibody, performed by our lab members on the embryonic small intestine sections.

FACS showed that the embryonic small intestine consists of 90 % of mesenchymal tissue, which is surrounding a thin tube with 10-20% epithelial cells (Fig. 11E). Taken together, establishing of embryonic cells isolation and FACS sorting conditions, was very important step to study further cellular heterogeneity, clonogenic capacity of cells and their genome-wide transcriptome.

[♣] Most of the results contained in this thesis are published (in modified form) as:
Nigmatullina L, Norkin M, Dzama MM, Messner B, Sayols S, Soshnikova N.
Id2 controls specification of Lgr5+ intestinal stem cell progenitors during gut development.
EMBO J. 2017 PubMed PMID: 28077488.

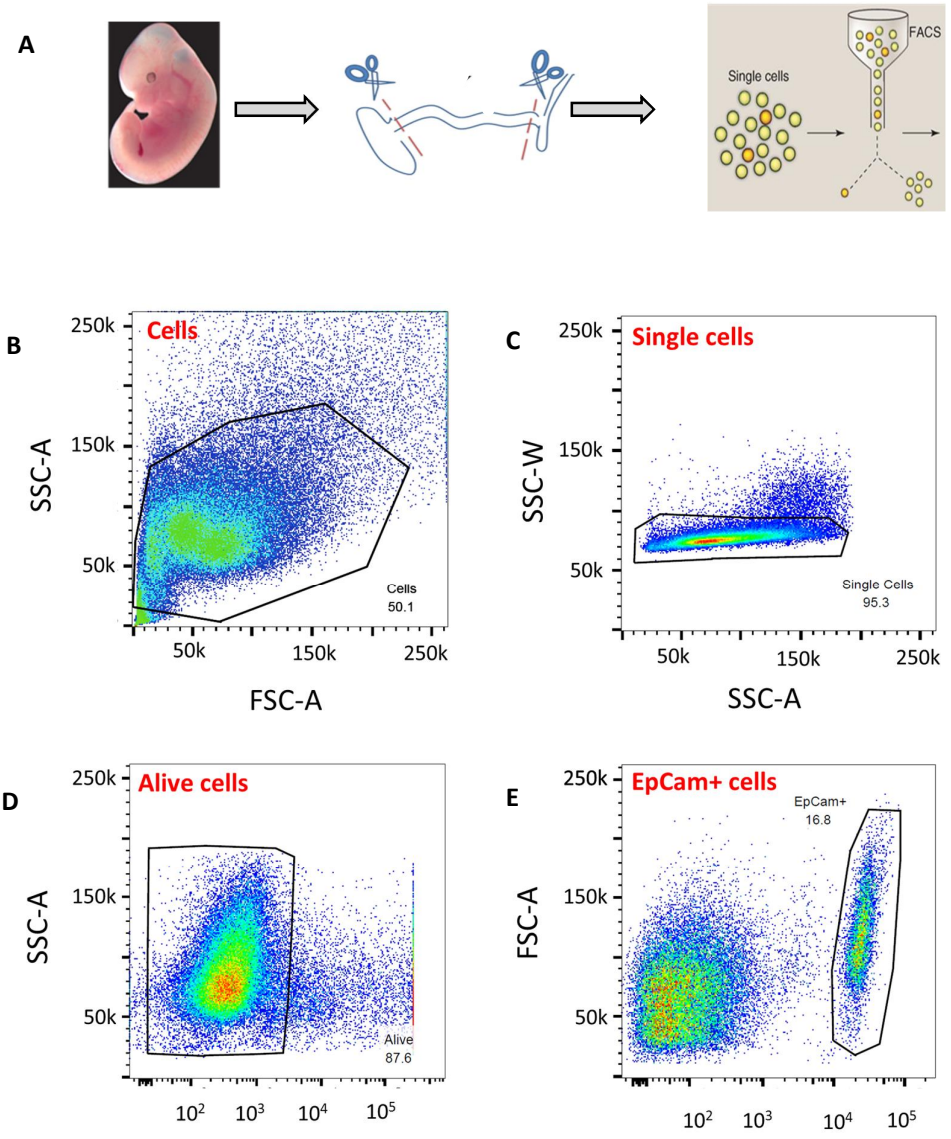

Figure 11. Embryonic intestinal cells isolation strategy. **A**: Dissection of the small intestine from the mouse embryo, followed by preparation of single cells suspension. **B-E**. FACS sorting strategy: Size selection and exclusion of cell debris (**B**); Single cell gating to exclude doublets (**C**). DAPI negative selection for alive cells population (**D**); Gating for EpCam positive epithelial intestinal cells.

5.2. Lgr5+ cells within embryonic gut epithelium.

In my PhD research, the most intriguing question was to elucidate the process, driving the formation of Lgr5+ cells within the embryonic gut epithelium *in vivo*. Unfortunately, to date, most of the studies on Lgr5 receptor activity are constrained by the lack of specific antibodies against its gene product. To overcome these limitations, I decided to verify the presence of Lgr5+ embryonic cell population by using of *Lgr5*$^{eGFP\text{-}CreRT2}$ knock-in mouse strain, where GFP-ires-CreRT2 cassette is expressed under the *Lgr5* gene locus (Barker, 2007, Fig 12C). In this mouse model cells/tissues, expressing *Lgr5* gene, could be identified by GFP-reporter activity. Being aware of the possibly variegated expression of the *Lgr5*$^{eGFP\text{-}CreRT2}$ cassette, reported for this transgenic mouse, our lab utilized *Lgr5* mRNA *in situ* hybridization (ISH) assay to examine expression of *Lgr5 in vivo* on numerous mouse embryonic sections from E11.5 to E15.5. Experiments, performed by our lab members, showed a small subset of cells, expressing *Lgr5* gene within the embryonic tube already at E13.5 (Fig. 12A). Interestingly, we didnôt observe a ubiquitous *Lgr5* gene expression neither at E13.5 nor earlier at E12.5, as it has been reported recently (Shyer, 2015). Embryonic endodermal marker *Shh*, highly expressed in intestinal tube, has been selected as a positive control for our ISH analysis (Fig.12B).

By using FACS sorting of Lgr5-eGFP-CreRT2 knock-in embryos, I confirmed that within EpCam^{+} small intestinal epithelia, 3-5% of cells are Lgr5^{GFP+} at E13.5, as it was detected by ISH (Fig. 12E). For the negative control, I used the wild-type (WT) littermate siblings from the same mother. This also allowed to gate a proper GFP plot for Lgr5+ cells (Fig 12D). To accurately quantify the activity of Lgr5$^{eGFP\text{-}CreRT2}$ cassette, I tested each sample separately, i.e. embryo per embryo. This strategy confirmed that there was no leakage or unspecific expression of GFP reporter in Lgr5^{GFP} negative embryos (Fig. 12D). Furthermore, low expression of Lgr5 was also shown by immunostaining against GFP on Lgr5-eGFP-CreRT2 embryos and absent in WT control (Fig. 13 C-D). Detailed analysis of stained sections enabled us to visualize the spacious distribution of GFP+ cells within the gut epithelium (Fig. 13B). Fig. 13C-D show that Lgr5+ cells spread not even, but by a gradient: Lgr5+ cells are not detected in anterior part, closer to stomach, but populate up to 90% of a posterior gut. Importantly, we received the same results by ISH against *Lgr5* mRNA. Thus, our data is contrast to ubiquitous GFP signal from Lgr5+ embryonic intestine, as reported by Shyer et.al (2015).

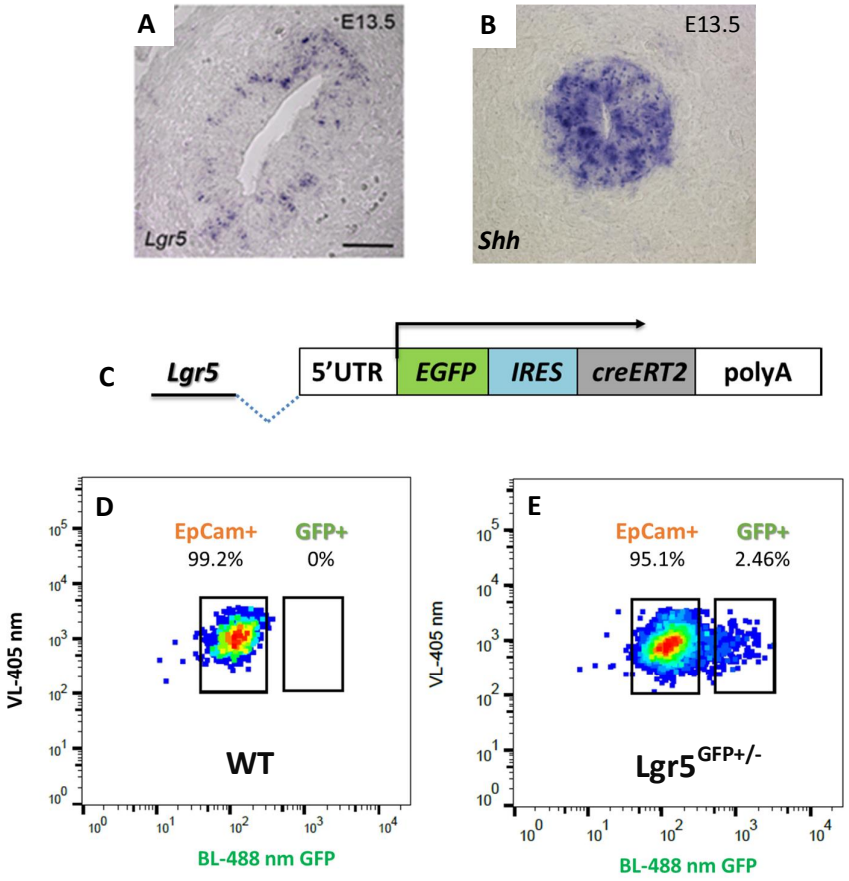

Figure 12. **Identification of Lgr5-expressing cell population at E13.5 *in vivo*.** ISH analysis performed on the E13.5 small intestine, revealing the presence of rare *Lgr5*-expressing cells (**A,** *provided by Dr. N.Soshnikova*) and ubiquitous *Shh* (**B**) gene transcripts within epithelium. **C**. Genetic construction of Lgr5-eGFP-CreRT mouse model. **D-E**. Embryonic intestinal cells, isolated from WT (**D**) and $Lgr5^{GFP\text{-}CreRT}/+$ (**E**) embryos, were stained with EpCam and analyzed for GFP signal by FACS. Discrete population of $Lgr5^{GFP+}$ cells is depicted. Scale bar, 30 µm.

I decided to check if such a minor Lgr5+ cell population at E13.5 is a subsequent result of Wnt signaling wave activity, taking place after E8.0. Several studies have reported that the Wnt signaling is important for a correct endoderm specification, particularly, for midgut and hindgut structures development (Spence, 2011; Fig. 13A). If the Wnt signaling is activated as soon as the endodermal-mesenchymal tube is formed and secreting bona fide molecules, responsible for stem cells formation, a higher number of Lgr5+ cells at earlier stages of embryo development would be detected.

However, FACS analysis at earlier stages didnôt confirm this hypothesis: E11.5 gut lacks Lgr5+ cells and E12.5 epithelium contained only 0.6% of $Lgr5^{GFP}$ per embryonic small intestine. Thus, most likely, activation of *Lgr5* gene transcription takes place between E12.5 to E13.5 stage, independently of early Wnt signaling at E8.0. Notably, GFP+ cells occupy mostly posterior part of the

growing small intestine. Thus, we assume that the Wnt activity, started in a posterior part, driving a subset of cells to become Lgr5+ due to a unique molecular signaling activity.

I have measured the dynamics of Lgr5-GFP expression within the growing embryonic gut tube. The amount of $Lgr5^{GFP+}$ cells was increasing during development, from 4.2% at E13.5 to 8.2% at E17.5, reaching the maximum at E15.5 - 9.8% (Fig. 13B) ï time of an active remodeling of intestinal epithelium. Our data indicate that at E13.5, transcriptional program, driving *Lgr5* gene expression is activated in a minor intestinal cell population, whereas the rest 95% of EpCam+ epithelial cells remains Lgr5 negative. However, the role of Lgr5+ cells at this stage should be further tested by *in vivo* lineage tracing in order to follow the fate of Lgr5+ progenies.

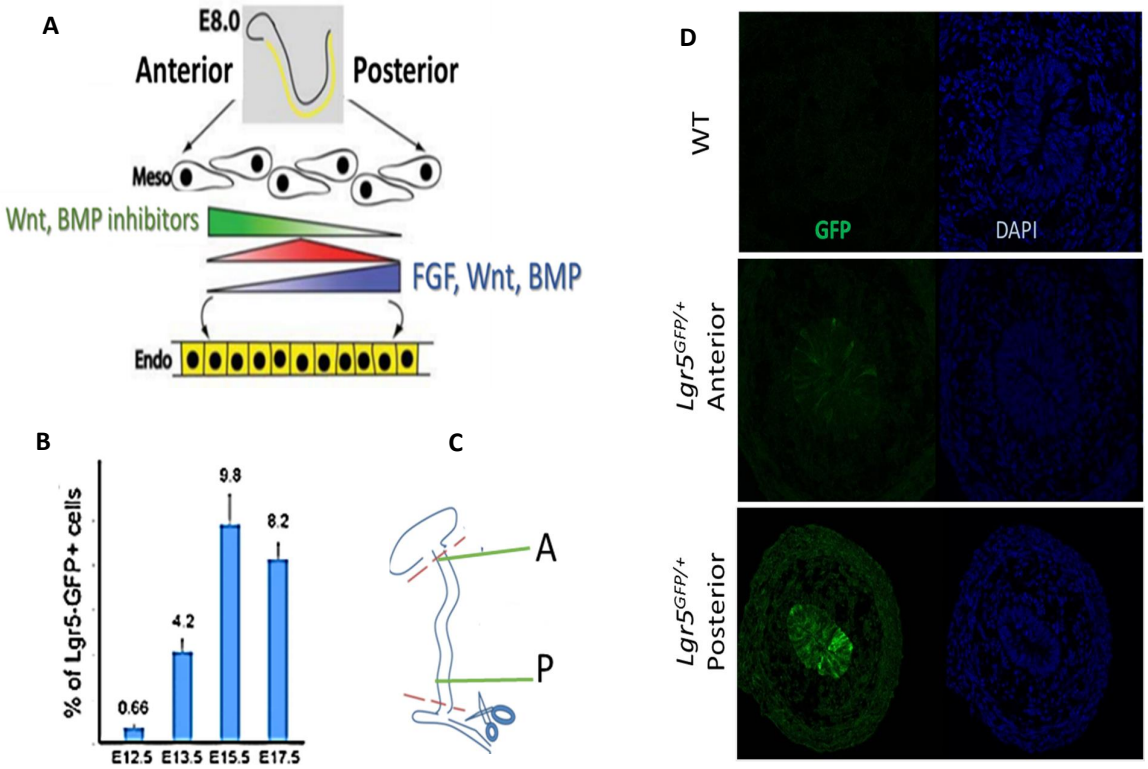

Figure 13. Identification of Wnt signaling activity in embryonic mouse gut epithelium. A. Signaling molecules, involved in anterior-posterior patterning of the intestine at E8.0 - Bmp, Wnt, Fgf and RA, expressed along the axis (adapted from Spence, 2011). **B**. Amount of Lgr5GFP+ cells within embryonic epithelium at stages E12.5-E17.5, measured by FACS. **C**. Schematic representation of the intestinal sections preparation. **D**. Immunostaining against GFP shows the distribution of $Lgr5^{GFP+}$ cells within E13.5 intestinal tube. A-anterior, P- posterior, error bars ±SD, n >3.

5.2.1. Lineage tracing of Lgr5+ embryonic intestinal cells *in vivo*.

In this approach, I took advantage of the same *Lgr5-eGFP-CreRT2* mouse strain, widely used in studies on adult animals. This mouse model allows us not only to quantify Lgr5+ cells by GFP reporter *in vivo* (see section 5.2.), but also to follow the fate of Lgr5-expressing cell population by Tamoxifen (Tam)-inducible Cre recombinase system during gut development.

First, to validate our mouse line as an intestinal stem-cell specific model and to check the efficiency of Lgr5+ cell labelling by Tam, I have performed Tam-induced tracing of $Lgr5^{Cre+}Rosa^{LacZ+}$ cells on adult P60 animals and dissected the guts after 5 days of tracing. As expected, single dose of Tam was enough to label ISCs. Cell fate of LacZ+ progenies could be visualized by blue ribbons of labelled villi (Fig.14A). Of note, in this experiment, I used the minimal dosage of Tam and only a single time injection has been performed. I observed the gradient of Wnt-responsive Lgr5 progenies - higher in anterior part and lower in posterior (Fig.14B). Additional control experiment with ubiquitous RosaLacz x RosaCre mouse lineage tracing confirmed the 99% efficiency of labelling (by Margarita Dzama).

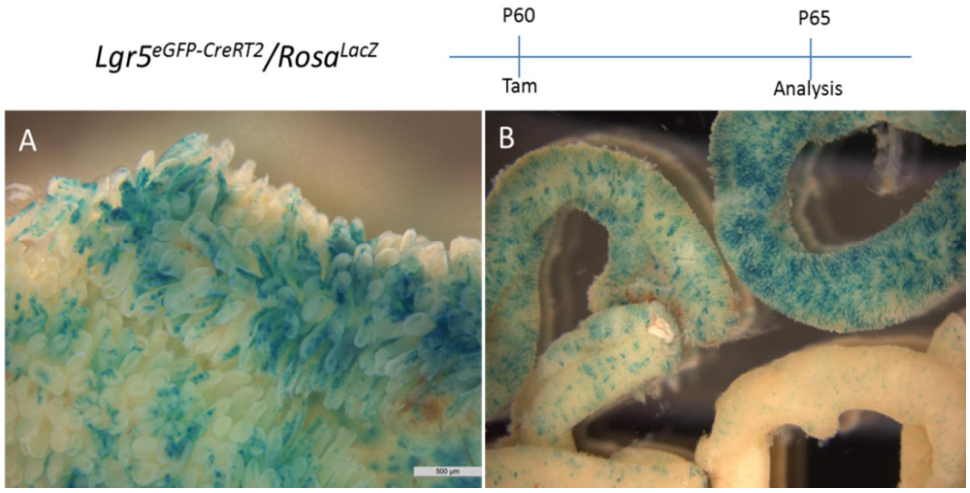

Figure 14. Lineage tracing of Lgr5+ ISCs in adult small intestine, by Tam injection of $Lgr5^{GFP-CreRT2}/Rosa^{LacZ}$ mouse. A. LacZ immunohistochemistry (blue cells) performed to detect *Lgr5+* progenies 5 days after a single Tam administration. **B**. The gradient of labelling within the whole intestine. Scale bar, 500µm.

To examine whether 4,2% of *Lgr5*$^{GFP+}$ expressing embryonic cells at E13.5 have a capacity to become ISCs, I performed a lineage tracing analysis. *Lgr5*$^{CreER/+}$;*Rosa*$^{LacZ/+}$ mice were treated with 10 mg/ml Tamoxifen at a single dose of 0.1 mg/g of body weight, oral gavage, at the time point indicated in the figure panels (Fig.15A). Of note, a higher dosage of Tam causes spontaneous abortions of pregnant mice, thus I kept the minimal concentration, required for a successful experiment. As tamoxifen injection can compromise the ability of pregnant mice to have natural birth, pups were delivered by cesarean section at E19.5ï E20. For a long lineage tracing experiment, following adult P60 stage, newborn mice were fed by adoptive lactating CD1 females. All lineage-tracing experiments were repeated in at least three different mice. Tamoxifen injection either at E12.5 or E13.5 gave very few *LacZ*$^{+}$ clones (from 3 to 10, resp.), visualized after 2 months of tracing (P60, Fig. 11A). Consistent to our FACS data from E14.5, *Lgr5*$^{+}$ cell tracing gave much more clones from this stage (Fig. 15A, 127±15). Notably, the most significant tracing was found at E15.5 (185±22). Although such induction gave rise to clones throughout the developing tissue, only ISCs clones that anchored to the crypt base survived long term. Those clones formed cohesive ribbons of blue cells emanating from the crypt and terminating on villi.

Immuno-histological stainings showed that *Lgr5*$^{LacZ+}$ labeled cells gave rise to all differentiated intestinal epithelial cell types, including enterocytes, chromogranin A positive entero-endocrine, PAS positive goblet and Paneth cells (Fig. 15B, 15C). Thus, embryonic *Lgr5*$^{+}$ intestinal epithelial cells are precursors of the adult intestinal stem cells, however *Lgr5* gene is not expressed ubiquitously at early developmental stages (in contrast to recently proposed model). Nevertheless, it also does not exclude the fact that other cell populations could not contribute to ISCs either. Thatôs why further characterization of embryonic intestinal cells on a molecular level was very important step in my study.

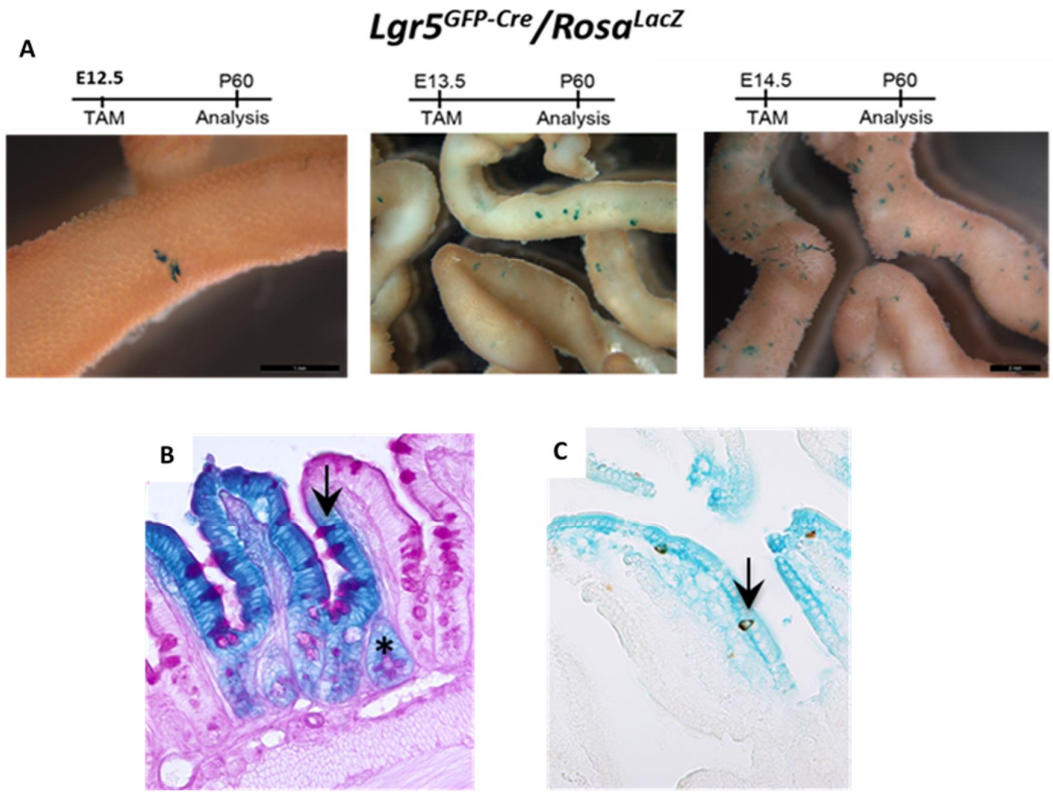

Figure 15. Lgr5+ cells analysis in a developing mouse small intestine. A. *Results are provided by M.Dzama.* Lineage tracing of Lgr5+ cells, labelled by Tam at E12.5, or E13.5, or E14.5, in *Lgr5*$^{GFP\text{-}CreRT2}$*/Rosa*^{LacZ} embryos demonstrates contribution of these cells to ISCs pool in adult P60 mouse intestine. **B-C**. Histological analysis of Lgr5+ lineage tracing sections revealed, that LacZ^{+} blue cells are not only enterocytes, but also PAS-staining positive Goblet (**B**, arrow) and Paneth cells (**B**, asteriks), chromogranin A positive enteroendocrine cells (**C**, arrow). Scale bar, 1mm.

5.2.2. Molecular signature of embryonic epithelial cells.

In order to gain insight into molecular signature of embryonic epithelial cells and their cellular heterogeneity, E13.5 EpCam^{+}Lgr5^{GFP+} (further as Lgr5^{+}) and EpCam^{+}Lgr5^{-} cells (as EpCam^{+}) were collected by FACS in amount of 500 cells per replicate and subjected to further RNA-sequencing analysis. The isolated cell populations were processed for total cDNA synthesis and library preparation. Due to a limited amount of material, I took advantage of SMART-Seq v4 Ultra Low Input RNA Kit for Sequencing (Clontech). In total four independent experiments for all procedures, including mice cross, FACS sorting and cDNA preparation have been performed.

Briefly, isolated total poly A+ mRNA was used for first and second strands of cDNA synthesis by template switching at the 5ô end. During such reverse transcription, defined PCR adapters have been added to both ends of the first-strand cDNA. This ensures the final cDNA libraries have the 5ô end of the mRNA, representing the original mRNA transcripts (Fig 16A). PCR-amplified cDNA was further purified by immobilization on AMPure XP beads (Beckman). The quality of all performed cDNA replicates was validated by Agilent 2100 Bioanalyzer and High Sensitivity DNA Kit (Agilent, Fig 16B,C). Final concentration of libraries was 45-60 ng/µL, resulting in 200-260 nM of material, available for further RNA-sequencing on Illumina platform.

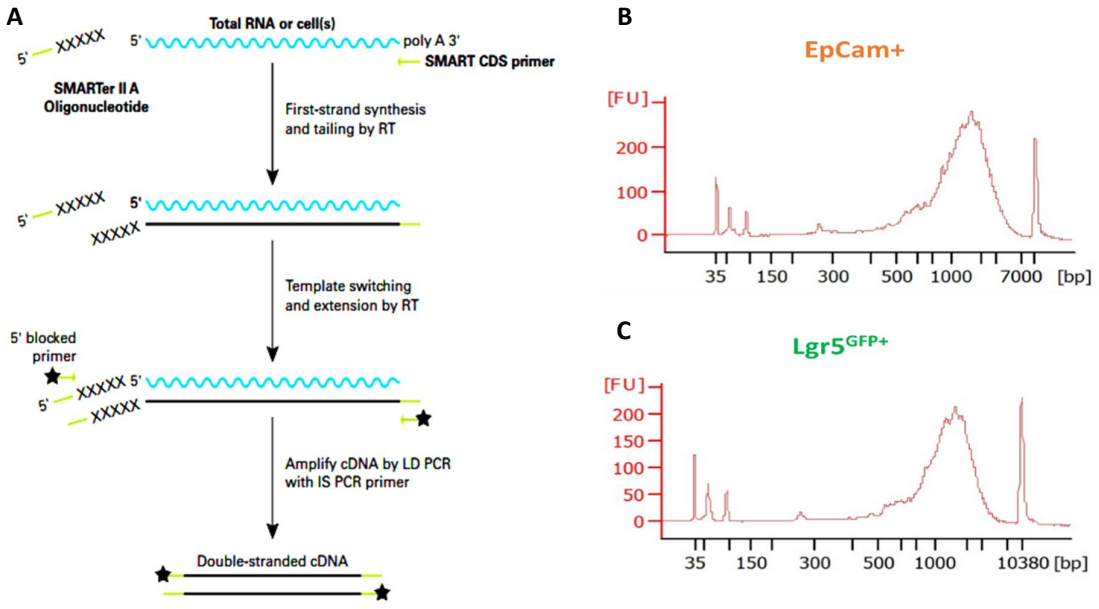

Figure 16. Embryonic E13.5 intestinal cells preparation for further RNA-sequencing analysis. A. Schematic strategy for ds cDNA libraries preparation using SMART-Seq v4 Ultra Low Input RNA Kit (Clontech protocol overview). **B-C**. Quality of the cDNA samples from EpCam^{+} (**B**) and Lgr5^{GFP+} (C) cell populations, measured by Bioanalyzer (Agilent) is showing that the libraries are not contaminated or degraded and optimal for further Illumina sequencing.

The gene expression analysis (by S. Sayols, IMB) of EpCam$^+$ and Lgr5$^+$ populations transcriptome data revealed more than 500 differently expressed genes (log2FC Ó 0.5, FDR < 0.01). The molecular signatures of both cell populations can be visible at the genome-wide level, by establishing pairwise comparison of transcriptional changes between EpCam$^+$ and Lgr5$^+$ cells (Fig.17). Isolated Lgr5$^+$ population was indeed enriched for *Lgr5*, which is normally uniquely expressed in stem cells (Fig. 18B; Schuijers, 2012). Remarkably, many intestinal stem cell markers were increased only in Lgr5+ cells already at E13.5, but not in EpCam+ population. These markers belong to a classical adult ISCs ñmolecular signatureò (described in chapter 3.2): *Lgr5* receptor, *Ascl2* transcription factor, *Smoc2* matricellular protein, *Tnfrsf19* receptor, *CD44* and several Wnt/b-catenin dependent genes (Fig. 17A). Conversely, EpCam+ cells demonstrated an up-regulation of genes, involved either in Wnt signalling inhibition processes (Fig. 18A) or in terminal differentiation of enterocytes. Thus, the transcriptional activity of *Fabp1/2* genes, producing intestinal fatty acid-binding proteins in adult enterocytes, as well as amino-peptidase enzyme (encoded by *Anpep*), a classical marker of enterocyte brush border, were detected only in EpCam+ cells and absent in Lgr5+ cells (Fig. 17A). Among other genes, typically abundantly expressed in mature enterocytes as transport proteins or metabolic enzymes (*Cyp2c65*, *Slc2a3, St8sia3*, *Rbp2*), we also detected an increased transcription of *Gata4* transcription factor in EpCam+ population. Deletion of *Gata4* affects lipid metabolism in enterocytes and causes impaired villi development due to changes in enterocyte gene expression program (Battle, 2008). More importantly, in contrast to Lgr5+ cells, EpCam+ samples were expressing a Wnt antagonistï *Sfrp5* gene. Of note, not all ñclassicalò adult stem cell markers were found expressed in early Lgr5+ population: embryonic gut is missing *Tcf4*, *Lrig1*, *Nr2e3*, *Prom1* etc. I confirmed the data obtained from RNA-sequencing by quantitative RT-PCR (Fig. 17B). DE-genes, detected in control EpCam+ cells (*Sfrp5, Onecut2, St8sia3*), were not expressed in Lgr5+ cells, whereas Wnt-responsive genes were upregulated in Lgr5+ samples. Altogether, I assume that E13.5 Lgr5+ cells just started to activate their ñstemnessò program and keeping many embryonic endodermal stage-specific genes expression (such as *Shh*, *Foxa2*, *Cdx2*, *Id2*). In general, the differences in gene expression between EpCam+ and Lgr5+ cells were maximum 4-5 fold.

Figure 17 - *Legend for the next page*. Results of RNA-sequencing for E13.5 intestinal Lgr5+ and EpCam+ cells. A. Bioinformatical analysis, illustrating gene expression profiles of Lgr5+ (x-axis) and EpCAM+ (y-axis) cells. Green ï the genes, significantly upregulated in Lgr5+ compared to EpCAM+ cells, orange - the genes, significantly upregulated in EpCAM+ compared to Lgr5+ cells (log2FC Ó 1, FDR < 0.01). **B.** qPCR data confirm the results of DE genes, shown by RNA-seq. Normalization control- *EpCam.* **C, D.** Screenshot from the UCSC genome browser showing transcription of *Sfrp5* (C) and *Lgr5* (D) genes in Lgr5+ and EpCam+ cells.

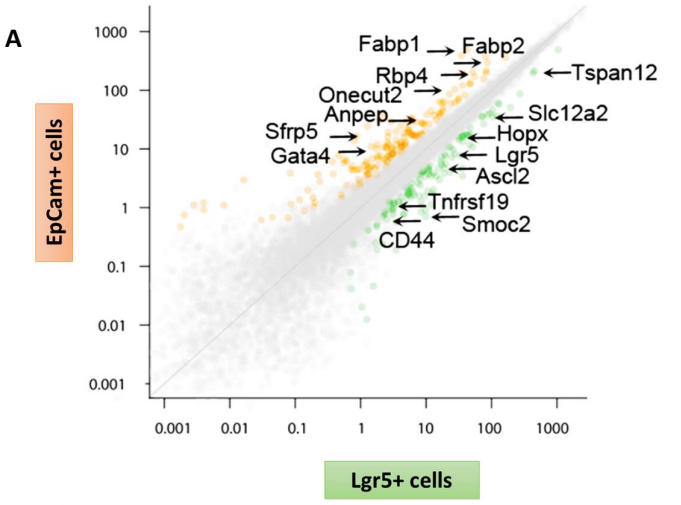
A
EpCam+ cells
Lgr5+ cells
Fabp1
Fabp2
Rbp4
Tspan12
Onecut2
Anpep
Slc12a2
Sfrp5
Hopx
Gata4
Lgr5
Ascl2
Tnfrsf19
Smoc2
CD44
1000
100
10
1
0.1
0.01
0.001

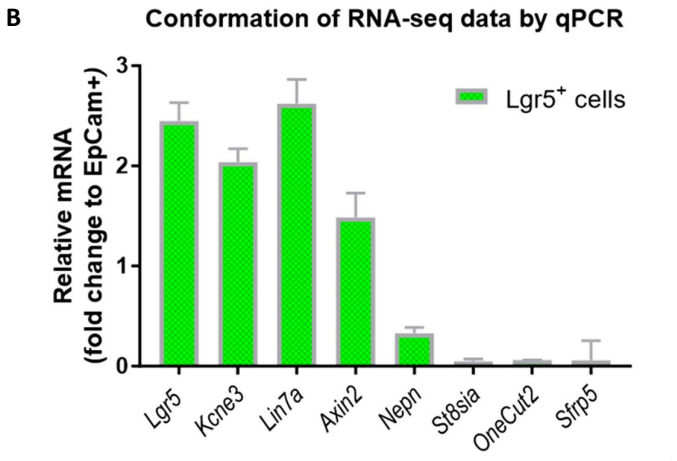
B
Conformation of RNA-seq data by qPCR
Relative mRNA (fold change to EpCam+)
Lgr5+ cells
Lgr5
Kcne3
Lin7a
Axin2
Nepn
St8sia
OneCut2
Sfrp5

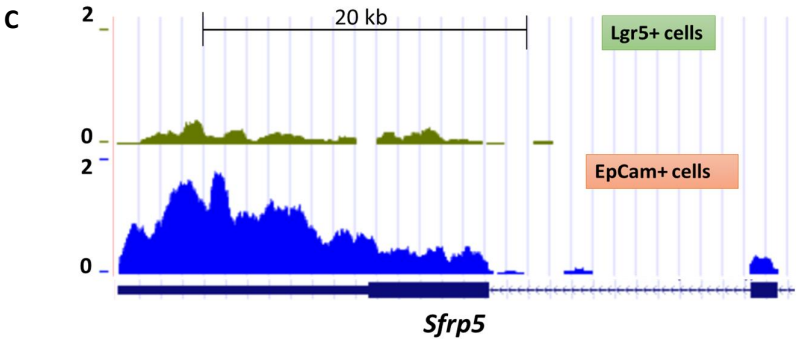
C
20 kb
Lgr5+ cells
EpCam+ cells
Sfrp5

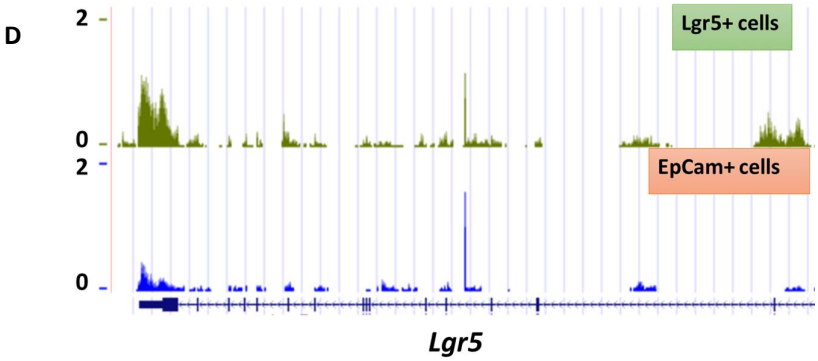
D
Lgr5+ cells
EpCam+ cells
Lgr5

5.2.3. Clonogenic capacity of embryonic intestinal cells *ex vivo*.

The *ex vivo* culture system described by Sato *et al.* (2009) allows propagation of so-called mini-gut organoid structures with all differentiated cell types when adult Lgr5+ ISCs are used as a starting material. I modified this protocol for culturing of embryonic small intestinal cells. Briefly, intestines from $Lgr5^{GFP+}$ embryos were dissected at E13.5, epithelial cells were sorted by FACS using pan-endodermal EpCAM marker and put into a Matrigel drop with medium on top. In such conditions these cells can grow in three dimensions (3D) and form organoids with adult intestinal stem cells. When E13.5 intestine was used, I observed that after 5 days in culture, in addition to adult-type organoids (Fig. 18A-C), a proportion of hollow spheres (further as *spheroids*) was generated (Fig. 18E-F). Although morphologically spheroid has a form of a gigantic cell (Fig. 18E), it is composed of hundreds of actively-proliferating cells inside. I could observe their high proliferation activity by anti-Ki67 immunostaining. During the first week after seeding of the cells, spheroids continued to grow in diameter and didnôt show any signs of differentiation. However, a drastic remodeling of spheroids starts after 1 week in culture. During their development, spheroids lose volume, become flat and differentiate into organoid-like structures at day 10 (Fig. 18F, 20A).

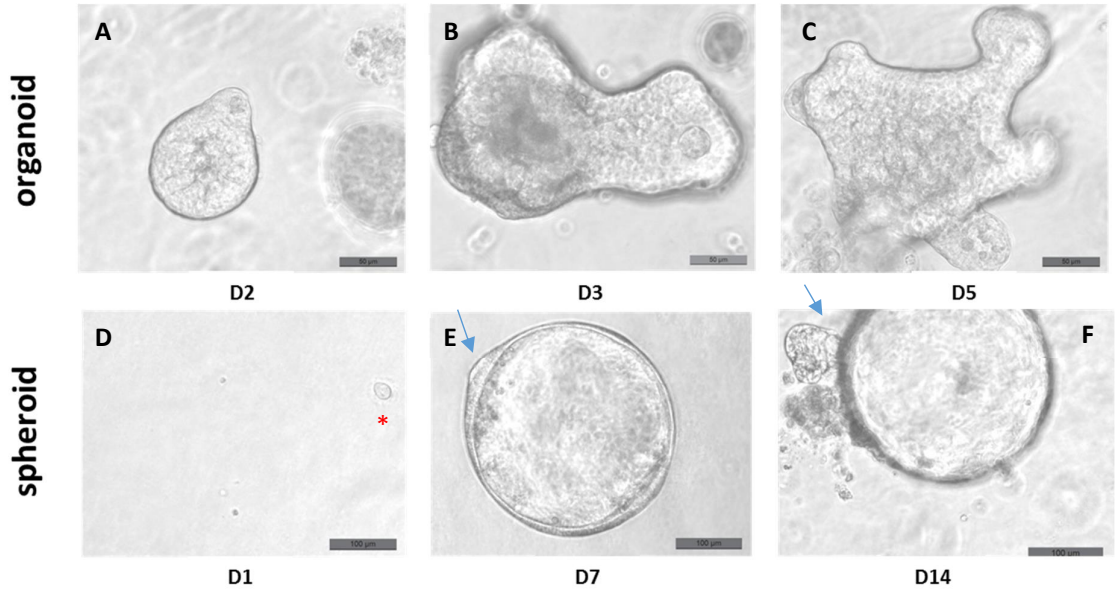

Figure 18. Clonogenic capacity of E13.5 intestinal epithelial cells, grown as *ex vivo* culture. A-C. Organoid formation takes place already after a few days in culture. **D-F.** Some of embryonic cells donôt become organoids immediately, but form so-called spheroid **(E),** where actively proliferating cells remain undifferentiated until day 7-10. After approximately 10 days in culture spheroids give rise to organoids. Arrow shows where the very first differentiation processes are activated. Scale bar, 100µm. D ï amount of days in culture.

Interestingly, the timing of such maturation could be controlled by concentration of the Wnt signaling growth factor - R-spondin, added to intestinal medium. Cells, starving for R-spondin-1, could not form organoids and were halted as spheroids. Independently, such phenomena were reported by two other research groups (Mustata, 2013; Fordham, 2013), when fetal intestinal cells formed spheroids which didnôt require R-spondin or Wnt ligands for its maintenance in cell culture.

Within one week mature organoids with Lgr5^{GFP+} ISCs, interspersed between granular Paneth cells, could be easily recognized by fluorescence microscopy (Fig. 19). I next examined the terminal differentiation of embryonic cells into intestinal cells *ex vivo*. I wondered whether organoids and spheroids at day 8, when they formed mini-gut-like structures, gave rise to all four intestinal cell types (Fig. 20A). Due to a very small size of the organoids, I had first to established conditions for harvesting, fixation, sectioning and immunostaining. Indeed, histological analysis of organoids showed lysozyme-positive Paneth cells, chromogranin A-positive enteroendocrine cells, alkaline phosphatase-positive enterocytes as well as PAS-stained Goblet cells (Fig.20B, lowest panel). Importantly, I identified only three intestinal cell types on spheroids sections, such as enterocytes, Goblet and enteroendocrine cells, but not Paneth cells (Fig.20B, upper panel)

Altogether, this suggests a conversion of spheroid-like structures into mini-gut organoids according to embryonic program of intestinal cells differentiation. Goblet and enterocytes could be observed already at E15.5 in new-formed villi, whereas Paneth cells appear only 3 weeks later, at stage P7-14, when crypt compartment with adult ISCs is established.

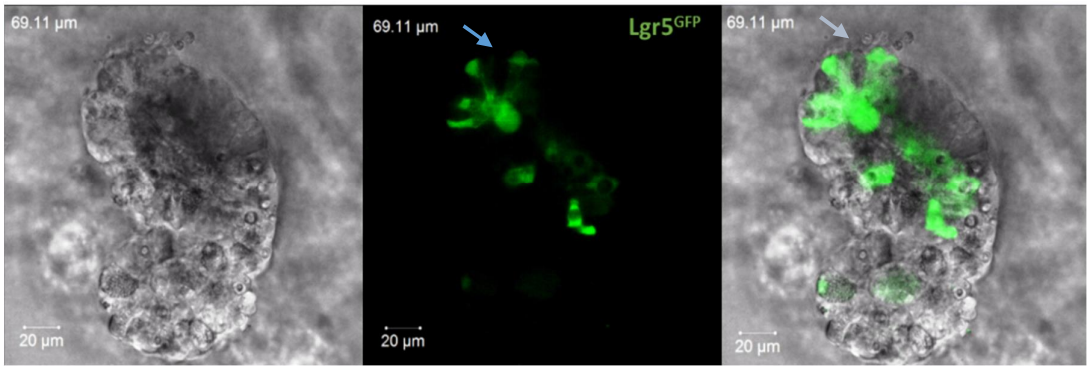

Figure 19. Microscopic analysis of Lgr5^{GFP+} organoid, derived from E13.5 plated cells. Blue arrow indicates a proper localization of a granular Paneth cell. A limited number of GFP+ ISCs is responsible for self-renewal and differentiation into absorptive or secretory cell lineages.

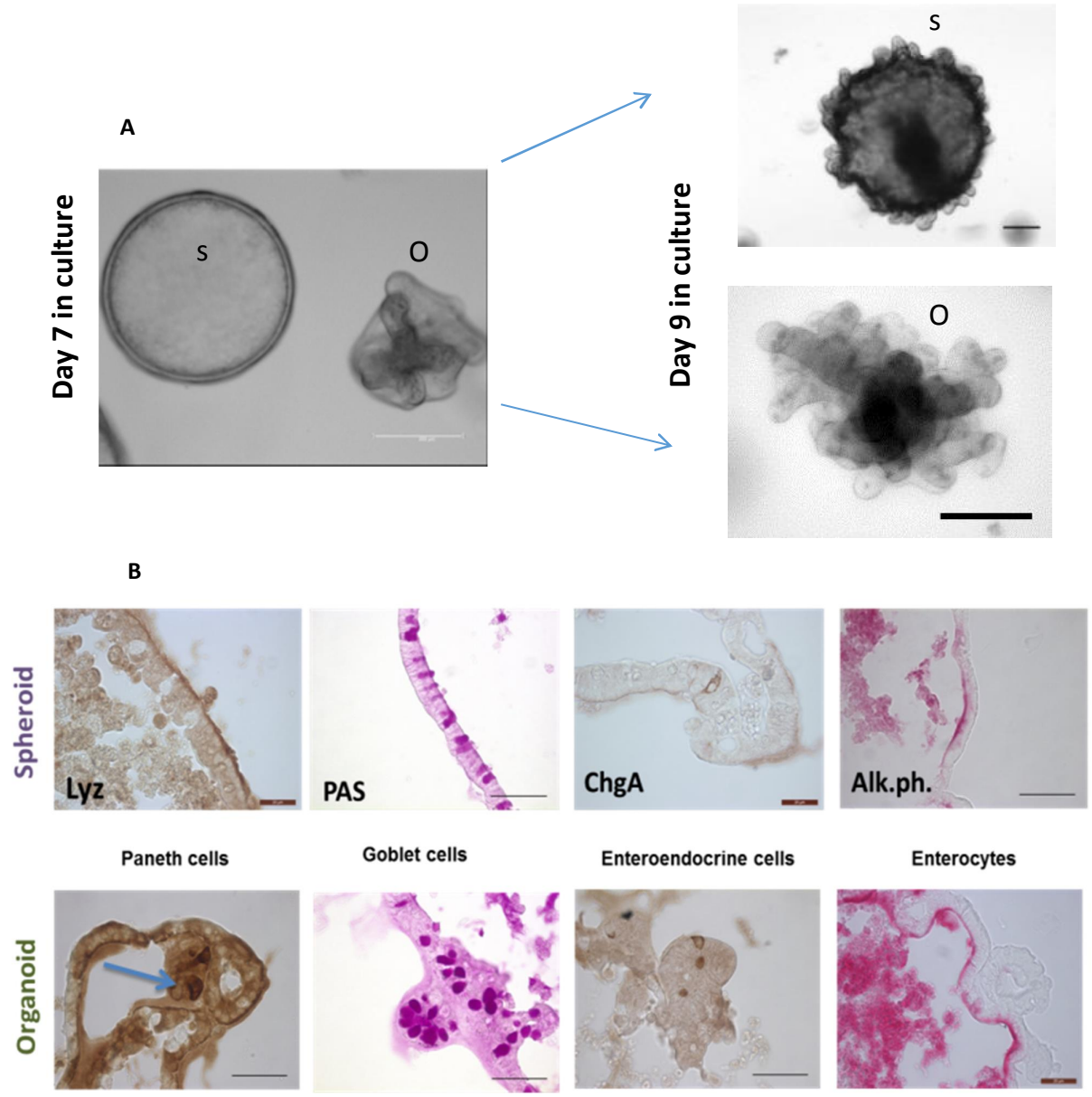

Figure 20. Embryonic intestinal organoid/spheroid culture from endodermal epithelial cells sorted at E13.5. A. Development of E13.5 isolated single endodermal cells into hollow sphere(S) and organoids (O). Both structures efficiently form mini-gut organoids after 7-9 days. Scale bar, 1mm and 200µm. **B.** Immunostaining analysis of grown organoids harvested at day 8 showed expression of all 4 intestinal cell types markers: lysozyme in Paneth cell, chromogranin A in enteroendocrine cells, alkaline phosphatase in enterocytes and PAS-stained Goblet cells. Spheroids collected from the same stage had no Paneth cells.

5.2.4. Clonogenic capacity of E13.5 Lgr5^{+} and Lgr5^{-} embryonic intestinal cells *ex vivo*.

Using the method, which I have successfully established for embryonic intestinal cells growth *ex vivo*, I decided to compare a clonogenic potential of EpCam^{+}Lgr5^{-} and EpCam^{+}Lgr5^{+} cells isolated at E13.5 and grown in cell culture. I sorted *Epcam^{+}Lgr5-eGFP^{high}* (Lgr5^{+}) vs. *Epcam^{+}Lgr5-eGFP^{-}* cells (control Lgr5^{-}), as described in chapter 5.2.2. The cells were sorted by FACS at density 500 cells/well and plated with adding of all growth factors (R-spo, Noggin, EGF), required for adult cell culture. Because the embryonic samples, dissociated to single cells undergo dissociation-induced apoptosis (anoikis), I added a Rho-associated kinase (ROCK) inhibitor Y-27632 to the medium. The protective ability of Y-27632 enables sorted cells to survive better and increase their cloning efficiency.

Figure 21 illustrates the growth of intestinal organoids and spheroids from EpCam^{+} (Lgr5^{-}) and Lgr5+ cell populations isolated at E13.5. After a few days in cell culture, EpCam+ cells started to form spheroids (Fig.21B), while the proliferation activity of Lgr5+ cells remain mostly unchanged (Fig. 21A). By 8 days of culture, I observed that both Lgr5+ and EpCam+ populations have a capacity to develop organoids and spheroids. However, a comprehensive analysis and calculations were constrained by the fact that Lgr5+ cells gave rise to at least 2-time smaller organoids/spheroids by their size. Notably, Lgr5+ cell ï formed organoids could not survive in a long-term experiment (>10 days), whereas EpCam+ population developed normal-sized organoids/spheroids. Altogether, the lower clonogenic potential was shown for Lgr5+ cells (Fig. 21C) - 0,4% for organoids and 0,2% for spheroids, for totally 20.000 cells sorted. These data indicate that at stage E13.5 EpCam+ and Lgr5+ has different potency to grow and give rise to their progenies.

Based on results of RNA *in situ* hybridization and genome-wide transcriptional profile, here I show that at E13.5 only a subset of epithelial cells express *Lgr5*, however these cells do not have a high clonogenic potential.

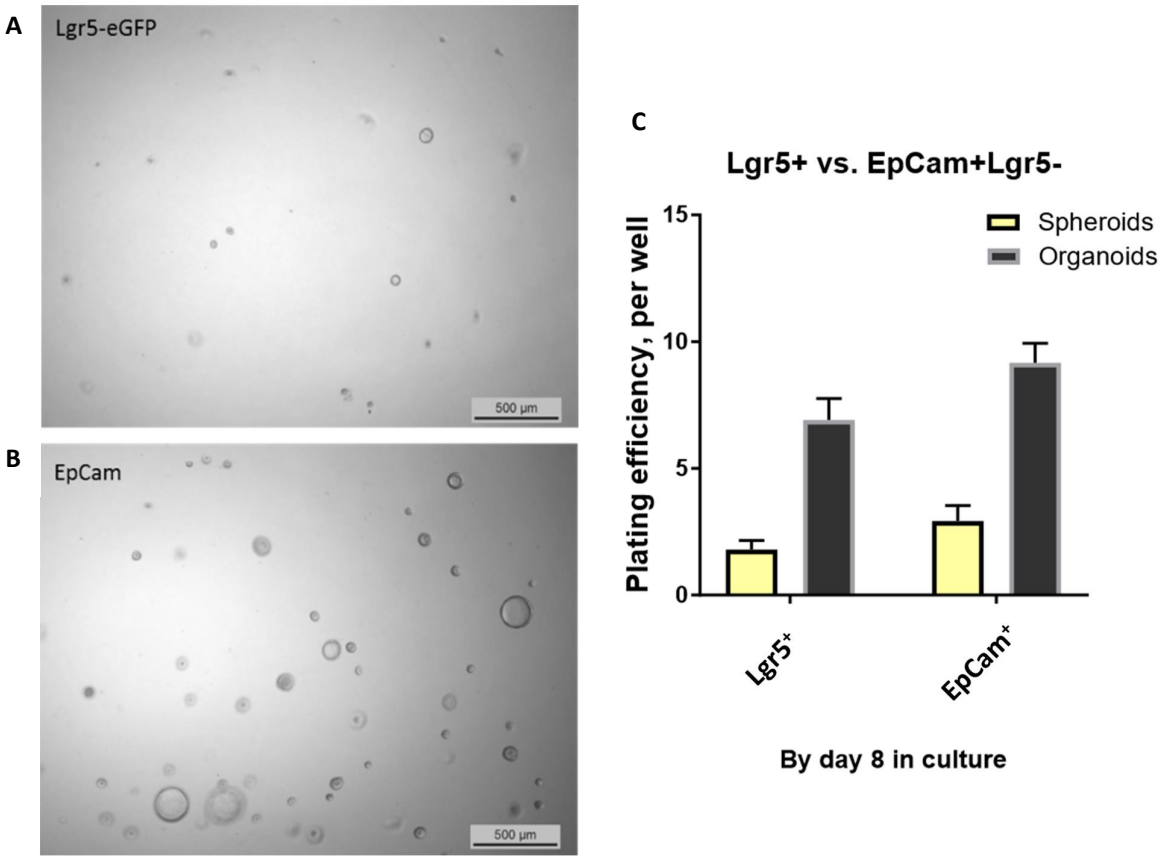

Figure 21. Clonogenic capacity of E13.5 sorted intestinal cells. Live phase-contrast imaging of Lgr5+ (**A**) and EpCam+ (**B**) cells grown for 5 days *ex vivo*. **C.** Average number of organoids/spheroids per well by the end of the time course (8 days) of the experiment. Cells were grown in duplicates for each biological replicate. Mean ±SEM; nÓ40; scale bar, 500µm.

5.3. Id2 as an endodermal marker of embryonic intestine.

5.3.1. Id2+ embryonic cells labelling using *Rosa*$^{tdTomato/eGFP}$ reporter system.

We attempted to design an experiment, where I would be able to visualize the heterogeneity of the intestinal epithelium, starting within the embryonic gut tube. We suggested that formation of the first Lgr5+ISCs precursors and subsequent cellular heterogeneity in the embryonic intestinal epithelium could take place after E11.5 by the following reasons: 1) our previous genome-wide chromatin data from E12.5 gut (Kazakevich, 2017) showed the presence of active histone marks on intestinal stem cell marker genes; 2) we detected first Lgr5-expressing cells at E12.5.

In order to provide a comprehensive expression profile in the small intestine, our lab collected sections of mouse embryonic stages, starting from E7.5 and performed numerous RNA *in situ* hybridization assays. Together we examined the expression of different signaling genes, such as *Shh*, *HNFa*, *Id1-Id3*, *Foxa2*, *TCF*s, *sRFP*s, *FGFs*, *LRPs* in embryonic gut tube (E7.5-E18.5) and in adult villi-crypt units (P60). Among those *Shh* and *Id*2 were expressed ubiquitously along embryonic intestinal axis (Fig. 12B, 22A). Accordingly, previous studies on embryonic intestine showed that the listed genes could be used as endodermal markers during the gut development (link). RNA-seq data for E13.5 stage (chapter 5.2.2) has evidenced a high transcriptional activity of *Id2* gene for both Lgr5^{+} and Lgr5^{-} cell populations (Fig. 22D).

Id2 gene encodes **i**nhibitor of **d**ifferentiation and is a target of Wnt/BMP signaling pathways. Id proteins regulate cell growth, cell fate determination and differentiation in stem cells and their progenitors during development and adult life (Lasorella, 2014). In mouse, *Id2* is highly expressed in the small intestine starting from E9.5-10.5, this gene product is abundant in both epithelia and mesenchyme (Fig.22A), but at late embryogenesis (E15.5-E17.5) its transcriptional activity significantly decreases. We did not detect *Id2* expression in adult intestine (Fig.22 B, C). Thus, we decided to select this gene as a ubiquitously expressed endodermal marker.

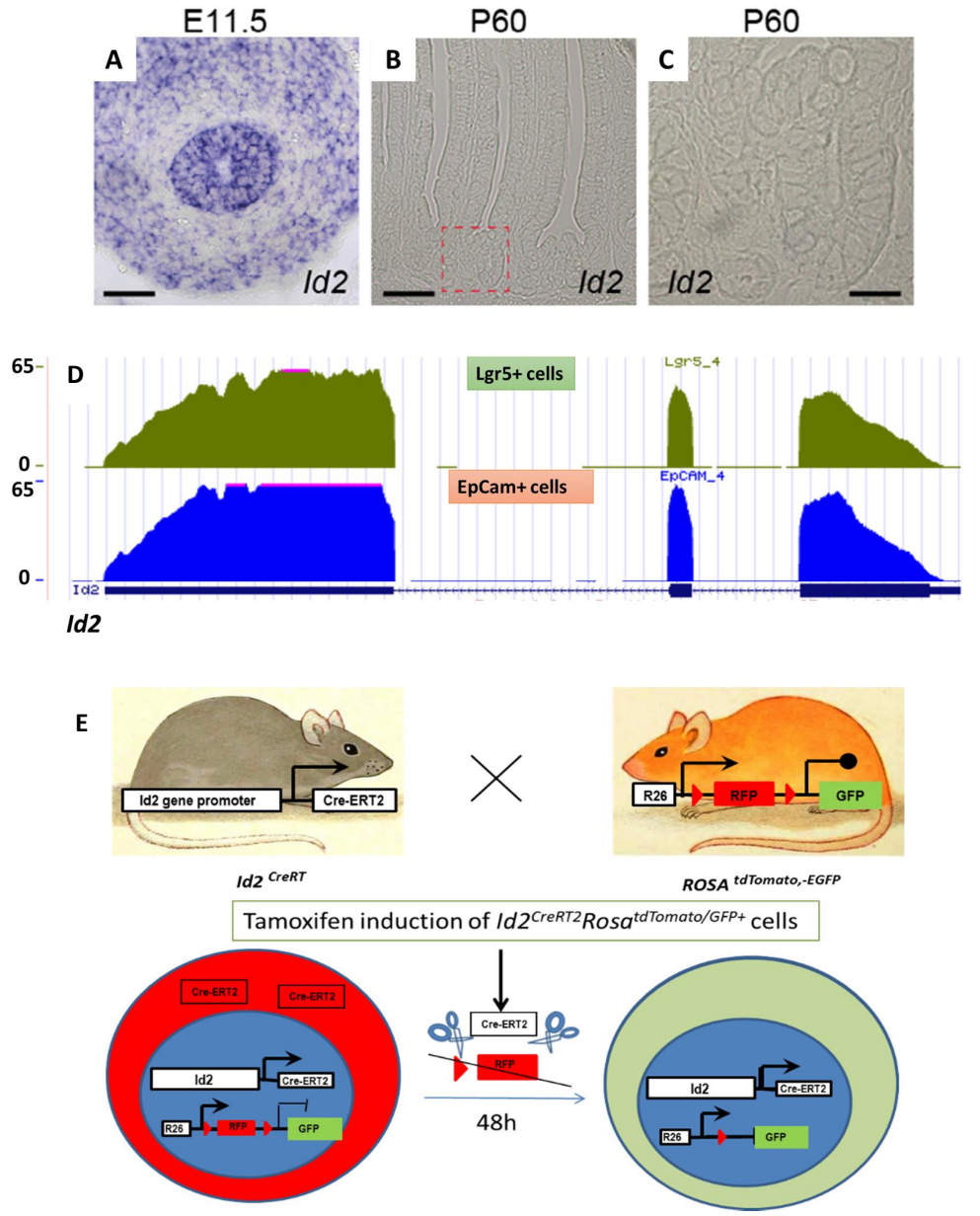

Figure 22. Expression of *Id2* gene in mouse small intestine. A-C. *Resuts and images are provided by M. Dzama and Dr. N. Soshnikova. In situ* hybridization performed on the small intestine reveals a high expression of *Id2* at E11.5 **(A)** and absence of *Id2* gene in adult epithelium: villi (**B**) or crypts (**C**). **D.** Screenshot from the UCSC genome browser showing transcription of *Id2* gene in Lgr5+ and EpCam+ cells. **E**. *Rosa*$^{(tdTomato;-eGFP)}$ reporter mouse cross with *Id2*^{CreRT}-mouse strain. Tamoxifen injection induces cell-specific Cre recombinase to cut loxP-flanked Tomato cassette that GFP gene constructed downstream starts to be expressed. All cells, expressing Cre at time point of Tamoxifen administration, will become GFP positive. Proliferation of GFP cells allows observing labelled progenies fate.

To identify putative Wnt-responsive Lgr5+ progenitors at E11.5, I decided to analyze the dynamics of cell population(s) within the actively growing epithelium. My interest were the following questions: 1) where first Lgr5+ cells come from? 2) is there any cell fate destiny at E11.5? Importantly, the addressed questions required to work on the animal level because the cellular complexity cannot be fully recapitulated *ex vivo.* To analyze the whole intestinal epithelium cells at E11.5, I needed an experimental strategy, where all intestinal epithelial cells would be labelled and manipulated *in vivo*. In this case, the mouse strain should contain a system with an embryonic intestine-specific chemically inducible promotor. For instant, Tamoxifen-inducible promotor, regulating Cre recombinase activity, should not be expressed globally, but in an intestinal epithelia-specific manner. Based on our previous *in situ* and RNA-seq data, *Id2* knock-in inducible reporter mouse, available for crosses, have been selected.

In this study, I aimed to analyze the proliferation activity of E11.5 intestinal cells by using lineage-tracing approach. The whole intestinal epithelium, positive for *Id*2 gene marker, would express Cre-recombinase under *Id*2 gene promotor (Fig.22E). When bred to $Rosa^{tdTomato/eGFP}$ reporter mouse, resulted $Id2^{Cre}Rosa^{tdTomato/eGFP}$ embryos after Tamoxifen administration will lose their red cassette (*tdTomato*) in all intestinal cells and become GFP^{+} forever (Fig.22E). In case when the whole epithelium is dividing at the same speed, I suggested, that after 3-5 days of tracing, I would detect the simultaneous shift of red $Id2^{Cre/+Tomato}$ cells into green $Id2^{Cre+GFP+}$ cells (Fig. 23A). If there is a subpopulation of cells, that doesnôt proliferate actively, I would see the intermediate yellow transient state cells by FACS.

$Id2^{Cre/+}Rosa^{tdTomato/eGFP}$ and control $Id2^{+/+}Rosa^{tdTomato/eGFP}$ embryos were injected with Tam at E11.5 and analyzed 1 and 2 days after Cre recombinase induction. When followed from E11.5 to E12.5, we observed only 3,3% of $Id2^{Cre}$ traced cells. Two days after tamoxifen injection, 5-7% of the *Id2*+ epithelial cells were labelled within the embryonic gut tube (Fig.23A). Unfortunately, this system demonstrated a very low labelling efficiency of *Id2*-expressing cells, since I was not able to trace 100% of epithelial cells. Remarkably, the desired level of Tam induction is difficult to control *in vivo*, it results mosaic expression of the Cre recombinase and subsequent GFP expression only in $Id2^{high+}$ population (as $Id2^{high\ Cre+}$ GFP+). Thus, tracing of $Id2^{Cre}/Rosa^{tdTomato/eGFP}$ cells couldnôt fully represent the whole gut development dynamics. Nevertheless, this experiment allowed to visualize a very interesting phenomenon: within 2 days after Tam administration, an ñintermediateò cell population ($Id2^{lowCre+,\ yellow}$) between highly proliferating $Id2^{Cre/GFP+}$ cells and not labelled $Id2^{low\ Cre+}$ Tomato cells was identified (Fig.23A). Most likely, this population has a lower proliferation activity: although the Tomato cassette was excised and GFP expression started, a certain amount of Tomato gene product gives a relatively high level of red fluorescent signal.

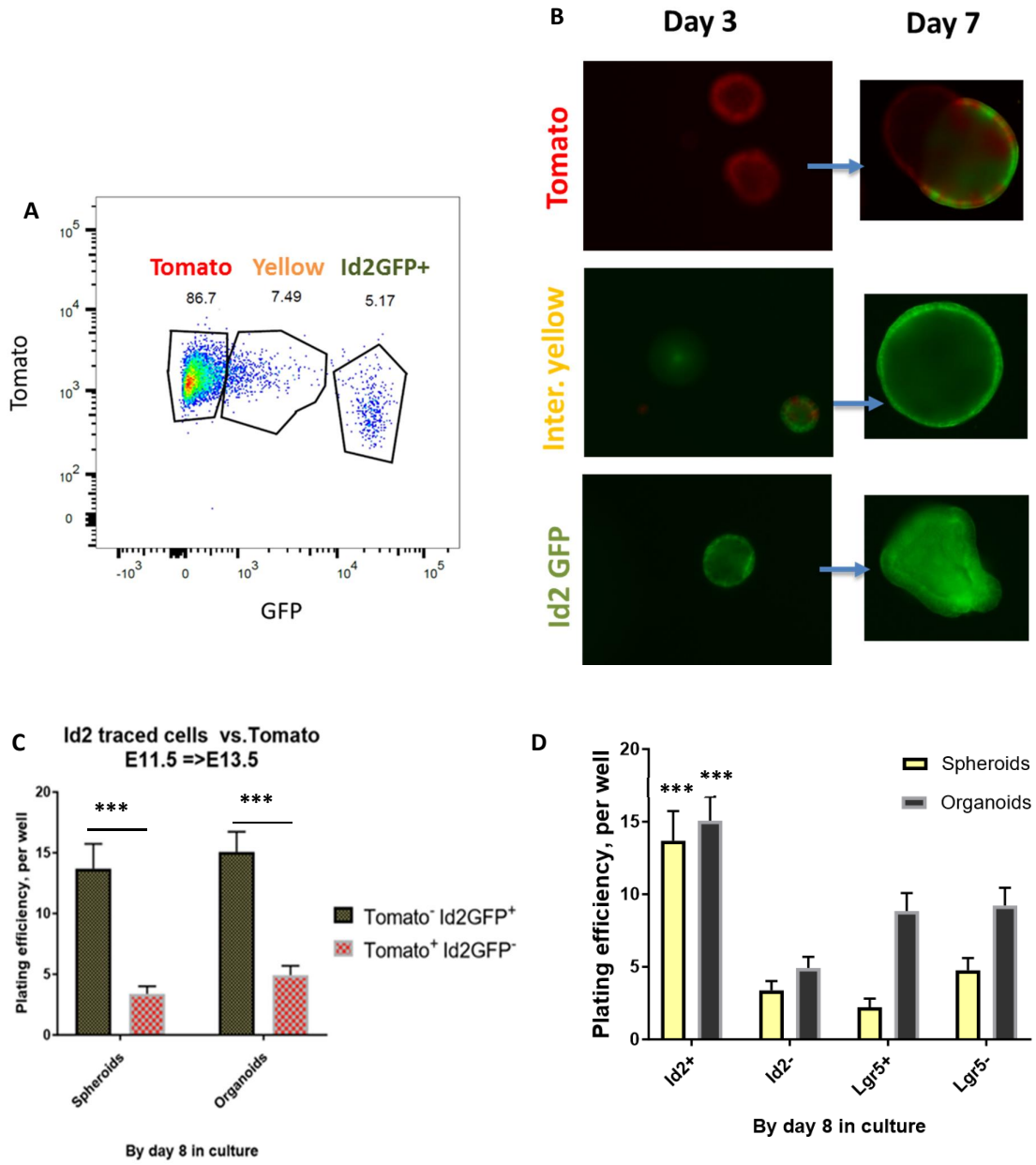

Figure 23. Id2$^{high\ Cre+}$ cells is a distinct cell population within embryonic gut epithelium. A. *Id2*^{CreRT}*/Rosa*$^{(tdTomato;-eGFP)}$ mouse embryo, analyzed by FACS after 2 days of Tam-induced lineage tracing. Discrete populations of unlabeled (Tomato), slowly-proliferating Id2$^{lowCre+}$ (Yellow) and fast-proliferating Id2$^{high\ Cre+}$ (Id2GFP+) are depicted. **B**. Proliferation activity of E13.5 isolated cell populations *ex vivo* at day 3 and day 5. Of note, unlabeled Tomato cells started to express GFP cassette by day 7, thus showing a basal activity of Id2Cre-mediated excision of *Tomato* gene. **C**. Quantification of organoids/spheroids number, formed from Id2^{GFP+} and Tomato^{+}Id2^{GFP-} cells *ex vivo*. **D**. Clonogenic capacity of all 4 sorted cell types: Id2^{+}, Id2^{-} (from *Id2*^{CreRT}*/Rosa*$^{(tdTomato;-eGFP)}$ lineage tracing) and Lgr5^{+}, EpCam^{+}Lgr5^{-} (from *Lgr5*$^{GFP+/-}$ embryo). Mean ±SEM; nÓ40; ***p<0.001, paired t-test.

Next I decided to collect Id2$^{low\ Cre+}$ Tomato/ Id2^{intermediate}/ Id2$^{high\ Cre+}$ GFP+ cells cells and compare their functional properties. Thus, 500 cells from embryonic Id2+ cells (Id2^{intermediate} and Id2+GFP), traced from E11.5 to E13.5 were grown in 3D culture, as well as not labelled Tomato (Id2$^{low\ Cre+}$ Tomato) cells. Whereas at day3 of cell culture I did not observe significant changes in growth, by day 7 I detected that the expression of GFP also takes place in slowly dividing Tomato cells (Fig.23B). Altogether, this data confirm that Tam-induced recombination can not be activated simultaneously in all cells. Furthermore, Id2$^{high\ Cre+}$ GFP+ population, grown in culture, showed at least three time higher clonogenic potential *ex vivo* (Fig. 23C). The amount of spheroids and organoids, formed from Lgr5+ and EpCam+Lgr5- was significantly low, comparing to Id2$^{high\ Cre+}$ GFP+ population (Fig. 23C; nÓ40).

Next I calculated the growing potency of all populations and compared them to Lgr5GFP+ and control EpCam+ from E13.5 without tracing. As shown in Fig 23D, within the embryonic intestinal epithelium there is a subpopulation of Id2$^{high\ Cre+}$ cells, which proliferates faster and has the highest clonogenic capacity *in vivo* (FACS) and *ex vivo*. Alternatively, heterozygosity in *Id2* gene might give an advantage in cell cycle and differentiation capacity of plated cells.

I wanted to re-evaluate our *Id2* lineage tracing approach by using two other reporter mice- *Rosa*$^{Stop/tdTomato}$, where all *Id2*+ labelled cells will become red upon Tam-induced excision of stop cassette, and *Rosa*$^{Stop/LacZ}$, where all labelled blue cells will be visible without fluorescent microscopy.

5.3.2. Id2+ embryonic cells labelling using RosaStop/LacZ reporter system.

Id2$^{Cre/+}$/ *Rosa*$^{Stop/LacZ}$ embryos, Tam-induced from E11.5, were analyzed at E15.5 ï timing of active remodeling processes in the gut tube. I used *Id2*$^{Cre/+}$*Rosa*$^{+/+}$ as well as *Lgr5*$^{Cre/+}$ /*Rosa*^{LacZ} embryos as negative controls. As seen on Fig. 24A, Id2$^{high\ Cre+}$ cells were labelled, however the labelling efficiency was still moderate. As expected, Tam-labelling of Lgr5Cre-expressing cells didnôt show any traced cells, because at E11.5 there was no Lgr5 gene transcriptional activity (Fig. 24B). Together with M.Dzama and Dr. N.Soshnikova we could examine the cell fate of Id2$^{high\ Cre+}$ cells *in vivo* by Tam labelling of mouse embryos at stages E9.5, E11.5, E13.5, E15.5 followed until adult stages (Fig. 24C-F). Our lineage tracing analysis demonstrates a numerous amount of Id2^{LacZ+} blue clones within adult small intestine after 2 month of tracing (Fig 24C). In adult gut epithelium LacZ+ signal was confined to crypt-villi units, corresponding to the localization of ISCs, TA cells and all differentiated intestinal cells. Further immunostaining against adult intestinal cell markers confirmed a presence of all cell types, originated from Id2^{Cre+}LacZ+ cells (Fig.24G-I).

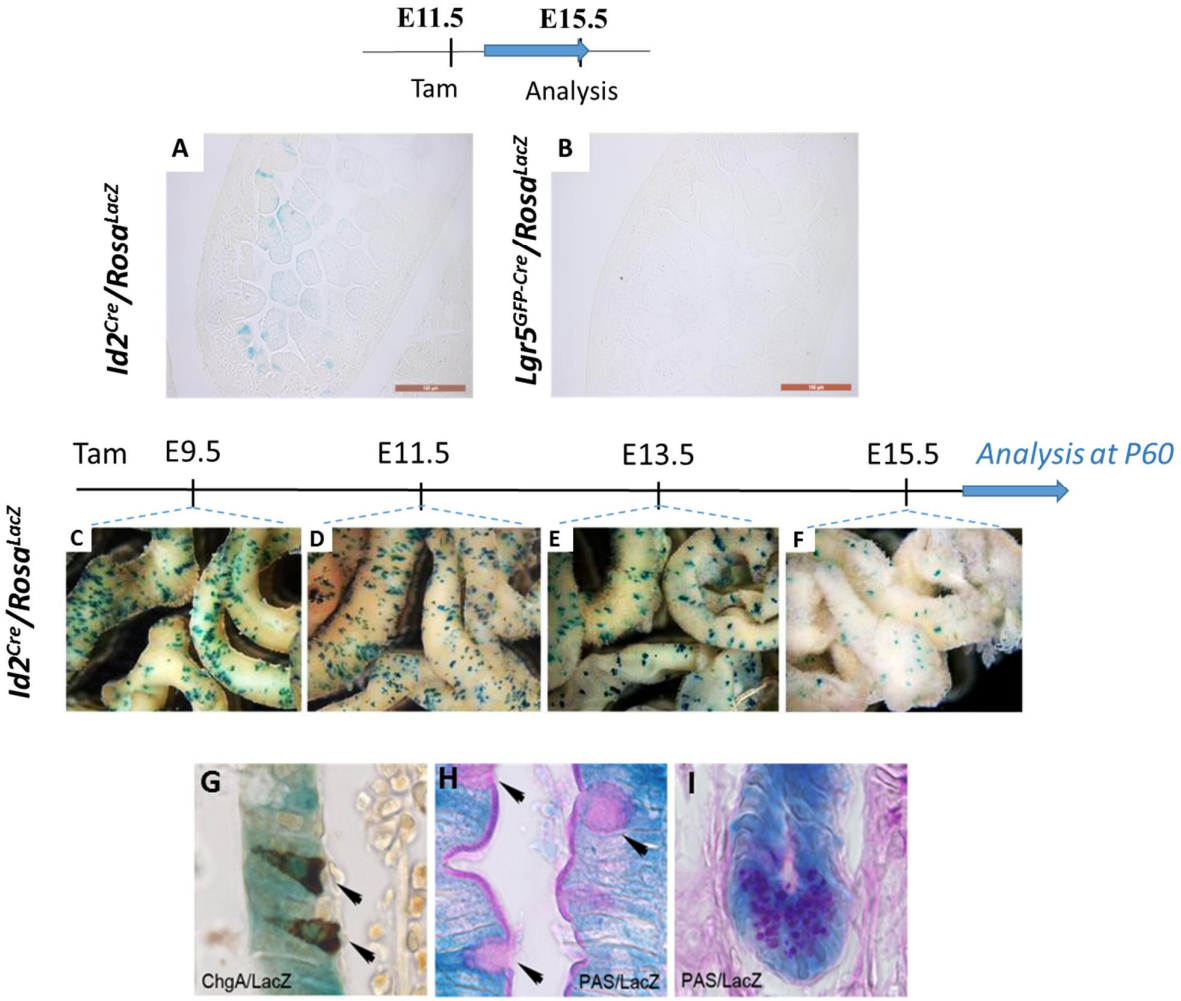

Figure 24. Id2+ progenies give rise to future ISCs pool. **A-B**. Tam-induced cell lineage tracing of $Id2^{Cre/+}/Rosa^{LacZ}$ (**A**) and $Lgr5^{Cre/+}/Rosa^{LacZ}$ embryos (**B**) injected at E11.5 and analyzed at E15.5. **C-F**. Tam-induced cell lineage tracing of $Id2^{Cre/+}/Rosa^{LacZ}$ adult mice, injected at E9.5 (**C**), E11.5(**D**), E13.5 (**E**) and E15.5 (**F**) and analyzed at P60 (*results and images provided by M.Dzama and N.Soshnikova*). **G-I** Histological analysis of $Id2^{Cre+}$ lineage tracing sections revealed, that $LacZ^{+}$ blue cells are not only enterocytes, but also chromogranin A positive enteroendocrine cells (**G**, arrow), PAS-staining positive Goblet (**H**, arrow) and Paneth cells (**I**). Scale bar, 500 nm.

5.3.3. Id2+ embryonic cells labelling using *Rosa*$^{Stop/tdTomato}$ reporter system.

High proliferation activity of *Id2*^{high} cells, their ability to contribute to adult ISCs pool *in vivo* as well as fast development *ex vivo*, led me to hypothesize that the very first Lgr5+ ISC progenitors may specify from this distinct cell population. In order to check this idea, an experiment with triple heterozygous cross using *Id2*^{CreRT}, *Lgr5*$^{CreRT\text{-}GFP}$ and *Rosa*$^{Stop/tdTomato}$ mice was designed. I aimed to follow the cell fate of E11.5 Id2$^{highCre+}$ cells by tdTomato label, while Lgr5$^{CreRT\text{-}GFP}$ knock-in cassette would start to be expressed only at E13.5. Co-localization of GFP+ *Lgr5*-expressing cells with labelled Id2^{Tomato} cells would demonstrate that Lgr5+ progenies originate from Id2$^{CreRT+\,high}$ population *in vivo*.

A new *Rosa*$^{Stop/tdTomato}$ reporter mouse has been ordered, since our previous results with using *Rosa*$^{tdTomato/eGFP}$ mouse did not satisfy the planned experiment strategy for two reasons: low labelling efficiency and the presence of eGFP under the ubiquitous Rosa promotor. Further control experiments on *Rosa*^{Cre}/*Rosa*$^{Stop/tdTomato}$ reporter mouse cross demonstrate the sufficient excision of stop cassette followed by Tomato expression (Ó97%), as confirmed after 1 day of Tam injection (Fig. 25A,B).

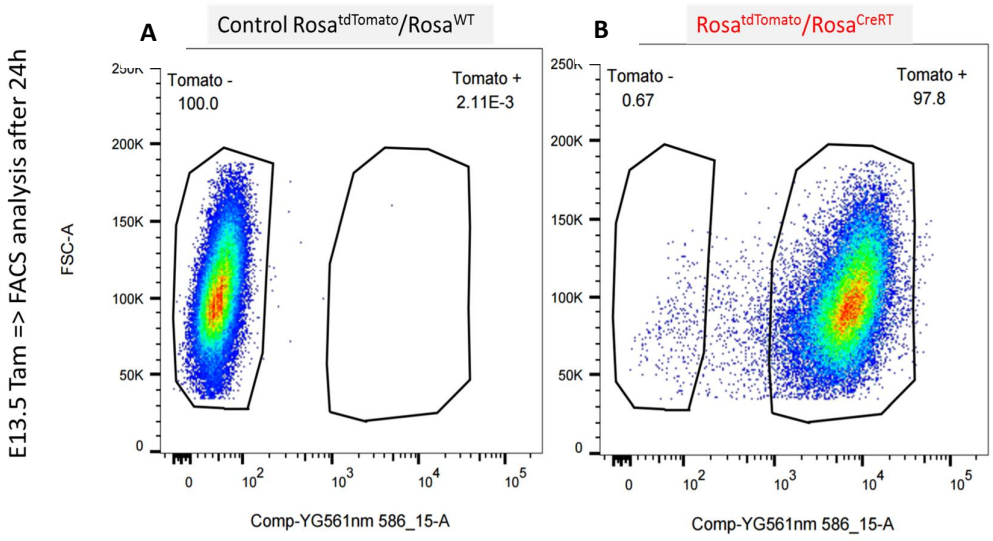

Figure 25. Cell fate labelling efficiency, examined on a control experiment with *Rosa*^{tdTomato} */Rosa*^{Cre} mice cross using FACS analysis.A-B. Lineage tracing of Rosa^{tdTomato}/Rosa^{WT} (**A**) embryo, injected at E13.5 and analyzed after 1 day of Tam induction, doesnôt show any unspecific tdTomato expression (A), whereas >97% cells of *Rosa*^{tdTomato} */Rosa*^{Cre} embryo intestinal epithelium become Tomato+(**B**).

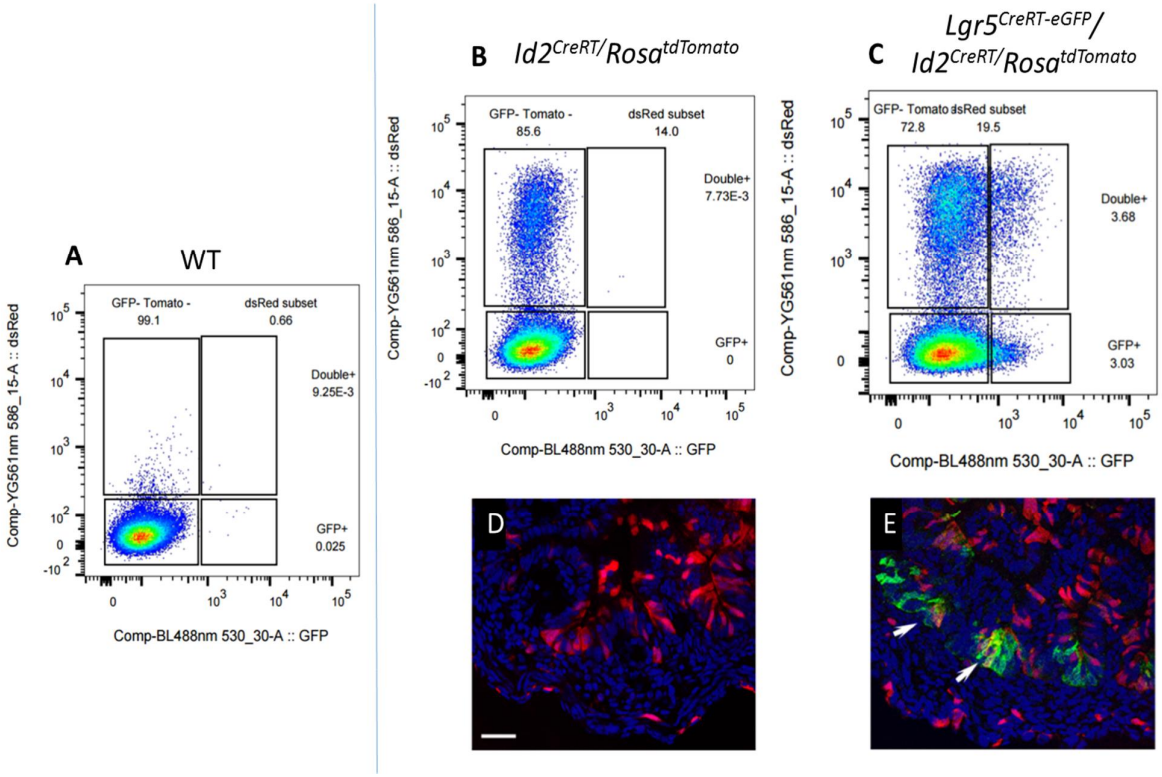

Figure 26. A fraction of Id2+ progenies, labelled at E11.5, is giving rise to E13.5 Lgr5GFP+cells. A. FACS analysis of WT embryos from Tam-injected $Lgr5^{CreGFP/+}$ $Id2^{Cre/+}$ / $Rosa^{tdTomato}$ mouse didnôt reveal unspecific GFP+ or Tomato+ transcriptional activity. **B-C**. FACS plots show an induction of Tomato expression in $Id2^{Cre/+}$ / $Rosa^{tdTomato}$ (**B**), whereas $Lgr5^{CreGFP+}$ /$Id2^{Cre/+}$ / $Rosa^{tdTomato}$ intestine contains a double-positive Tomato+GFP+ cell population, derived from E11.5 *Id2*-expressing cells (**C**). **D-E.**. Immunofluorescent analysis of small intestines from $Id2^{Cre/+}$ / $Rosa^{tdTomato}$ (**D**) and $Lgr5^{CreGFP+}$ /$Id2^{Cre/+}$ / $Rosa^{tdTomato}$ (**E**) sections, stained with anti-GFP antibodies, demonstrates the spatial distribution of Id2+ labelled cells at E15.5. Double-positive $Tomato^{+}Lgr5^{GFP+}$ cell population, derived from $Id2^{Cre+}$ progenies, is located in actively-proliferating intervilli pockets (white arrows). Scale bar, 40 µm, n>3.

In order to check if an increased amount of $Lgr5^{+}$ ISCs originates from $Id2^{highCre+}$ heterozygous progenitors during embryogenesis, I performed a cell lineage tracing on triple mutant $Lgr5^{CreRT-GFP/}Id2^{Cre}/Rosa^{Stop/tdTomato}$ mouse cross at E11.5 and analysed each embryo 2 and 4 days alterï at E13.5 and E15.5, respectively (Fig.26). Of note, labelling with a new $Rosa^{tdTomato}$ reporter was more efficient, the labelling ratio was variegating from 15-20% (for E13.5 analysis) and >25% (for E15.5) of all epithelial cells (instead of 3-6% with $Rosa^{tdTomato;eGFP}$); all Tomato+ cells were detected only in $Id2^{Cre+}/Rosa^{tdTomato}$ embryos, but never in $Lgr5^{CreRT-eGFP}/Rosa^{tdTomato}$. I have measured the amount of $Lgr5^{GFP+}$ cells that was originated from $Id2^{+/-}$ genetical background ($tdTomato^{+}$ labelled). Thus,

labelling of *Lgr5*$^{CreRT\text{-}GFP/}$*Id2*^{Cre}/*Rosa*$^{Stop/tdTomato}$ embryo at E11.5 , analyzed at E13.5, shows that approximately 10% of all *Id2*$^{Cre+}$ /*Rosa*^{tdTomato} gave rise to Lgr5+ progenies (Figure 26C, see Q1 and Q2 quadrants). Summarizing, in our experiment 25-30% of Lgr5^{EGFP+} cells originate from Id2 $^{highCre+}$ population (Fig. 26C, Q2- Q3). When the embryos were analysed prior to villi-intervilli specification at E15.5, I saw that the amount of red labelled *Lgr5*$^{CreRT\text{-}GFP}$ cells increased twice (25%), showing that those cells continue to proliferate and contribute to future ISCs pool.

5.3.4. Molecular characteristics of Lgr5^{GFP+} cells, derived from *Id2*$^{+/-}$ cell population at E11.5.

In order to study further the cellular heterogeneity within the developing intestinal epithelium, I decided to collect Lgr5+ cells, derived from Id2$^{+/-}$ cell population at E11.5 and a Lgr5GFP+, that were not labelled by Tomato. I wanted to understand the molecular identity of these two populations as if they belong to distinct cell types.

Lgr5^{GFP+} and Id2$^{+/-}$Lgr5^{GFP+} cells, as well Id2$^{+/-}$Tomato^{+} and EpCam^{+} Tomato^{-}Lgr5^{GFP-} samples from E11.5 induced by Tam, were collected for further RNA-seq and *ex vivo* cell culture at E13.5. Unfortunately, results of RNA-seq revealed no significant DE genes, identified between Lgr5+ and Id2$^{+/-}$ Lgr5^{GFP} cell populations. In some instances, we also observed a variation of labelling results, depending on Tamoxifen batch. FACS quantification of GFP+ cells at E13.5 and E15.5 demonstrated an elevated number of Lgr5+ cells, heterozygous for *Id2* gene, when compared to WT Lgr5 GFP+ embryos (Fig.27A). Further clonogenic potential assay showed that *Id2*$^{+/-}$ cells, negative for *Lgr*5, have the highest growing capacity *ex vivo* (Fig. 27B).

Altogether, our study shows that Lgr5+ cell progenitors appear independently of occurs independently of *Id2*^{high} population. Most likely, determination of Lgr5+ cells occurs in any cell before E11.5. Unfortunately, currently available methods do not allow to quantify precise amount of cell populations within the developing gut epithelium. In order to characterize the cell lineage choice, taking place at E11.5, a single cell RNA-seq should be further established and performed. Presumably, maturation of Lgr5+ cells is driven by mesenchymal signaling molecules or the intensive refolding of the intestinal epithelium determines the cell fate of Id2^{+} endodermal cells.

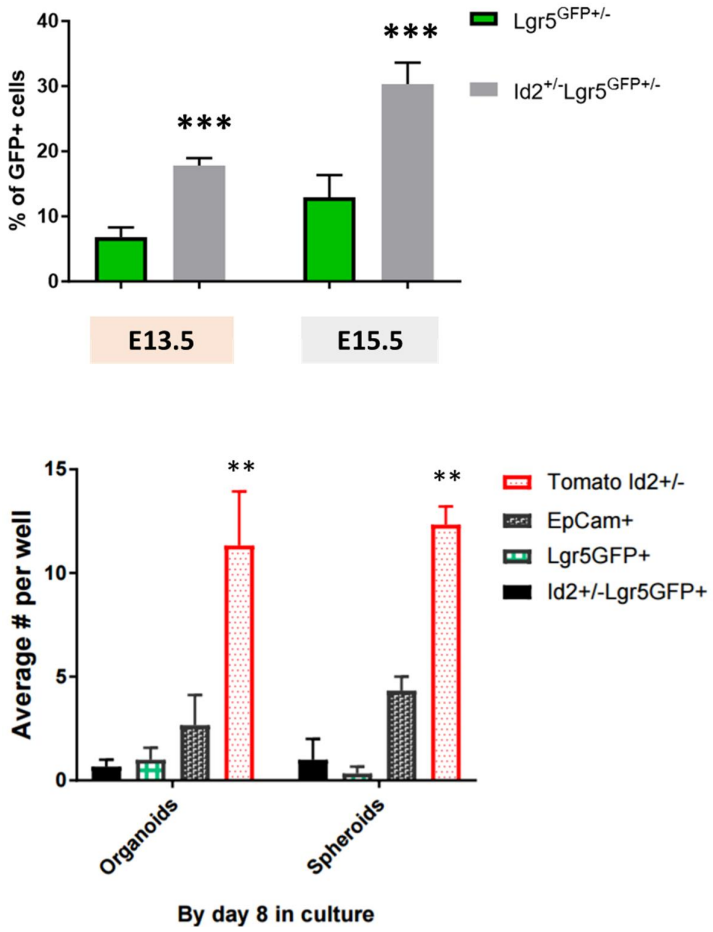

Figure 27. Id2 heterozygosity increases the number of Lgr5 GFP+ cells. **A.** FACS quantification of Lgr5-EGFP+cells, collected from $Lgr5^{GFP+/-}$ and $Id2^{+/-}Lgr5^{GFP+/-}$ samples at stages E13.5 and E15.5. **B**. Clonogenic potential of $Lgr5^{GFP+/-}$ and $Id2^{+/-}$ $Lgr5^{GFP+/-}$ populations, Tam-induced at E11.5 and isolated 2 days later. Error bars, mean ±SEM. Significance was calculated with t-test; **p<0.01, ***p<0.001.

5.4. Id2 KO in early gut development.

Lgr5$^{GFP/+}$ mice crossed into *Id2*$^{CreRT/+}$ background display increased number of Lgr5GFP+ cells and high proliferation capacities, implying that *Id2* gene itself may act upstream of Wnt signaling and may play role in Lgr5+ cells formation.

To uncover the early phenotypic effect of *Id2* gene in *Lgr5*$^{+}$ ISCs cells pool appearance during gut development and the molecular consequences caused by loss of *Id2* gene activity, I crossed *Id-Cre* heterozygous mice carrying a Cre-recombinase-oestrogen-receptor-T2 (*Cre-ER*) allele targeted to the *Id2 gene* locus to *Lgr5-eGFP-CreRT2* mouse (Fig. 28). Deletion of *Id2* exon in resulting *Id2*$^{cre/Cre}$ embryos was confirmed by PCR genotyping. The advantage of such a triple heterozygous mouse cross is a possibility to test each embryo, resulted as Id2 WT (Id2 WT Lgr5$^{GFP/+}$), Id2 het (Id2$^{Cre/+}$Lgr5$^{GFP/+}$) and Id2KO (Id2$^{Cre/Cre}$Lgr5^{GFP+}) from the same mother under the same experimental conditions. Indicated mouse cross strategy has been applied for the most of my further experiments (Fig.28).

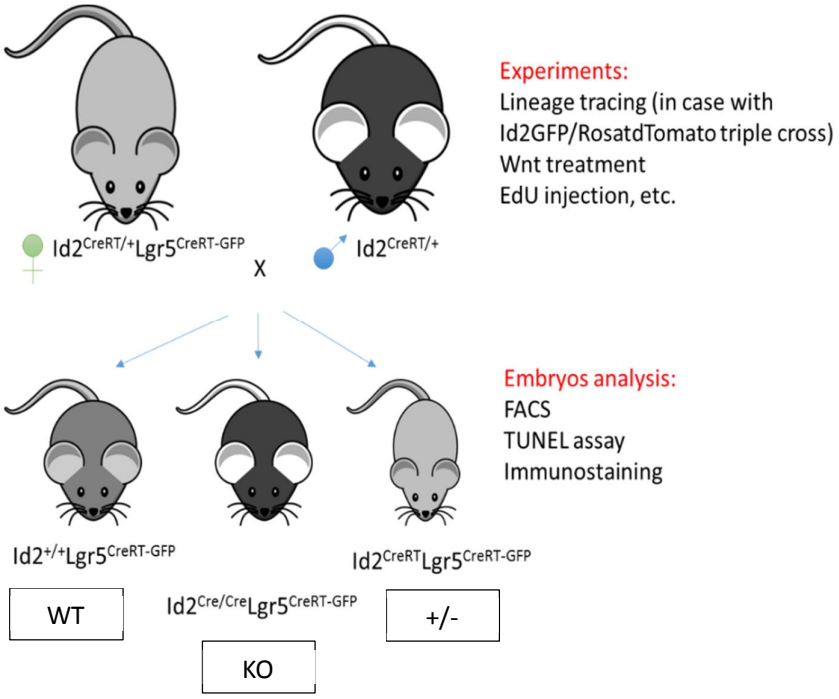

Figure 28. Generation of *Id2*-null embryos by Id2het x Id2 het x Lgr5 GFP+/- mouse triple cross. This experimental approach enables us to test both WT and Id2KO embryos from the same offspring.

I tested if the amount of Lgr5+ cells, appearing at E13.5 could be affected in *Id2*-null (Id2KO) embryos. Firstly, I measured the level of Lgr5GFP+ cells in $Id2^{Cre/Cre}Lgr5^{eGFP\text{-}Cre}$ triple mutant embryos by using FACS. When E11.5 intestine was used, I observed that, in contrast to control Id2WT Lgr5-GFP embryos, Id2 KO epithelial cells had 30% Lgr5-GFP+ cells at this stage (Fig.30A,B). In order to understand when *Id2* gene knock-out potentially leads to upregulation of Lgr5 expression, I checked the earliest stage of intestinal tube formation ï E9.5. Because of a very limited amount of embryonic endodermal material at this stage, I couldnôt perform FACS-based quantification of GFP+ cells. However, immunostaining against GFP showed that at E9.5 WT small intestine has very few Lgr5-GFP+ cells (2-5 per section, Fig. 29B), however much more of Lgr5-GFP + cells were detected in Id2 KO gut epithelium, where the whole posterior part was positive for GFP (Fig. 29A). Immunostaining on E11.5 gut epithelium supported our hypothesis that the amount of Lgr5+ cells is significantly increased in absence of *Id2* (Fig. 29C), whereas WT gut remains Lgr5GFP-negative (Fig. 29D). Thus, *Id2* gene dysfunction affects early activation of Wnt target - *Lgr5* gene expression. But are those cells that start to express Lgr5 earlier, just represent Wnt stem cell signature as E13.5 Lgr5

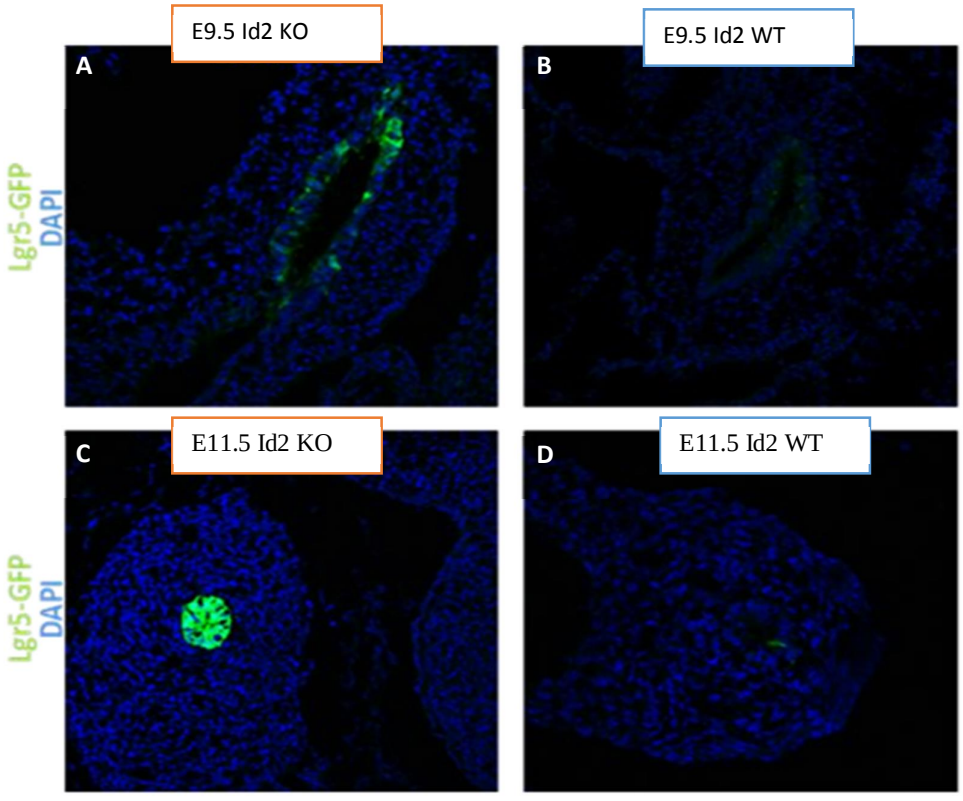

Figure 29. Immunostaining against GFP on E9.5 and E11.5 Id2 KO intestines. Early activation of $Lgr5^{GFP+}$ cells is shown for Id2 KO embryonic samples from E9.5 (**A**) and E11.5 (**C**), whereas control Lgr5EGFP+ do not express Lgr5 at E9.5 (**B**) and E11.5 (**D**).

cells in WT embryo or do Id2KO Lgr5+ cells develop abnormally? Could we identify any Wnt ligands available for Lgr5 receptor in a surrounding mesenchyme?

Significant upregulation of *Lgr5* transcription in early Id2 KO embryos prompted us to perform complementary studies of RNA profiles in WT and *Id2*-null embryonic intestines and mesenchymal tissue underlying the epithelium. I decided to isolate the cells at E11.5 ï the earliest embryonic stage when the gut could be visualized, dissected from each mouse embryo and purely sorted by FACS. I used the same sorting conditions as for previously described E13.5 Lgr5+ cells (see chapter 5.2.2.). Mesenchymal cells we sorted as EpCam^{ï} population (Fig. 30A, B). Since *Lgr5GFP*+ expression is absent in WT intestine at E11.5, I collected only EpCam+ and mesenchymal EpCam- populations for our Id2WT control samples. (Fig. 30A).

250 cells were collected for further cDNA preparation for each sample with 3 biological replicates. The identical genomic libraries preparation protocol has been used (chapter 5.2.2). DNA integrity profile and the concentration values showed a good samples quality. Interestingly, the highest peak, specific for Id2 WT mesenchyme, is absent in Id2-deficient sample (Fig. 30C). As we saw after RNA-seq analysis, this peak relates to an abundant transcriptional activity of *Id2* gene itself (Fig. 30C, arrow). Although the first intron of *Id2* in our *Id2*^{CreRT} mouse is disturbed, preventing Id2 protein translation, we see that the rest of the gene body is transcribed.

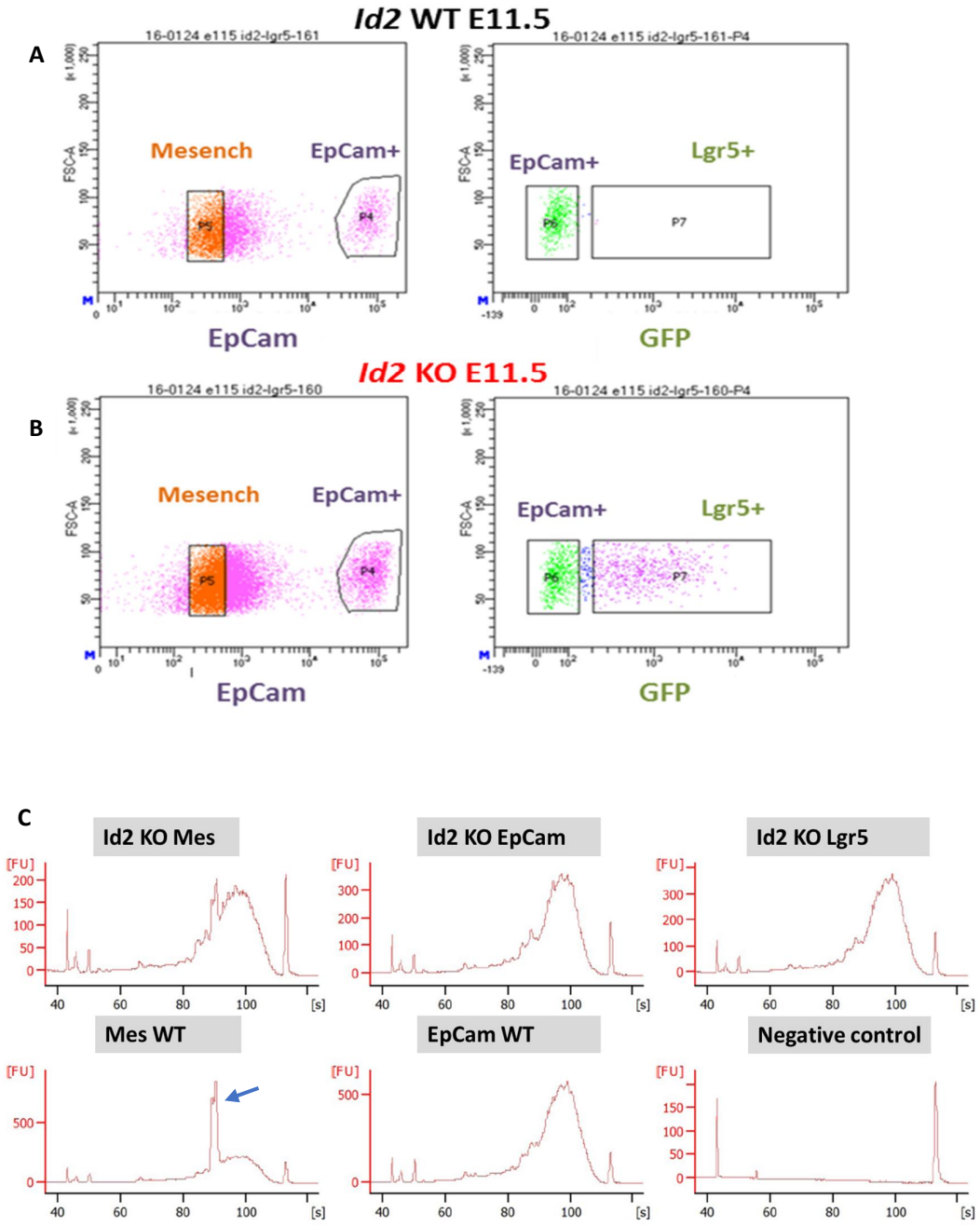

Figure 30. RNA-seq of E11.5 Id2KO and WT intestinal cells. FACS-gating strategy for collecting epithelial and mesenchymal cells, isolated from control Id2 WT (**A**) and Id2KO Lgr5 GFP+ (**B**) embryonic material. **C**. Efficiency of cDNA library preparation was measured by Bioanalyser. Arrow indicates a specific high transcriptional peak in mesenchymal samples.

5.4.1. RNA-sequencing of E11.5 Id2 KO small intestine epithelium.

Results of RNA-seq revealed significant differences in genes expression between Id2 KO and WT embryos samples. When we compared Lgr5KO cells to control EpCam WT, more than 1000 differentially expressed genes (p-value<0,01) were found (Fig. 31A). Almost the same amount of DE-genes was detected between Id2KOLgr5^{+} and Id2KOLgr5^{-} cells (over 800 genes, Fig.31C). However, we found less changes in genes expression when compared EpCam+ cells from both Id2KO and Id2 WT (338 DE genes). Interestingly, when we analyzed Id2KO Lgr5+ population, we detected not only the genes, upregulated in E13.5 WT gut (chapter 5.2.2.: *Lgr5*, *Smoc2, Tnfrsf19*), but also a few new unique genes, specific for Wnt signaling (Fig. 31C). Thus, Wnt6 and Wnt11 ligands are expressed exclusively in Id2 KO+ cells as well as *Snai2* epithelial-mesenchymal transition transcription factor (Fig. 32A). *PDGFa* - **p**latelet-**d**erived **g**rowth **f**actor-**A**, which has been reported to be specifically expressed at E15.5 in intervillus pockets, is already upregulated at E11.5 in Id2 KO epithelium. On the other hand, Id2 WT EpCam+ cells also have important upregulated genes, enhancing cell proliferation: Rbl29 and Rpl2 ribosomal proteins, Ccl3 chemokine and Igf1 insulin-growth factor (Fig. 31A). In general, *Id2*-mutant epithelium demonstrates an upregulation of many cell cycle progression and proliferation genes, such as *Ccnb1*, *Ccnd2*, *Aurkb*, *Smoc2* etc (Fig. 31B), regardless of Lgr5+ expression. Our data demonstrates that intestinal epithelium is composed of actively dividing cells in both Id2 KO and WT samples.

We tested further how different are the RNA profiles of Lgr5+ vs Lgr5- cell populations within Id2 KO intestine. Interestingly, Id2 KO Lgr5+ cells show upregulation in intestinal ñmaturationò genes such as vimentin, collagen and keratin. Additional ISCs markers that were not found in normal E13.5 Lgr5 cells, were upregulated in Id2KO Lgr5 cells, such as *Lrig1* and *Prom1*, indicating that Id2 KO Lgr5 cells are more differentiated into ISCs already at E11.5 (Fig. 31C). On the other hand, enterocytes markers, highly upregulated in E13.5 Lgr5^{-} population, didnôt appear earlier in Id2-null embryos. As shown in Fig. 31D, at E11.5 *Id2* KO embryos have significant upregulation (20-times fold change) of *Lgr5* gene expression. Immuno-histochemical analysis of E11.5 *Id2* KO embryonic intestine demonstrated expansion of Lgr5+ GFP cells (Fig. 29C,D).

It is believed that a trio of transcriptional regulators - Ascl2, Tcf4 and nuclear b-catenin, regulates transcriptional activity of Wnt signaling genes in the small intestine (link). Thus, the particular interest of my research was to examine if a high expression of these genes is responsible for establishing adult ISCs molecular signature. Surprisingly, neither *Ascl2* nor *Tcf4* were upregulated in Id2-deficient mouse epithelium. In opposite, their expression level remained unchanged. Additionally, I performed numerous stainings against b-catenin on E11.5 Id2 WT and Id2KO intestinal sections. I couldnôt detect nuclear accumulation of b-catenin in Id2-mutant embryos. The data of E11.5 RNA-seq was very important to gain insight into the molecular properties of *Id2*-deficient mouse epithelium.

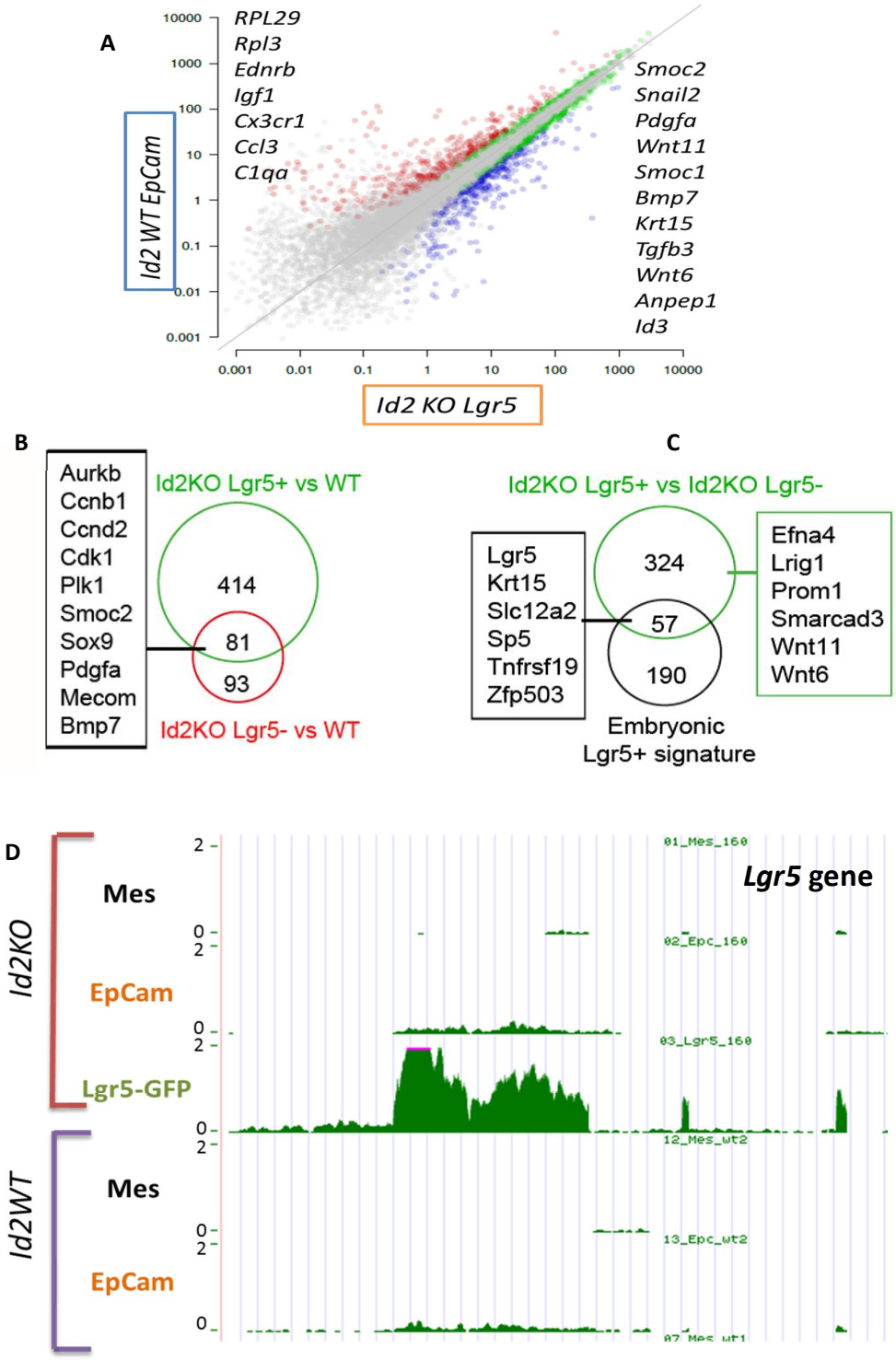

Figure 31. Results of E11.5 Id2 KO cells RNA-sequencing. Pair-wise scatter plot analysis of changes in gene expression showing the molecular signatures of Id2 WT *EpCam*$^{+}$ and Id2 KO *Lgr5*$^{+}$ (**A, B**) or Id2 KO *Lgr5*$^{+}$ vs Id2 KO EpCam cell populations (**C**) (n=3).The list of top upregulated genes is shown for each cell population (**A-C**). **G-H.** E11.5 RNA-seq data for *Lgr5* gene expression in Id2 WT vs. Id2 KO samples, viewed by USCS Genome Browser. 20-times fold upregulation of *Lgr5* gene transcription is shown for Id2KO Lgr5+ cell population.

5.4.2. RNA-sequencing of Id2KO mesenchyme E11.5.

Our analysis of Id2 KO vs. Id2 WT mesenchymal cells did not show a high number of DE genes (150 genes, $\log_2$FC>1; FDR<0.01). *Esr1*(estrogen 1 gene, expressed from $Id2^{CreER/CreER}$ background, was one of the most upregulated genes in Id2KO epithelium. We detected an upregulation of 10 other genes, that mostly belong to metabolic pathways (*Slc7a9*, *Pnliprp2, Hemk1*, *Scd*). Interestingly, *Wnt 11* was also expressed higher in *Id2* KO mesenchyme. Among the rest 140 downregulated transcripts we found mostly the genes, specific for erythropoiesis, such as embryonic globin genes (*Hbb-y*, *Hba-x*, and *Hbb-bh1*), master transcription factor of erythropoiesis - *Gata1*, and hematopoietic-specific factor *Klf1*, involved in erythroid genes expression.

In collaboration with a PhD student M.Norkin, we confirmed results of RNA-seq data by RT-PCR using primers for *Lgr5*, *Ascl2*, *Wnt 11*, *Wnt6*, *Smoc2*, *Snai2* etc. Unfortunately, attempts to detect *Wnt 11*, *Wnt6* and *Lgr5* by RNA *in situ* hybridization filed due to the amount of transcripts that are apparently under the detection limit, at least by this technique.

Transcriptomic profiles of mesenchymal, EpCam+ and $EpCam^{+}Lgr5^{+}$ clearly showed a unique RNA profile of Id2 KO samples at E11.5 epithelium. Our data demonstrated that at this developmental stage WT embryonic endodermal cells do not have an active Wnt signaling, as they do not express any ISCs markers. Yet, early activation Wnt signaling target genes, including *Lgr5*, is caused by epithelial-specific *Id2* gene loss (Fig. 32B).

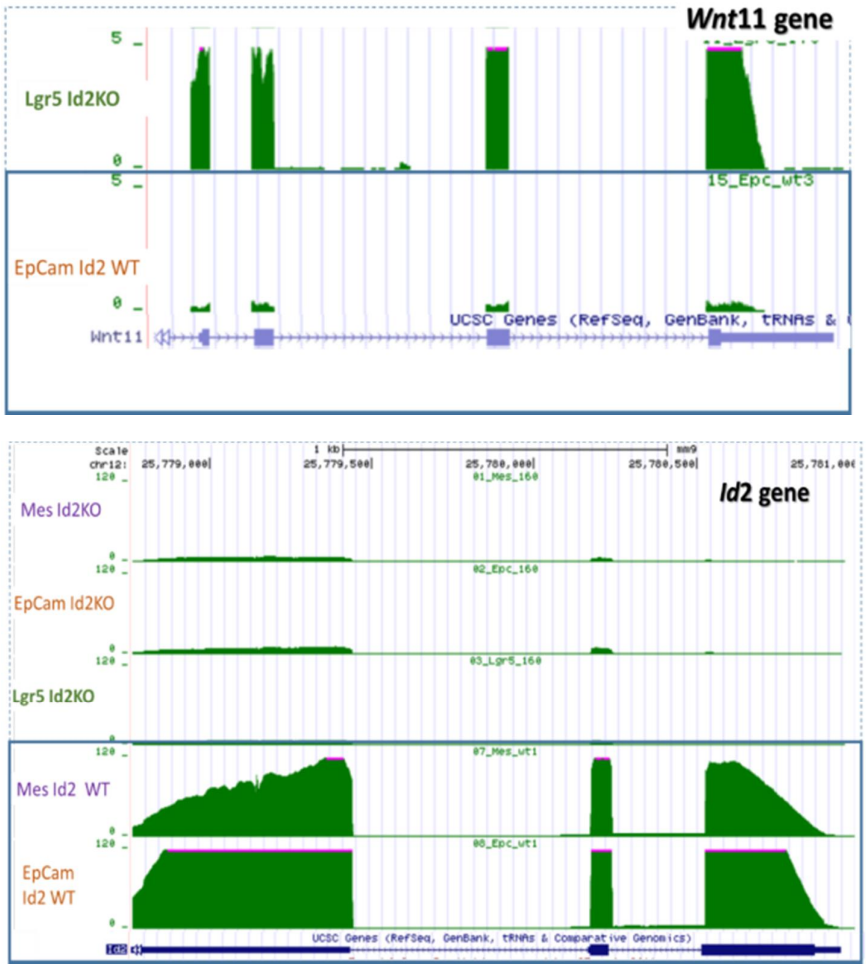

Figure 32. E11.5 Id2KO RNA-seq results shown on UCSC Genome Browser. A-B. Illustrative view of transcriptional activity profile for *Wnt 11* (**A**) and *Id2* (**B**) genes in Lgr5+(green), EpCam+(orange) and mesenchymal cells (violet). Decreased expression of *Wnt11* in Id2WT (**A**) and *Id2* in Id2KO (**B**) embryos is indicated by the considerably fewer reads mapping to the exons compared with control populations.

A

5.5. *Id2* KO embryos small intestine development at E15.5.

5.5.1. *Id2KO* Lgr5+ cells distribution *in vivo.*

To evaluate further the functional consequences of early Wnt signaling activation in intestinal epithelium development, I analyzed embryos at E15.5 ï the stage when villus formation occurs, starting proximally and proceeding distally. By this time, in villi terminally differentiated absorptive (enterocytes) and secretory (goblet and neuroendocrine) cells are present. Between the folds of villi highly proliferative intervillus regions start to express adult ISC markers, such as *Lgr5*, *CD44*, *Tcf4*, establishing a proper stem cell environment before crypts formation. As I demonstrated earlier for E11.5 and E13.5 stages, *Id2* was essential to restrict stemness of intestinal Lgr5+ cells. In such case, the increase of Wnt signaling before epithelium reorganization at E15.5 would possibly lead to: 1) abnormal differentiation of enterocytes in villi due to expansion of Lgr5+ stem cells, or 2) blockage of Lgr5+ cells redundancy by compensatory mechanisms. To further explore these alternatives, I investigated here the role of *Id2* loss at E15.5.

I measured the amount of $Lgr5^{GFP+}$ cells at E15.5 in $Lgr5^{eGFP\text{-}CreRT}$ (Id2 WT) mouse embryos and compared to $Id2^{Cre/Cre}Lgr5^{eGFP\text{-}CreRT}$ (Id2 KO). Intestinal epithelium was split into 2 pieces and analyzed separately for anterior and posterior parts, since the signaling molecules and organoids forming capacity were demonstrated to be different for these regions (de Santa Barbara, 2003). Accordingly, here I show that at E15.5 WT embryos have up to 15% of Lgr5GFP+ cells in anterior intestine and much more ï 40% - in posterior part (Fig. 33B, 34C). We hypothesize that the Wnt signaling gradient, started from posterior intestine at E11.5, determines the number of Lgr5+ progenies in intervilli. As expected, *Id2*-heterogeneous small intestine has 1,5-fold increased amount of Lgr5+ GFP+ progenies, both for anterior and posterior parts. However, immunostaining analysis of $Id2^{+/-}$ samples revealed that all Lgr5GFP+ cells were localized only in intervillus pockets and never in villi (data not shown).

Interestingly, Id2 KO $Lgr5^{GFP+}$ cells, appeared as a minor population at E9.5 small intestine, didnôt disappear by E15.5. Neither their amount was close to $Id2^{+/-}$ embryos. In contrast, during active proliferation of epithelial cells prior to villi formation, $Lgr5^{+}$ cells occupy around 60% of anterior and up to 90% of all posterior cells in the gut (Fig. 33C, 34C). Moreover, the intensity of GFP signal in Id2KO cells is much higher for the majority of Lgr5+ cells, whereas $Id2^{+/-}$ Lgr5+ cells are not $Lgr5^{GFP+high}$(Fig. 33B,C). Such a dramatic change in intestinal cells population heterogeneity could be clearly observed in a histogram analysis of the baseline fluorescence intensity of EpCam+ cells. Fig. 33D demonstrates that majority of Id2KO posterior cells becomes GFP+, whereas more than 50% of the whole intestinal epithelium is represented by $Lgr5GFP^{high+}$ cells.

In order to visualize the distribution of Id2 KO $Lgr5^{GFP+}$ cells in the small intestine, immunostaining against GFP was performed. In the posterior part of the intestinal epithelium, GFP+ cells are evenly distributed, occupying both villi and intevilli regions (Fig. 34B). However, a highest

GFP signal was detected in intervillus pockets. The amount of Id2 KO Lgr5^{GFP+} cells in anterior part is not high and mostly found in intervillus pockets. I examined Id2 WT Lgr5^{GFP+} embryos, but rare GFP cells were found only in intervillus regions in posterior part, whereas anterior part contained very few

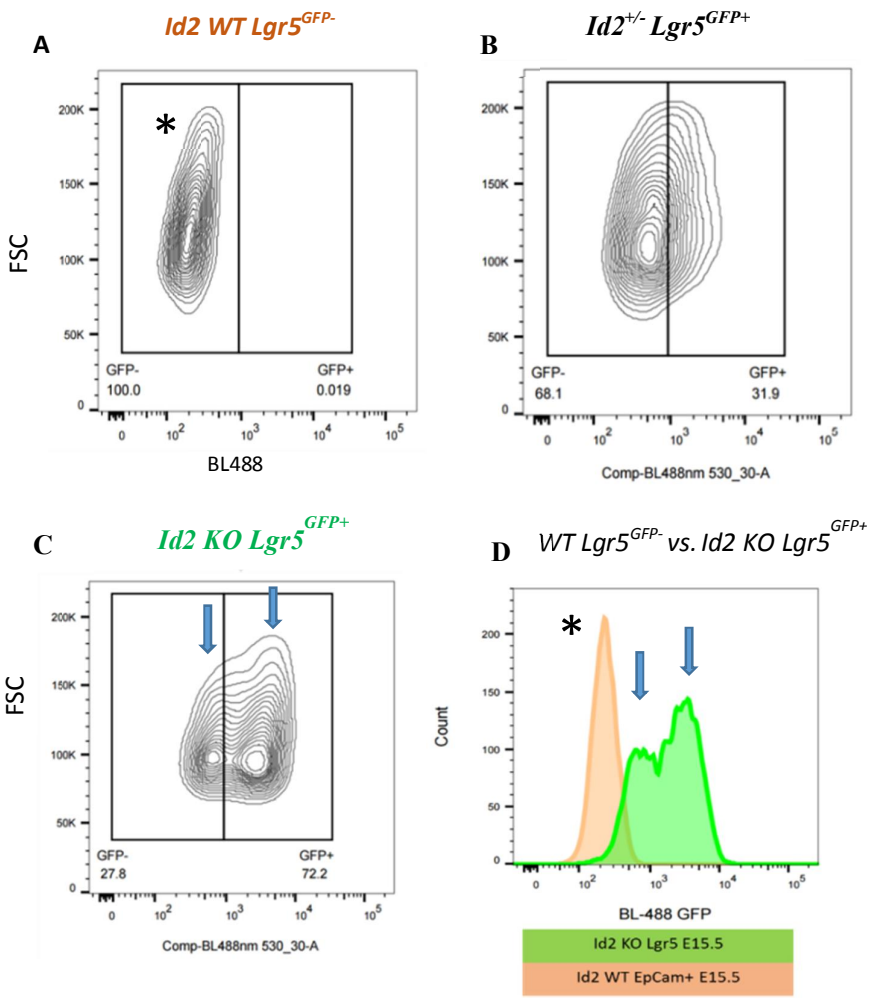

Figure 33. Representative FACS plots of GFP+ cells from Id2 WT, Id2 het and Id2KO embryos at E15.5. A-C. The gating strategy shown illustrates: a negative control for GFP+ signal in *Id2WT Lgr5*$^{GFP-}$ embryo (**A**, asterisk); GFP+ cells population in *Id2*$^{+/-}$*Lgr5*$^{GFP+}$ (**B**) and *Id2 KO Lgr5*$^{GFP+}$ (**C**) embryos. **D.** Fluorescence histograms of each gated population indicate a shift in the visual peak of GFP intensity in Id2 KO cells, compared to WT control. Thus, the whole posterior gut of *Id2*-null epithelial cells consists of Lgr5GFP^{low+} and Lgr5GFP^{high+} cells (blue arrows).

GFP+ cells per gut sections (Fig. 34A).

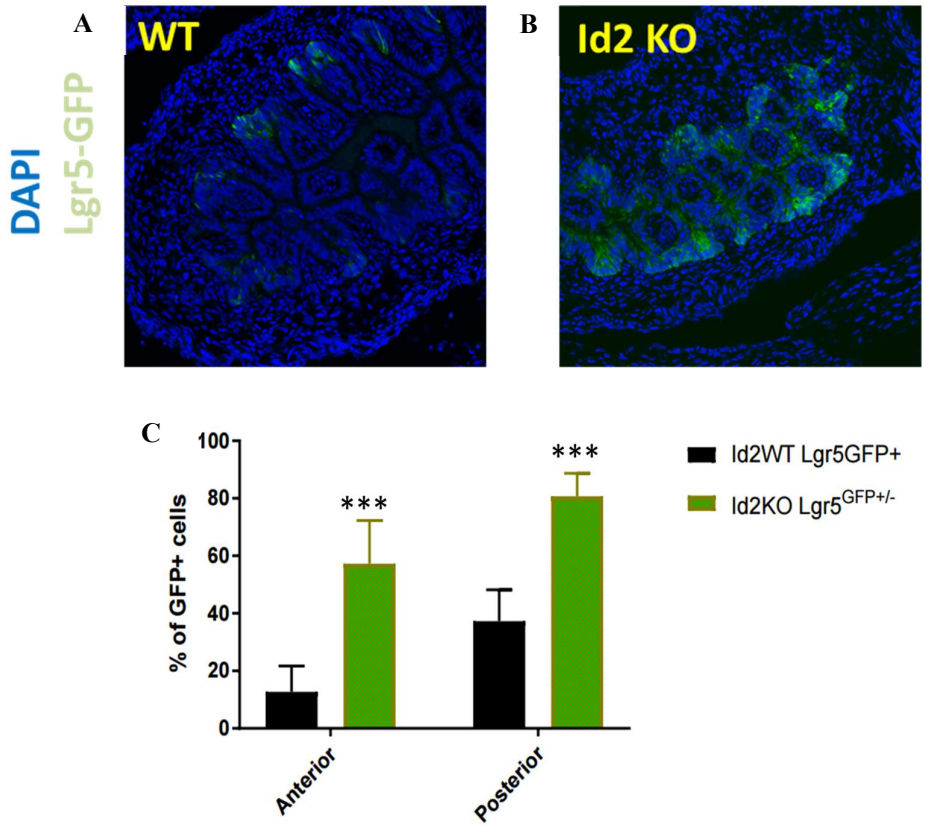

Figure 34. Id2-deficient intestinal epithelium has an increased number of Lgr5-GFP+ cells. A-B. Immunostaining against GFP shows a limited amount of Lgr5GFP+ cells in Id2 WT Lgr5GFP+/- posterior gut (**A**), whereas up to 90% of Lgr5GFP+ cells occupy both in villi and intervilli compartments in Id2KO samples (**B**). **C**. FACS quantification of Lgr5GFP+ cells in *Id2 WT Lgr5*$^{GFP+/-}$ vs *Id2 KO* samples revealed an increase in Lgr5GFP+ cells for both anterior and posterior part. Error bars, mean ±SD. Significance was calculated with t-test; **p<0.01, ***p<0.001.

5.5.2. Results of qRT-PCR analysis of E15.5 epithelium.

To characterize consequences of such a dramatic upregulation of Lgr5 stem cell marker in E15.5 intestinal epithelium, I collected 500 $Lgr5^{GFP+}$ cells from both Id2 WT and Id2 KO embryos, as well as control $EpCam^{+}Lgr5^{GFP-}$ cells for further qRT-PCR analysis. Together with M.Norkin we tested whether Id2KOLgr5+ cells has the same ISCs signature when we compare their gene expression profiles to normally developed WT cells.

Interestingly, many Wnt signaling genes, such as *Lgr5* gene itself, *Smoc2*, *Lrig1*, were upregulated 2-4 times in a posterior gut, whereas anterior cells didn't show dramatic differences in their genes expression. We have tested many targets from our E11.5 list with differentially expressed genes list, including *Snai*2, *Wnt*11, *Wnt*6, *R-spo*1, *R-spo*3 and *Id*1-*Id*3.

The uncoupling results between $Lgr5^{GFP+}$ signal intensity by FACS (up to 90% of the whole gut epithelium) and *Lgr5* gene expression level by qPCR was unexpected. I assume that a high Lgr5GFP+ signal, counted by FACS, represents GFP protein accumulation as a consequence of early Wnt signaling activity. However, by E15.5 molecular mechanisms, initiated by dramatic epithelial reorganization at E14.5-E15.5, are establishing a proper stem cell niche in non-cell-autonomous manner. Thus, any unrelated ISCs genes activity in villi is blocked by compensatory signals, most probably, from surrounding mesenchyme and BMP clusters. This idea was further confirmed by joint experiments with M.Norkin. qPCR results of E17.5 Id2KO Lgr5GFP+ cells don't show any significant differences in their genes, when compared to WT cells (data not shown). Consistent to our data, we observed that in Id2KO mice the amount of Lgr5GFP+ cells is decreasing, when compared to E15.5 stage.

Furthermore, proliferation activity of Id2KO Lgr5 intestinal epithelium was measured by using Click-iT EdU Cell Proliferation Assay (ThermoFisher). Briefly, a pregnant mouse was subjected to a single injection of EdU - a chemical analog of thymidine, 30 min before sacrifice. EdU is incorporated into fast-cycling cells during their DNA synthesis. Staining with Pacific blue fluorescent secondary antibody allows us to measure the amount of proliferative cells by FACS or to analyze the tissue sections at 450 nm intensity. Immunostaining analysis of Id2KO epithelium with control EdU-treated Id2 WT gut sections didn't demonstrate any significant changes in their proliferation activity (Fig. 35C, F). The same results were obtained in collaboration with M.Dzama, where we quantified the amount of EdU+ cells by FACS (data not shown). In accordance to these results, I could not detect a nuclear localization of ß-catenin or increased amount of *Tcf4* or *Sox9* genes by immunostaining on E15.5 gut sections.

Further I have performed immunostaining analysis of Id2 KO Lgr5 small intestine sections for cytoplasmic EpCam, as we saw an increased amount of EpCam+ cells by FACS. Interestingly, I have detected a significant upregulation of EpCam on translational level (Fig.35 D,E). Normally EpCam is

a cell surface molecule and a loss of its intracellular domain with subsequent accumulation in cytoplasm predicts cancer progression.

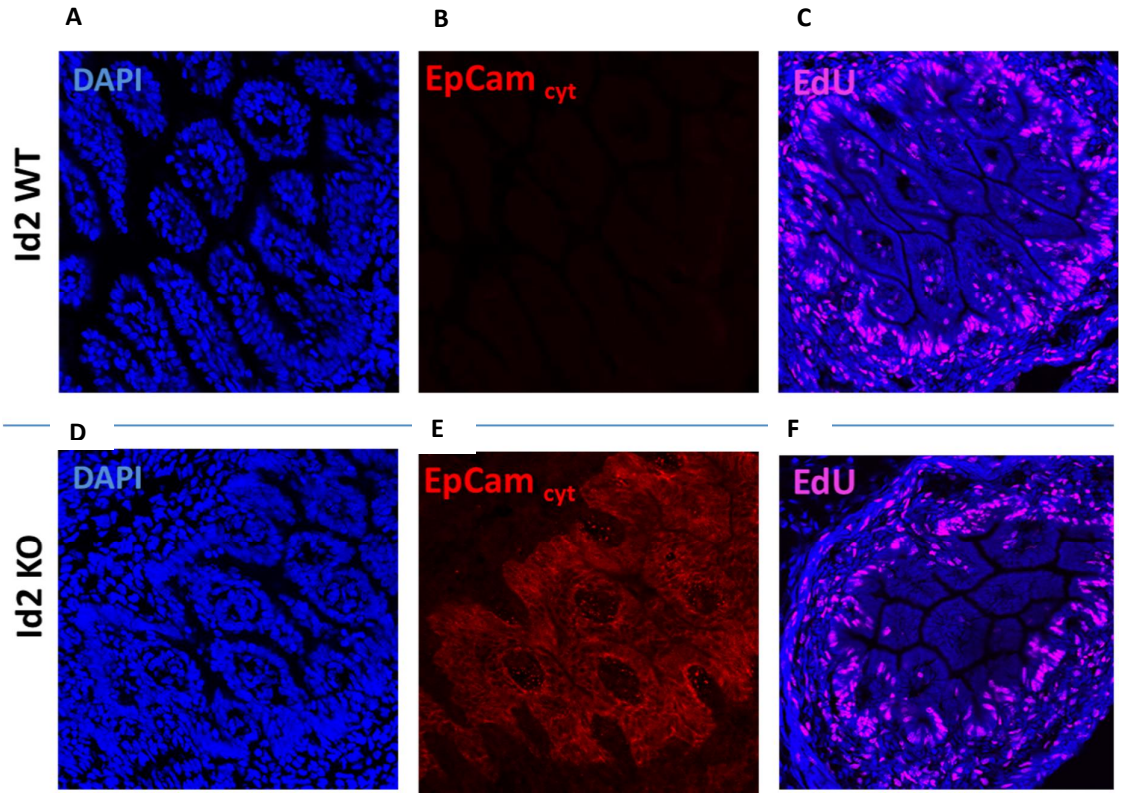

Figure 35. Intestinal homeostasis of Id2KO embryos at E15.5. A,B,D,E. The small intestine was examined for the presence of intracellular domain of EpCam by specific antibody staining against its C-terminus in WT (**A,B**) and Id2KO (**D,E**) embryos. **C,E**. EdU was injected into E15.5 pregnant mouse 30 min prior to euthanasia, and the embryos were collected for anti-EdU staining. Proportion of EdU-positive cells in WT (**C**) and Id2KO (**F**) epithelum does not differ. $n = 2$.

5.5.3. Clonogenic capacity of E15.5 Id2 KO cells *ex vivo.*

In order to characterize the clonogenic capacity of E15.5 isolated intestinal cells to form organoids and spheroids, I have applied *ex vivo* cell culture assay. In this approach, I separated the small intestine into 2 parts ï anterior and posterior. As reported earlier for newborn mice intestine (Fordham, 2013), posterior cells give rise to organoids, whereas anterior cells form predominantly spheroids.

I have collected 500 cells from each of the following samples: anterior Id2WT $EpCam^{+}Lgr5^{GFP-}$; Id2WT $EpCam^{+}Lgr5^{GFP+}$; Id2KO $EpCam^{+}Lgr5^{GFP+-}$; Id2KO $EpCam^{+}Lgr5^{GFP-}$, as well as for posterior part. Each sample was plated in a separate well and examined for its growing potential. Mustata et al. (2013) reported that cells, separated from the whole intestinal epithelium at E15.0, give rise to organoids (>95%), but already at E16.0 the proportion of generated spheroids and organoids refers as 40:60, respectively. When I analyzed E15.5 cultures cells, I also could observe this distribution, but more detailed ï on a cell population level. The relative proportion of spheroids and organoids formed from Id2 KO and Id2 WT cells was studied. Analysis of structures, derived from Id2KO and control WT embryos, revealed no significant differences for anterior part. Interestingly, anterior cells have a capacity to form both spheroids and organoids, regardless of *Id2* gene activity (Fig. 36A). In contrast, WT epithelial cells from posterior gut generated only organoids (Fig. 36C, 36D). When I examined posterior *Id2*-deficient samples, I observed a significant advantage in their growth, proliferation and differentiation in comparison to WT cells (Fig. 36B, D, E). Thus, *Id2* KO cells (both EpCam and Lgr5+) grow more efficiently, forming organoids as well as undifferentiated spheroids. Notably, Id2 KO Lgr5-negative cells have the highest proliferative capacity as spheroids without further differentiation into organoids (Fig. 36E). Therefore, at stage E15.5 Id2 KO cells actively proliferate and keep undifferentiated state in culture conditions. These results indicated that epithelium in Id2 KO cells prior to villi-intervilli formation could undergo severe differentiation problems *in vivo*. Among the supplements, added in our culture system, both spheroids and organoids required R-spondin 1 for their growth and survival. However, once a big budding organoid was formed, it could survive withour R-spo 1 for a 10 days at least. In contrast, organoids formed from E13.5 cells, are more sensitive to R-spo presence in medium.

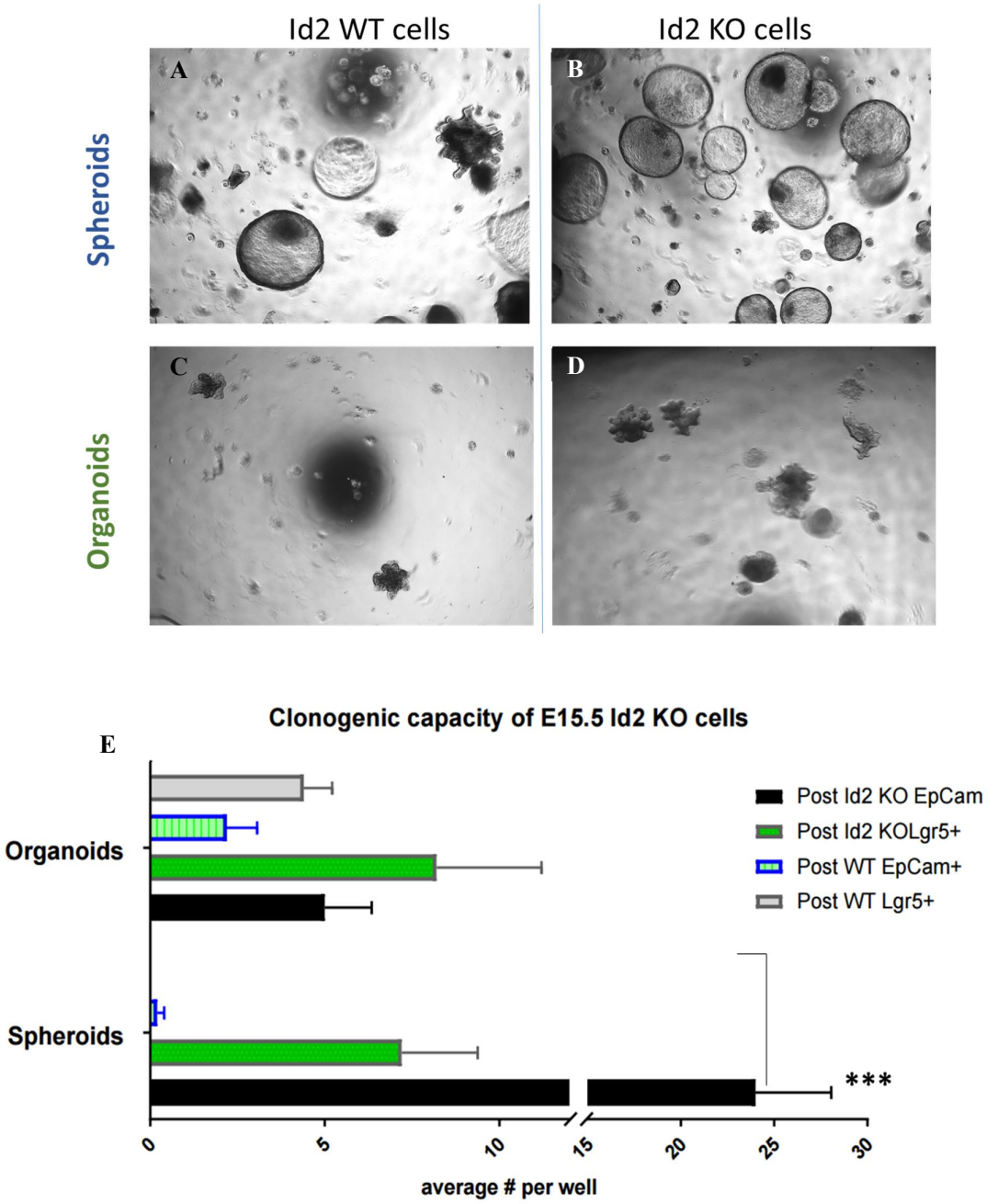

Figure 36. Clonogenic potential of Id2KO intestinal cells at E15.5 *ex vivo*. A-D. Control WT cells, derived from anterior gut, have a capacity to form both spheroids (**A**) and organoids (**C**) after 5 days in cell culture. *Id2*-null epithelium gives rise to numerous undifferentiated spheroids (**B**, posterior gut) as well as organoids (**D**). Error bars, mean±SEM, n>20. Significance was calculated with t-test, ***p<0.001.

5.5.4. qPCR-RT on E15.5 organoids and spheroids, grown for 1 week in culture.

To characterize further the identity of Id2KO-derived highly proliferative cells, grown *ex vivo*, I have collected organoids and spheroids from Id2-deficient posterior part. Our qRTï PCR analysis demonstrates that *Id2*-deficient cells are indeed missing *Id2* gene expression, when compared with WT posterior organoids, normalized to *Tbp1* (Fig. 37). Surprisingly, we have detected an enormous upregulation of markers for epithelial to mesenchymal transition (EMT), as well as cancer markers *Trop2* and *Cnx43* (Fig. 37). It has been reported earlier that *Cnx43* and *Trop2* are markers of embryonic undifferentiated cells in spheroids (Mustata, 2013), never found in organoids. Indeed, in our experiment all WT organoids are negative for these genes. However, organoids and spheroids, formed by Id2KO cells have increased level of *Cnx43* and *Trop2*. ISC signature genes, such as *Lgr5*, *Smoc2* and *Axin2* were upregulated in Id2KO organoids and spheroids. *Lrig1*, identified as a DE gene in our E11.5 Id2KO RNA-seg is also increased exclusively in Id2KO derived structures.

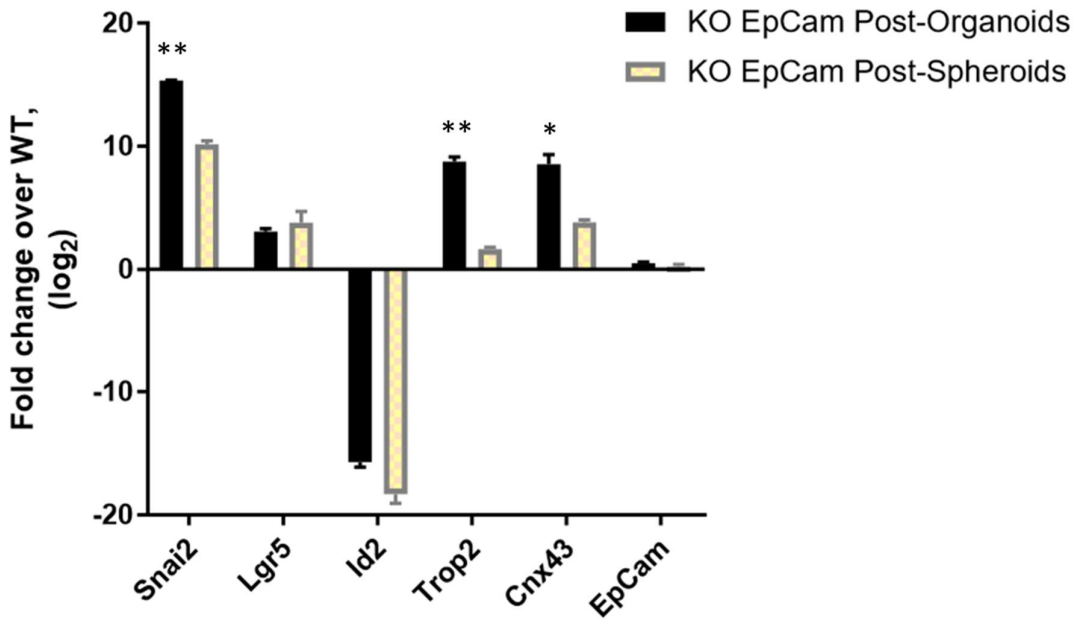

Figure 37. qRT-PCR analysis of Id2KO cells, collected at E15,5 and grown for 8 days *ex vivo*. Id2KO EpCam+ cells revealed the highest difference in their proliferation and differentiation in comparison to WT-derive organoids/spheroids. Error bars, mean±SD, p*<0.1; p**<0.01, t test, n=3.

5.5.5. Chemical compounds screening *ex vivo*.

To determine the molecular mechanism, driving Lgr5 ISCs specification in the absence of *Id2* gene product, *Id2*-null intestines were studied in 3D *ex vivo* cell system. Particularly, I investigated the impact of the mesenchyme, which is expressing Id2 as well, however missing in the ñmini-gutò culture conditions. As discussed earlier, Id2KO small intestine from posterior part forms predominantly spheroids, whereas we couldnôt observe any spheroids in WT control. Accordingly, other studies on embryonic intestinal cells demonstrated that the posterior part gives rise only to organoids (Fordham, 2013; Mustata, 2013). To investigate the mechanism leading to increased proliferation and delayed differentiation of *Id2*-deficient intestine, I have applied a chemical compounds screening assay. Here I sought to modulate Wnt signaling pathway by appying the following conditions:

1. Normal medium with R-spo and all essential growth factors (control +**R spo**);
2. R-spondin-1 depleted medium, which will block Lgr5/R-spo triggered Wnt activation (**-R spo**);
3. Treatment with the glycogen synthase kinase 3ϐ inhibitor TWS119, which will activate Wnt signaling (+**TWS**);
4. Disruption of ϐ-catenin/TCF transcriptional complex by ICG-001 component and suppression of the Wnt/ϐ-catenin mediated gene transcription (+**ICG001**);
5. Blockage of Wnts secretion by Wnt-C59 compound ï an inhibitor of mammalian PORCN acyltransferase (+**Wnt C-59**)
6. Stabilization of Axin protein by XAV 939 compound, which will inhibit the poly-ADP-ribosylating enzyme tankyrase and stimulate ϐ-catenin degradation (+**XAV**)
7. Treatment with DAPT, an inhibitor of ɔ-secretase, which downregulates Notch pathway activity (+**DAPT**);
8. Inhibition of Notch signaling by TAPI-1, that inhibits a TNF-alpha converting enzyme, or TACE, required for Notch cleavage and activation (+**TAPI-1**).

Before testing all chemical compounds on a very limited amount of E15.5 derived Id2KO cells, I aimed to establish the culturing conditions for WT embryonic cells. Briefly, 500 cells, sorted per well, were grown for 1 week in culture with all necessary growth factors. Then the cells were re-plated in a new Matrigel drop without R-spondin and the drugs were added accordingly (Fig. 38 A-F).

Although Wnt C-59 and XAV 939 have been reported to inhibit Wnt signaling, I could not observe any significant phenotype in WT organoids development (Fig. 38E,F). Forced activation of Wnt by TWS agent was ineffective as well (Fig. 38C), because the amount of organoids remained unchanged. As Notch signaling target gene *Trop*2 was upregulated in Id2 KO cells, I tested two inhibitors of Notch: DAPT and TAPI-1. Treatment with DAPT caused massive cell death already after 2 days of culturing (not shown). However, TAPI-1 treated organoids lost their typical budding

structure and developed spheroids instead. Interestingly, such de-differentiation effect did not last long ï after several days in TAPI-enriched medium all cells turned apparently into post-mitotic secretory cells, because no clear boundaries between Paneth cells and ISCs have been observed (Fig. 38H). In contrast, control organoids developed crypts with 2-3 Paneth cells on tips (Fig. 38I)

Among three growth supplements, required for ISCs maintenance *ex vivo* ï R-spondin1/ EGF/ Noggin, only R-spondin 1 was necessary for E15.5-derived organoids and spheroids. According to previous studies on embryonic gut epithelium (Mustata, 2013; Fordham, 2013), E16.0 cells form spheroids and survive without R-spondin1 supplement. Thus, embryonic intestinal cells are Wnt-independent. Of note, this statement considers additional supplements in culture, for example, Prostaglandin or DAPT. However, in our system only E13.5 cells do not differentiate and form spheroids, unless R-spondin is added. When E15.5 cells were tested, R-spondin was necessary for both Id2 WT / KO spheroids and organoids. Thus, our observations *ex vivo* showed that R-spondin 1 is absolutely required for survival and development of intestinal spheroids into organoids (for Id2 KO).

Collectively, our data on modulation of Wnt/b-catenin signaling activity *ex vivo* by chemical compounds demonstrates inefficiency of the applied method to gain insight into molecular processes, responsible for precocious specification of Id2KO cells. Presumably, the working concentrations for each of the chemical component were not fully optimized due to a limited number of embryonic cells, available for each testing experiment. Additionally, *ex vivo* cell culture conditions are constrained by lack of mesenchyme-specific signals.

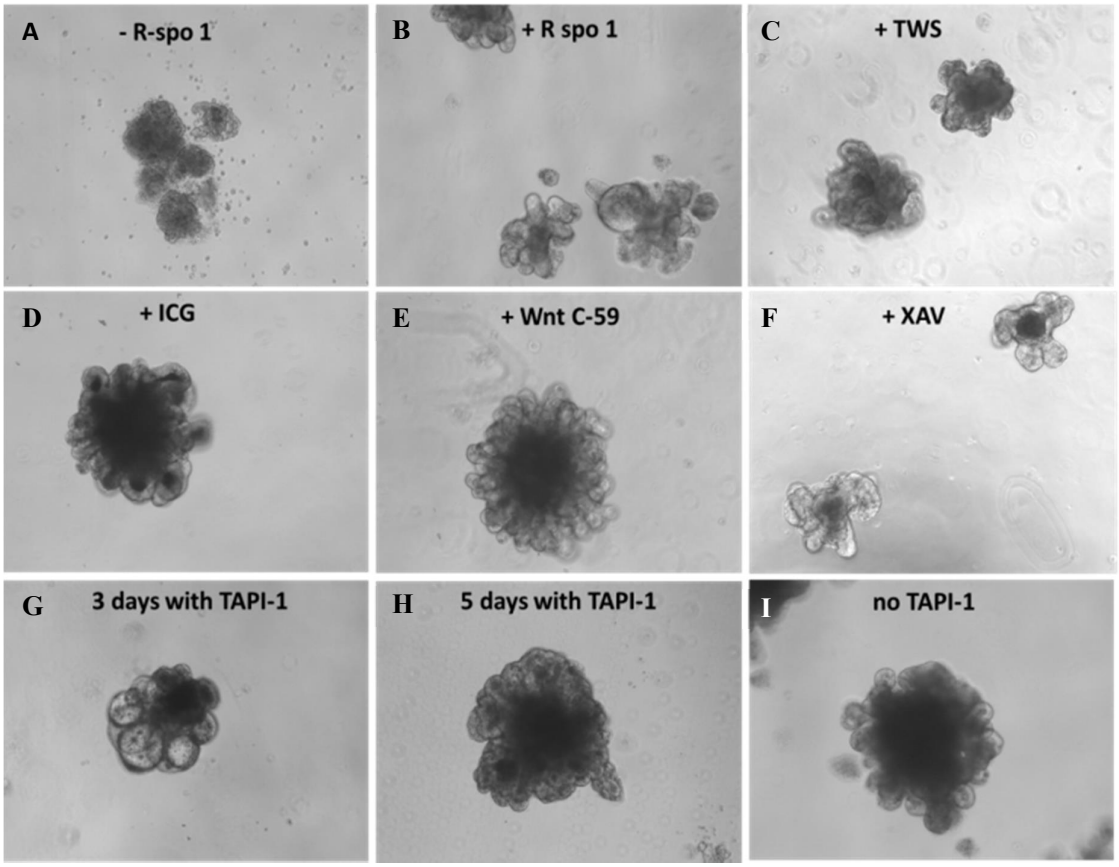

Figure 38. Effects of Wnt/ß-catenin and Notch signaling- specific modulators on E15.5 cells growth *ex vivo*. A. In the absence of R-Spo1, intestinal cells undergo cell death within 5 days, **B**. R-spo + conditioned medium is essential for growth and survival of plated cells. C. TWS-enriched conditional medium does not reveal and advantage in cell growth, when compared to untreated control.**C-F.** Effect of Wnt inhibitors ex vivo: treatment with ICG(**D**), Wnt C59 (**E**) and XAV(**F**) does not show changes in organoids development. In contrast, cells, treated with Notch inhibitor TAPI-1, after 3 days in culture form spheroids (**G**), which will be differentiated into organoid within 2 days (**H**), while control cells are not affected (**I**).

5.5.6. Wnt treatment *in vivo*.

An alternative and more reliable approach to inhibit Wnt signaling is to block the production of all active secreted Wnts *in vivo*. This can be achieved by targeting a key enzyme in the process of Wnt biosynthesis, the membrane bound O-acyltransferase PORCN. It has been reported before that the mammalian Wnt signaling is sensitive to PORCN expression levels, as inhibition of PORCN activity by a small molecule Wnt C-59 inhibitor abrupts Wnt activity (Proffitt, 2013). Although our *ex vivo* experiment didnôt show any Wnt associated phenotype in organoids, we anticipated that Wnt C-59 administration *in vivo* will prevent a Wnt-dependent signaling in embryos. Thus, I assessed the role of secreted Wnts in the small intestine development, particularly in Id2KO embryos.

In order to efficiently block PORCN prior to epithelium re-organization at E15.5, the following experiment has been conducted: Wnt C-59 was administered once daily to the pregnant mice at E13.5, E14.5 and E15.25 (Fig. 39A). Control animals (vehicle) were treated with 5% DMSO at the same time points. The embryos were collected at E15.5 and the small intestines were subjected to further FACS analysis, immunostaining and RT-PCR analysis. Upon Wnt C-59 treatment, a significant loss of Lgr5GFP+ cells was observed in WT embryos ï up to 6-fold decrease (Fig. 39D) in comparison to control samples, as it was shown by FACS (Fig. 39B) and anti-GFP immunostaining (Fig. 39C). Interestingly, Id2KO embryos were affected less ï up to 3-fold downregulation of Lgr5GFP+ cells for posterior small intestine (Fig. 40A,B), yet the intensity of GFP signal has been reduced for both villi and intervilli regions (from 10^4 to 10^3 shown by FACS, also Fig. 40B).

Further investigation of Wnt C59-treated gut sections revealed no significant changes in their morphology. Particularly, Hematoxilin & Eosin staining didnôt show any abnormality in gut development (data not shown). In order to test whether the reduction of Lgr5GFP+ cells upon Wnt C-59 administration is due to apoptotic cell death, I have applied TUNEL assay. As shown in Fig. 41C, inhibition of Wnt secretion did not cause massive apoptotic events in the intestinal epithelium, in comparison to vehicle control. Additional experiment with Wnt inhibition in Id2KO Lgr5+ cells at E9.5+E10.5 was performed to check rescue of a mutant phenotype at E11.5, when *Id2*-deficient epithelium has a unique transcriptional profile. Changes in genes expression of Wnt C59-treated samples, as well as in a negative control, were analyzed by qRT-PCR. Our data confirm that Wnt signaling target genes, such as *Lgr5*, *Smoc2*, *Wnt6* , specific for E11.5 Id2KO gut, are absent upon Wnt inhibition *in vivo* (data not shown). Altogether, these results indicate that the early specification of Wnt-responsive Lgr5+ cells is driven by Wnt signaling activity within *Id2*-deficient epithelial cells. Importantly, this phenotype could be rescued by Wnt C59 administration during the earlier stages of the gut development.

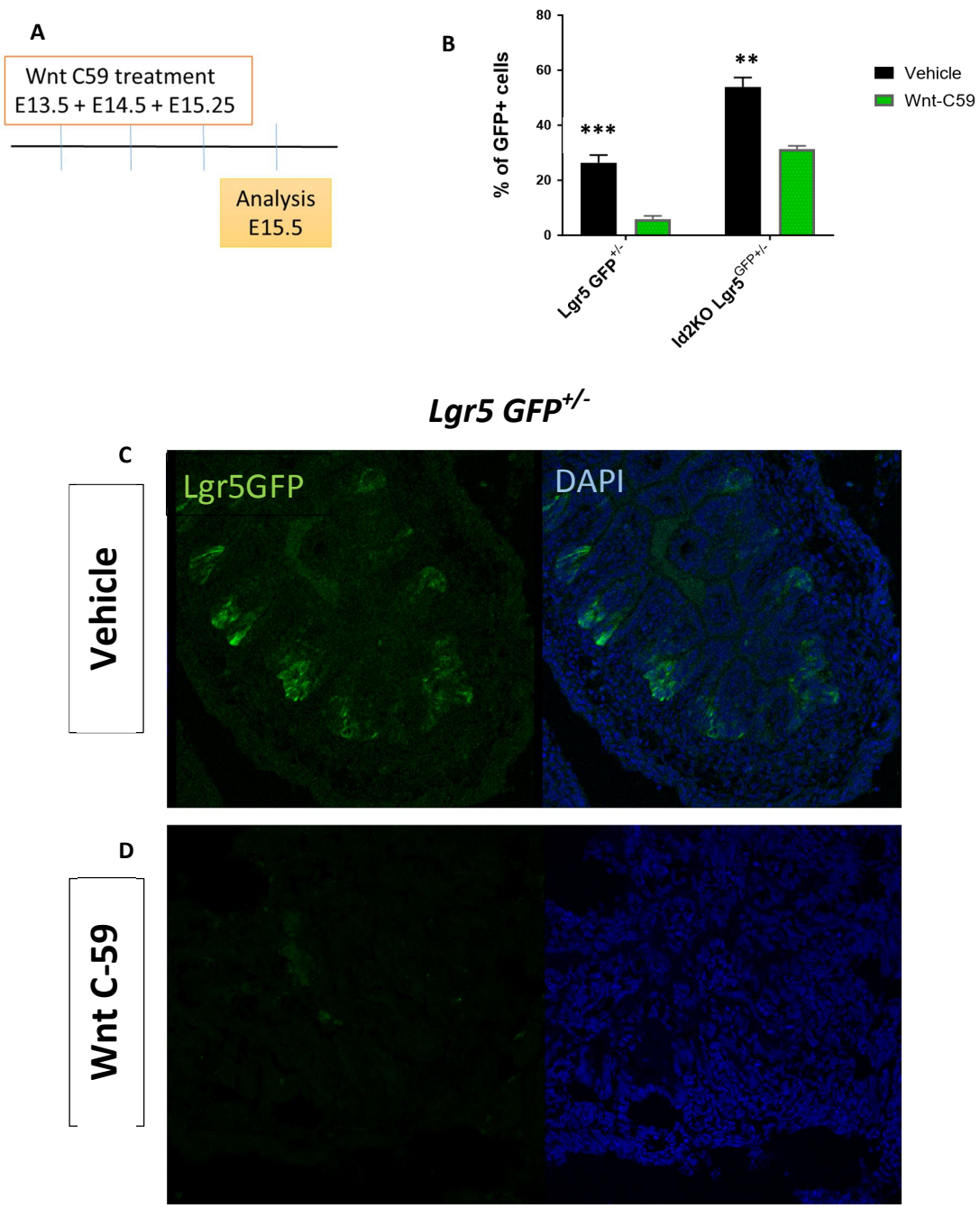

Figure 39. E15.5 intestinal epithelium is responding to inhibition of Wnt signaling *in vivo*. A. Experimental approach in which Wnt C59 inhibitor is administrated at E13.5+E14.5+E15.25 prior to villi-intervilli specification at E15.5. **B-D.** Upon Wnt C59 treatment the amount of E15.5 Lgr5GFP+ cells, measured for WT (black) and Id2KO (green) samples, is significantly reduced. This data in confirmed by immunostaining against GFP in *Id2WT Lgr5*$^{GFP+/-}$ sections (**C,D**). p**<0.01; p***<0.001, n=3.

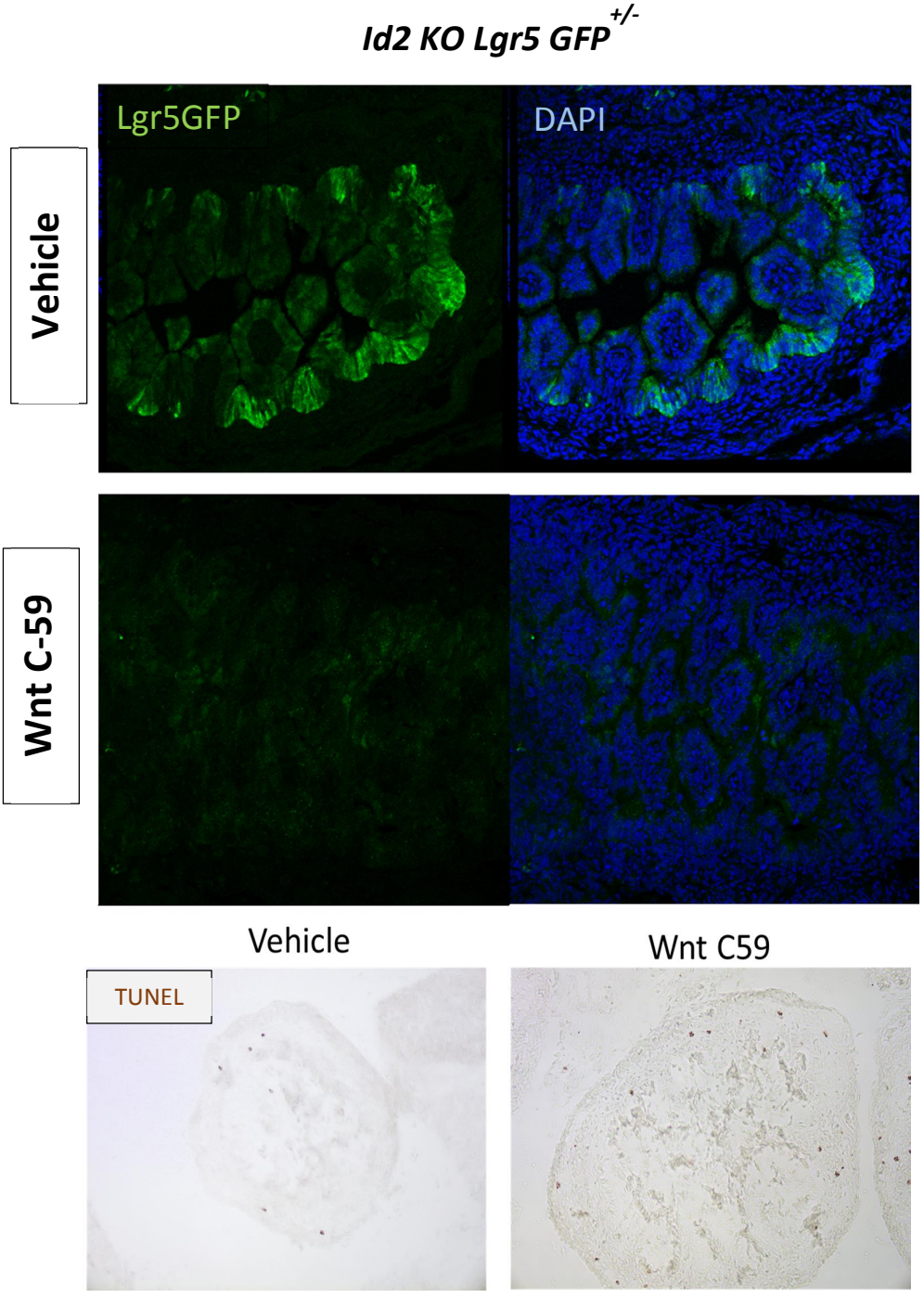

Figure 40. ***Id2*-deficient intestinal epithelium is responding to inhibition of Wnt signaling *in vivo*.** **A-B.** *Id2 KO Lgr5* $^{GFP+/-}$embryos, treated with Wnt C59 inhibitor at E13.5+E14.5+E15.25, displays a loss of Lgr5GFP+ cells at E15.5 (**B**), as compared to a control vehicle-treated sample (**A**). **C.** TUNEL assay (Promega) did not detect apoptosis in both vehicle- and Wnt C59-treated epithelial cells.

5.6. Id2 KO embryos small intestine development at neonatal stage.

Based on previous studies from Russel *et al*, 2004, intestinal abnormalities in *Id2*-null mouse development could be detected only after E18.5. *Id2-null* intestinal epithelial cells fail to have terminal differentiation and their active hyperproliferative state leads to neoplastic lesions in the small intestine. However, this phenotype was considered as a cell cycle arrest, but never related to early activation of *Lgr5* gene. Importantly, our comprehensive analysis of Id2KO epithelium indicates that *Id2* gene regulates the activity of Wnt signaling during the embryogenesis.

Here I examined intestinal morphology of newborn Id2 KO mice. According to Russel, 2004, E18.5 *Id2-null* intestine has adenomas regions, in which secretory Goblet cells are either overrepresented or completely absent. However, our detailed analysis of Id2 KO sections showed reduced amount of secretory Goblet cells throughout the whole intestinal epithelium (data not shown). Furthermore, cell proliferation assay with EdU-injected embryos allowed to visualize the regions with actively proliferating cells. As expected, in WT embryo proliferative cells are localized in intervillus compartment (Fig. 41A), whereas Id2KO-specific adenoma has a high proliferation in both villi-intervilli regions (Fig. 41B). Those abnormally dividing cells within mutant embryonic gut caused improperly differentiated structures, such as: cells hyperplasia (Fig. 41B), or merged villi (Fig.42C) or merged crypt compartments (Fig 42B), or shorter villi with keratinized intervillus epithelium (Fig. 42D) in comparison to healthy wilt-type state (Fig. 42A). In general, newborn Id2KO mouse small intestine has less differentiated villi formed.

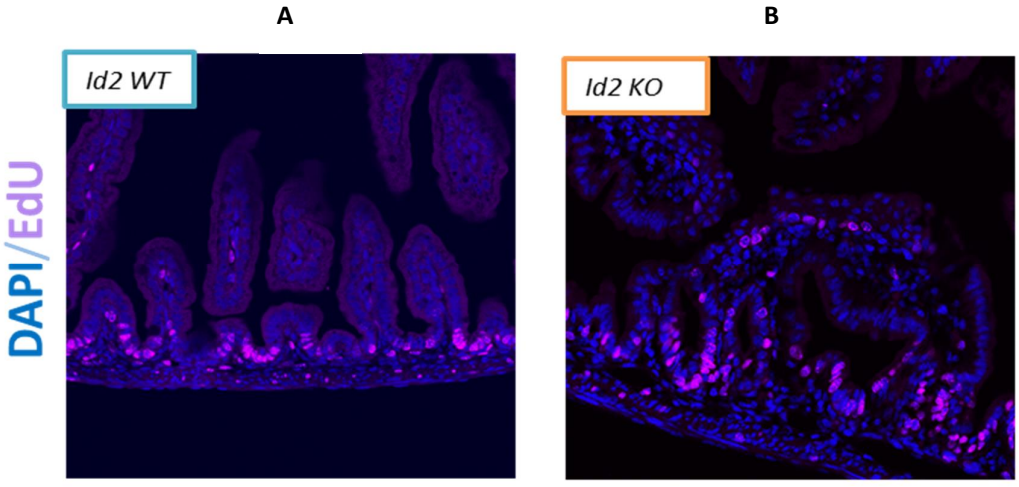

Figure 41. Cell proliferation identified by anti-EdU immunostaining on newborn mice. A-B. Pink color indicates the distribution of proliferating cells in WT (**A**) and Id2KO (**B**) intestinal epithelium.

I hypothesize that abnormally appeared Lgr5 stem cells actively divide and establish crypt-like hyperplastic regions within the embryonic gut (Fig. 41B). Consistent with our qPCR data analysis, performed on E15.5 Id2KO embryo samples, enormous upregulation of a cancer marker - nuclear

Trop2, is detected *in vivo* at stages E18.5-P0 (Fig. 42E, F). Therefore, Id2 KO neonate mice develop a tumor so early, already at neonatal stages, since *Id2* gene, suppressor of early Wnt activation in gut, is not expressed. *Id2* gene loss causes abnormal tissue differentiation, accompanied by nuclear Trop2 accumulation. Our hypothesis was further tested by Id2KO Lgr5 cells lineage tracing (chapter 5.8).

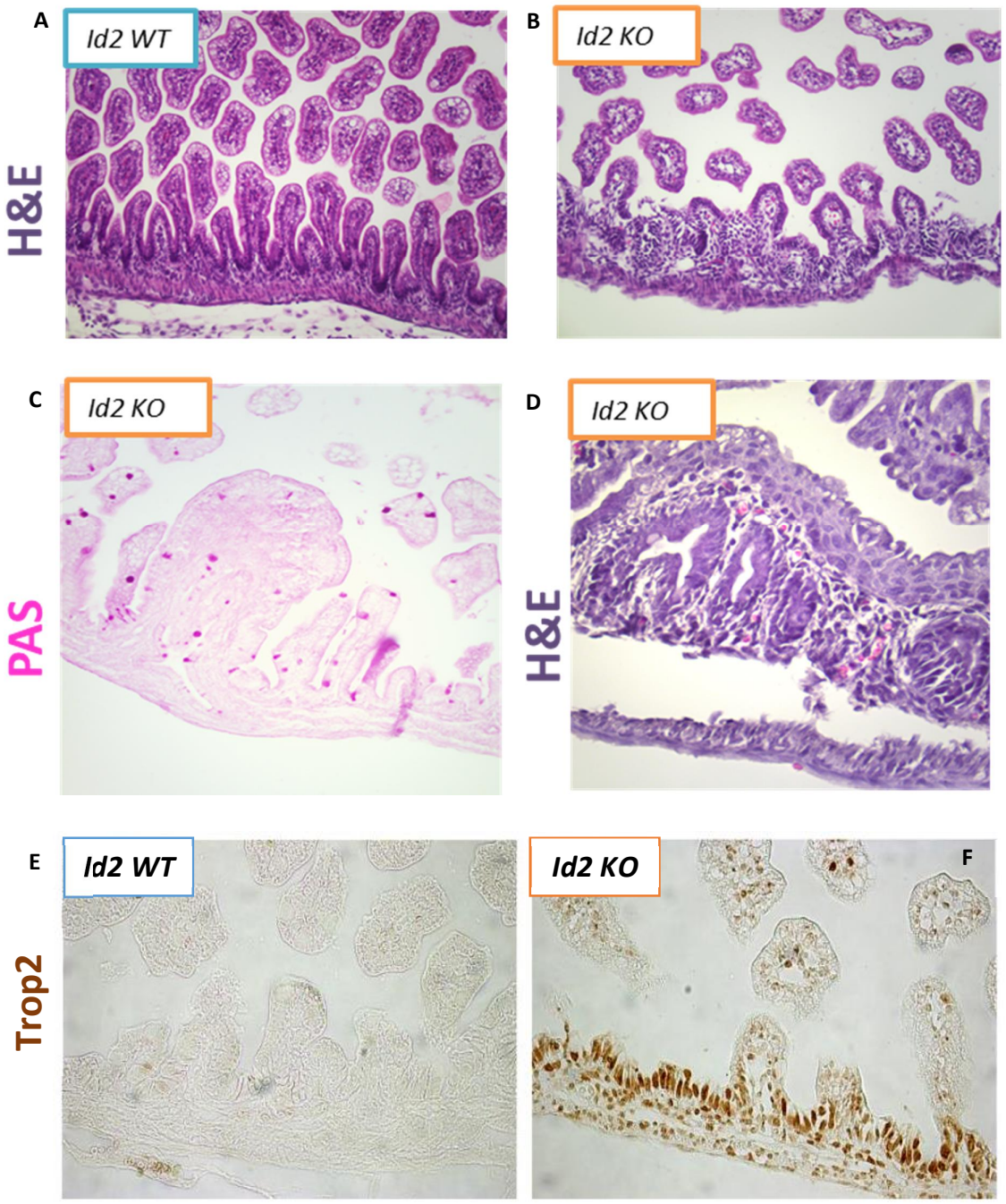

Figure 42. Immunohistological analisys of newborn mice demonstrates differentiation abnormalities, caused by *Id2* gene loss. A-D. Hematoxylin &Eosin staining of Id2 WT section (**A**) indicates a normal morphology of the small intestine. Severe intestinal abnormalities, observed in Id2KO sections: shortened villi (**B**), hyperplastic lesions (**C**), keratinized epithelium (**D**). **E,F.** Identification of nuclear Trop2 accumulation by immunostaining against its c-terminal intracellular domain (**F**). Notably, WT intestinal cells are Trop2-negative (**E**).

5.7. *Id2* KO adult mice small intestine phenotype.

Whereas Id2KO newborn mice could not be distinguished by their size from WT littermates, adult *Id2*-null mice had a reduced size and weight (35% less weight, Fig 42A, B). During dissection of the Id2 KO small intestine, a few small visible polyp-like structures within epithelium were observed (Fig. 42G). Despite of the significant abnormalities in embryonic development, adult intestine of Id2KO mice does not show expected severe cancer progression (Fig. 42H). However, further immuno-histochemical studies (IHC) showed differentiation abnormalities not only in those polyps, but throughout the whole epithelium. Thus, PAS staining of *Id2* mutant small intestine demonstrated significantly reduced number of secretory lineage cells ï Goblets in villi and Paneth cells in crypts (Fig. 43D, H). Interestingly, adenoma formed in the anterior gut, harbored abnormally high amount of Lysozyme positive both Paneth and Goblet cells and was classified as tubulovillous adenoma (Fig. 42G). However, in adult tissue Lgr5-GFP expressing cells were localized normally ï in crypts within ISCs (Fig 42 E, H) for both WT and KO tissues, with slightly higher level of GFP expression in posterior Id2 KO gut. In contrast to neonate stage, villi in Id2 KO mostly developed normally with the only differences in crypts composition (Fig. 42C,F). When stained with DAPI and b-catenin, the mutant Id2 tissue could be recognized by unusual cells shape in ISCs crypt compartment (Fig. 43A,B,E,F). Id2 KO crypts have cells twice less by size and nuclei occupy the whole cell shape, but in WT DAPI-stained nucleus is localized on a cell periphery because of the Lysozyme-containing granules (Fig. 43E). Indeed, further PAS and anti-Lysozyme stainings showed that Id2 KO small intestine has less Paneth cells (instead of 5 - only 1 or 2), constantly degranulated from lysozyme (Fig.42F, 43C, G).

Furthermore I examined the cellular composition in Id2-deficient intestinal epithelium by multicolored FACS analysis using cell-specific antibodies against Paneth/Goblet cells (UEA-1 TRITC), ISCs/enteroendocrine cells (CD24), performed on Id2WT Lgr5 GFP+ or Id2KO Lgr5GFP+ mouse samples (Fig. 44A,B). Consistent to immunostainings, Id2KO posterior gut contains a higher amount of $Lgr5^{GFP+}$ cells (Fig. 44A, middle panel). Interestingly, an additional cell population, positive for secretory lineage (UEA-1 high, CD24high) is present in Id2KO anterior epithelium (Fig. 44A, right panel). I assume that these cells are derived from tubular adenomas, that are enriched for secretory cells and found exclusively in anterior gut (Fig. 42G).

In summary, adult Id2 KO mouse has less abnormality in the small intestine in comparison to neonates. This could be explained by compensatory programs occurring after crypt formation and Paneth cells development on a second week after birth. The other reason could be that after E15.5 when villi-intervilli differentiated, Lgr5-gene expression in villi is inhibited by molecular signals coming from mesenchymal niche. In general, we canõt exclude the role of surrounding mesenchymal cell-to cell interactions that could provide Wnt ligands/antagonists and other essential signals for a proper gut homeostasis.

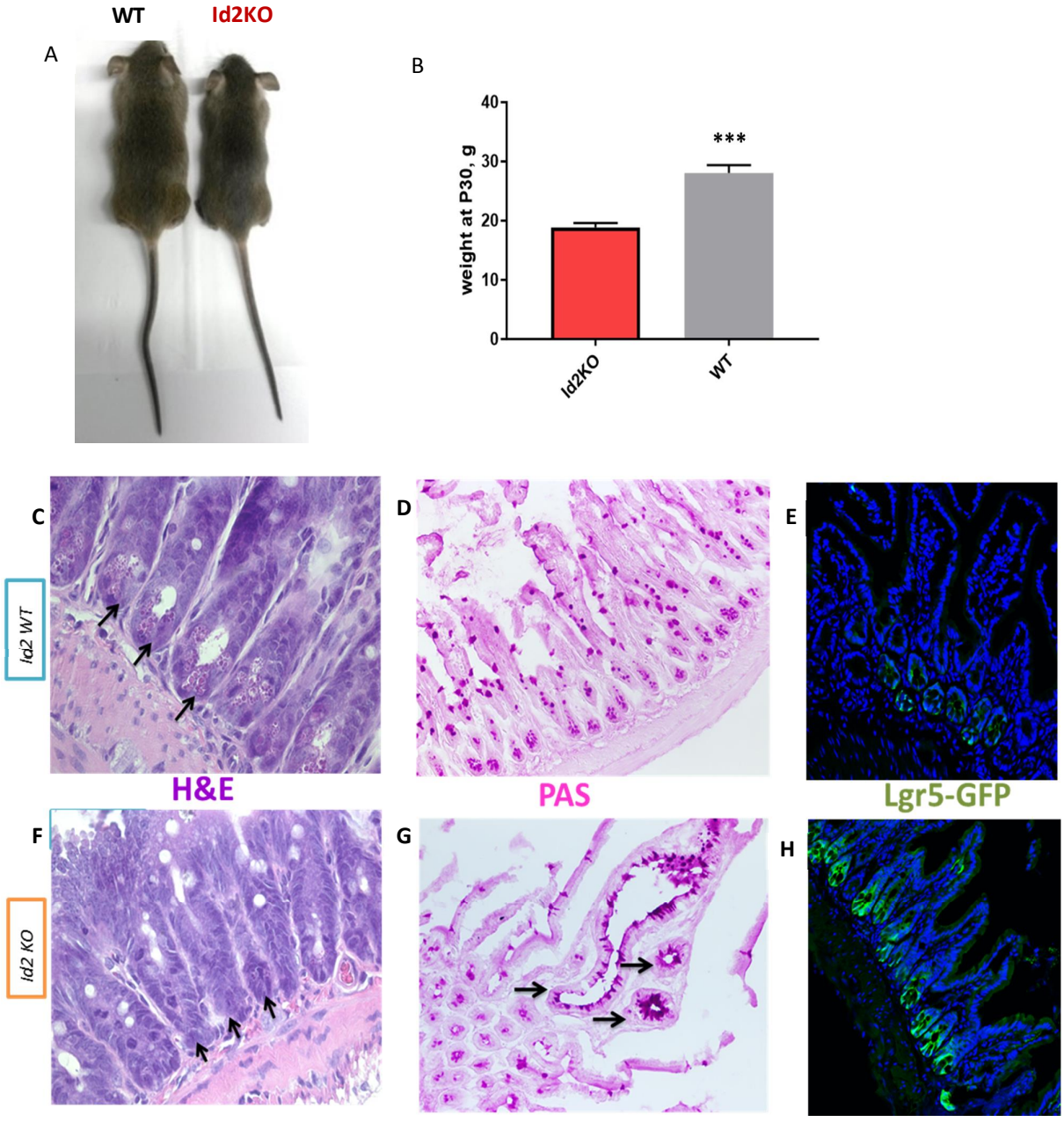

Figure 42. Adult *Id2*-mutant mice display severe abnormalities in intestinal epithelial cells differentiation. A-B. Id2 KO animals are retarded in growth, as the weight and size of these animals is significantly reduced, when compared to WT control (**A, B**). **C-H.** Cells morphology of WT intestinal sections (**C, D, H**) shows a healthy state of the gut epithelium. In contrast, intestinal cell differentiation abnormalities were found in Id2KO small intestine: degranulation of Paneth cells (**F**), tubulovillous adenoma (**G**). An elevated number of Lgr5GFPhigh cells, identified in Id2 mutant section (**H**) in comparison to Id2 WT Lgr5 $^{GFP+/-}$ control sample (**E**).

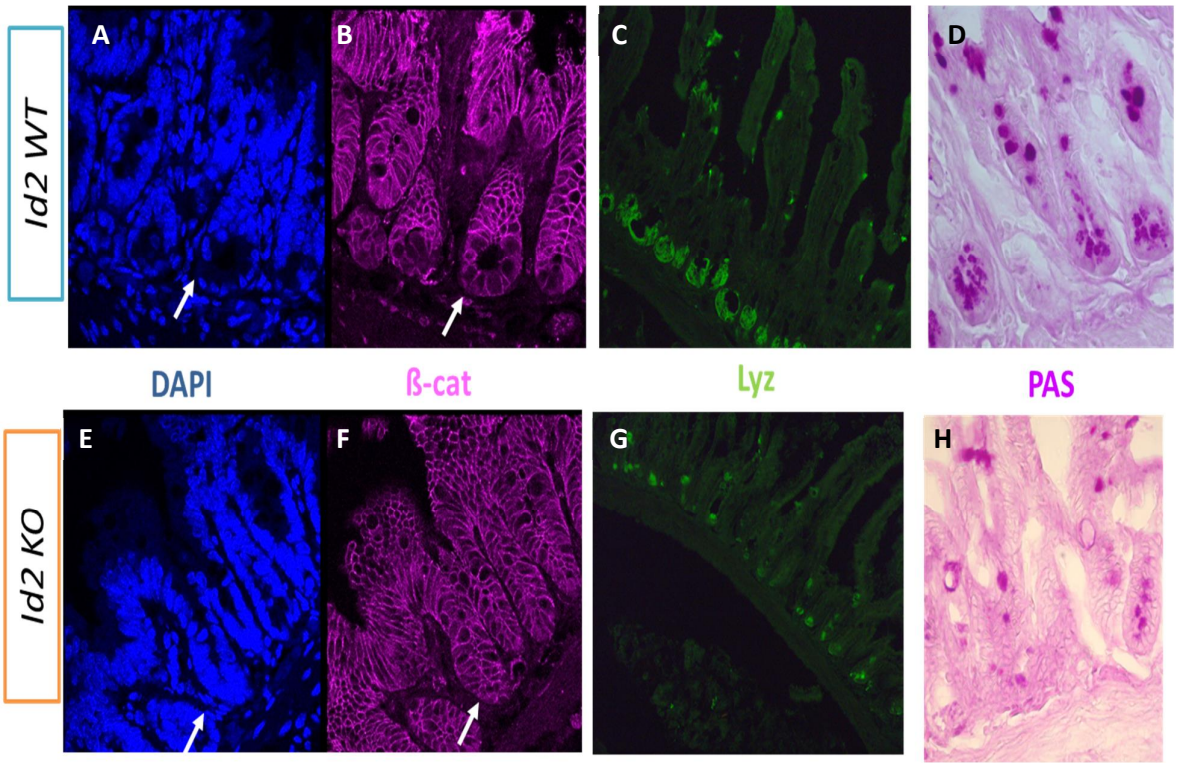

Fig 43. *Id2*- deficient cells analysis in adult mouse intestinal epithelium. A-H. DAPI staining shows a WT cell nucleus (**A**) located on a periphery of the stem cell compartment, but not in Id2 KO crypts (**E**). These data is confirmed by anti b-catenin staining (**B,F**). Hematoxilin & Eosin stainings of Id2 KO crypt regions (**H**) shows no granules in Paneth cells when compared to pink-colored granule pockets in WT (**D**) Lysozyme antibody staining indicates abnormalities in Paneth cells differentiation (**C,G**). White arrows show cell-to-cell boundaries.

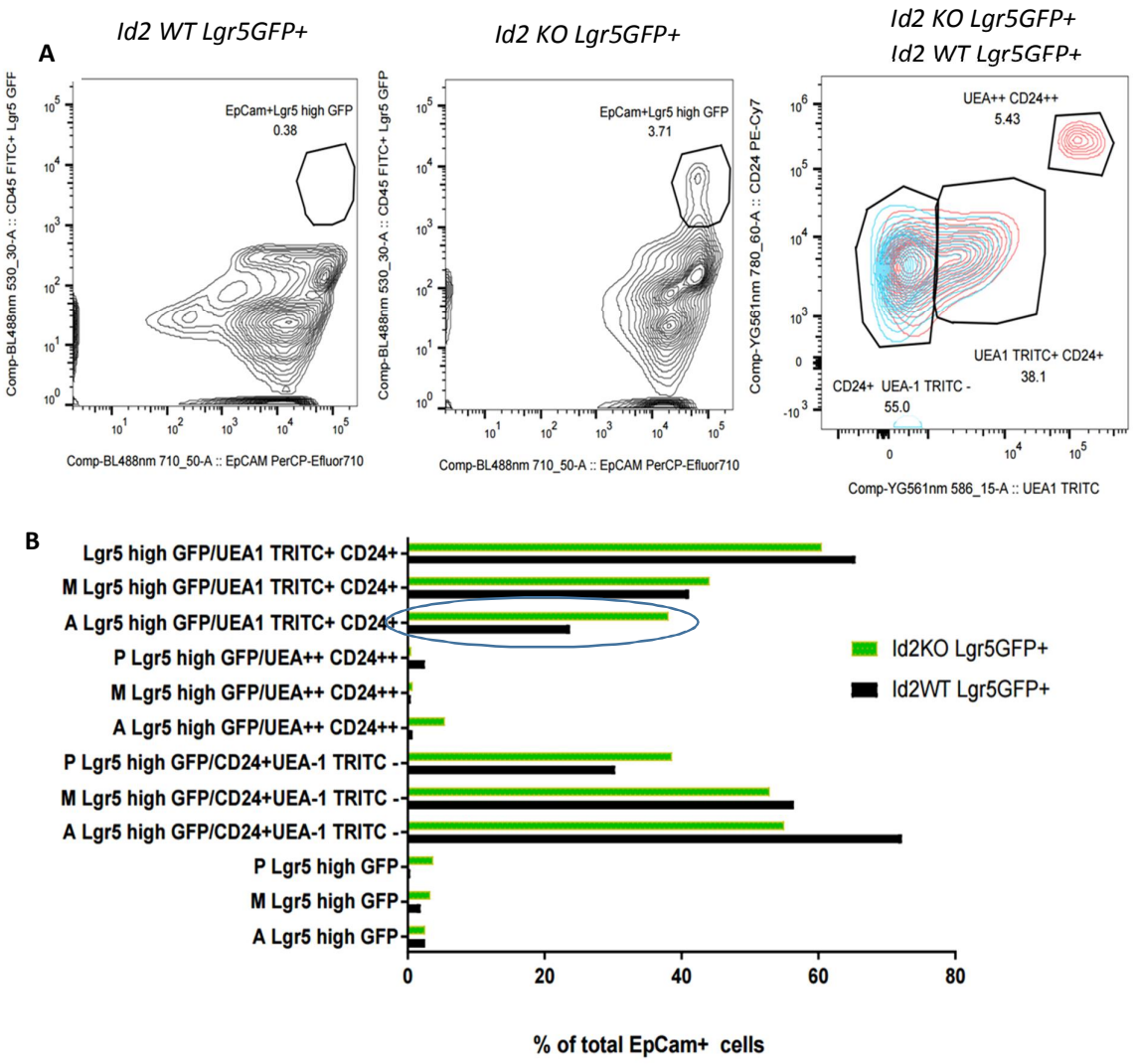

Figure 44. FACS-based analysis of *Id2 KO Lgr5*$^{GFP+/-}$ intestinal epithelium by using cell type-specific antibodies against secretory cells (UEA-1 TRITC) and ISCs/TA/enteroendocrine cells (CD24). A. FACS gating plot illustrates a presence of Lgr5GFP high population in Id2KO posterior gut (middle panel) when compared to Id2 WT Lgr5GFP control (right panel). Additional UEA-1/CD24-enriched population (red) is specific for an anterior Id2KO gut. **B**. Quantification of stained cell populations in anterior (A), middle (M) and posterior (P) epithelial cells. In a blue circle ï secretory population, found in Id2KO anterior gut.

5.8. Cell lineage tracing of Id2KO Lgr5+ cells at E11.5.

Finally, to understand the capacity of precociously specified Lgr5GFP+ cells in *Id2*-null intestinal epithelium to become adult ISCs and contribute to the intestinal homeostasis, I have performed a long-term lineage tracing. In order to distinguish early-activated Id2KO Lgr5+ cells, we have designed a following experimental strategy: $Id2^{GFP}$ knock-in mouse is used for generating $Id2^{GFP/GFP}$ (Id2KO) genotype. Importantly, *Id2* gene is silent in adult state, thus Lgr5GFP+ cells could be visualized on $Id2^{GFP/GFP}$ genetical background. Tamoxifen induction at E11.5 of $Id2^{GFP/GFP}Lgr5^{Cre\ GFP}Rosa^{tdTomato}$ embryo specifically labelled only precocious Id2KO *Lgr5Cre*-expressing cells. As shown in Fig. 45C, E11.5 labelled Id2KO LGR5+cells gave rise to Tomato+ ISCs in adult mouse with a cohesive ribbon of red differentiated cells. Conversely, neither $Id2^{GFP/GFP}Rosa^{tdTomato}$ (Fig. 45A), nor $Lgr5^{Cre\ GFP}Rosa^{tdTomato}$ (Fig. 45B) embryos were labelled upon Tam administration.

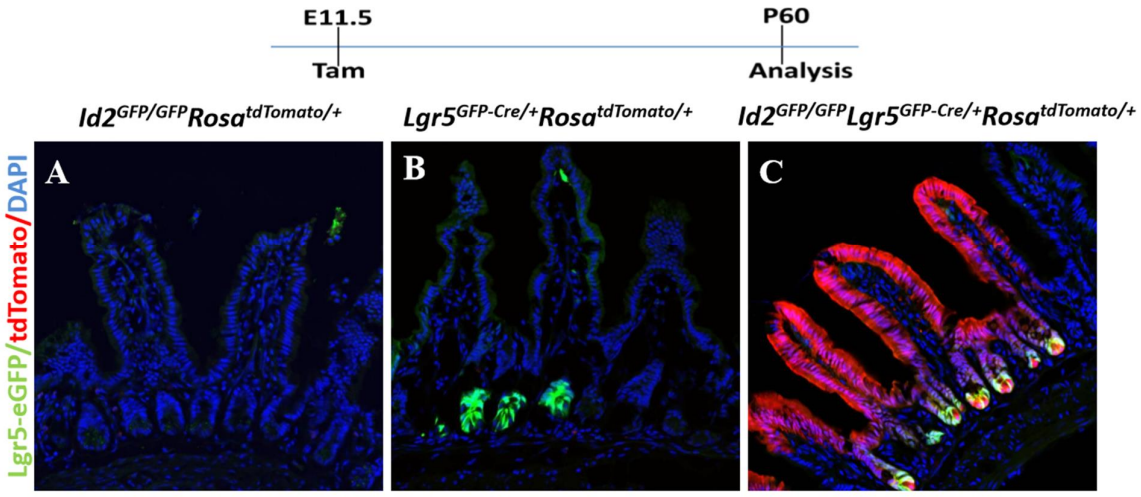

Figure 45. Impact of precociously specified Id2KO Lgr5GFP+ cells on adult intestinal homeostasis. A-C. Results of lineage tracing of Lgr5GFP-Cre expressing cells, labelled at E11.5 in $Id2^{GFP/GFP}Rosa^{tdTomato}$ (**A**), $Lgr5^{Cre\ GFP}Rosa^{tdTomato}$ (**B**) and $Id2^{GFP/GFP}Lgr5^{Cre\ GFP}Rosa^{tdTomato}$(**C**) embryos and analyzed at P60. This data shows that in *Id2*-deficient embryos, earlyï activated Lgr5+ cells develop into adult ISCs *in vivo*.

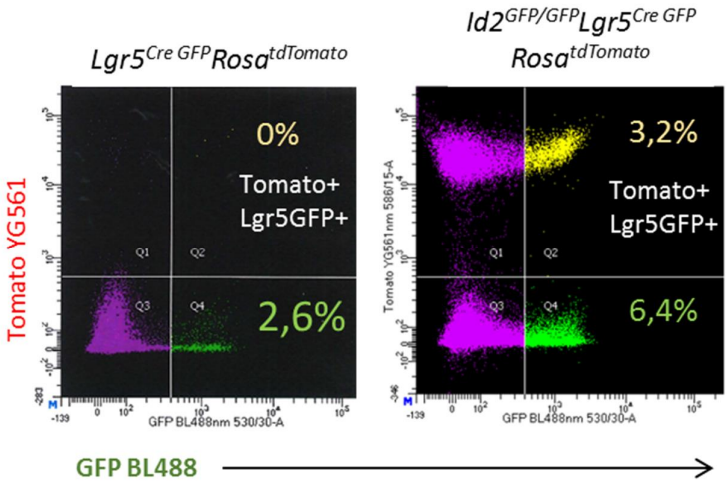

Figure 45. Precociously specified Id2KO Lgr5GFP+ cells have a significant contribution on adult posterior gut. Results of FACS analysis for E11.5 labelled Lgr5Cre-GFP+ expressing cells collected form $Lgr5^{Cre\ GFP}Rosa^{tdTomato}$ **(left panel)** and $Id2^{GFP/GFP}Lgr5^{Cre\ GFP}Rosa^{tdTomato}$ **(right panel)** This data indicates that in *Id2*-deficient embryos 50% of all ISCs are derived from earlyï activated Lgr5+ cells.

Further FACS quantification of E11.5 Tam labelled embryos revealed that Id2KO posterior intestine contains 3-fold increased amount of Lgr5GFP+ cells (Fig. 46B), confirming our previous results of anti-GFP immunostaining (Fig. 42H) and FACS analysis of P60 *Id2*-mutants (Fig. 44A, middle panel). Importantly, in a posterior Id2KO epithelium up to 50% of all LGRGFP+ cells are derived from E11.5 population. Control $Lgr5^{Cre\ GFP}Rosa^{tdTomato}$does not show any Tomato-labelled GFP+ cells (Fig. 46A). In order to characterize the transcriptional profiles of Id2KO-derived cells, I have collected 500 Lgr5GFP+ cells from anterior, middle and posterior gut epithelium and subjected them for further RNA-sequencing. Bioinformatical analysis of Lgr5GFP+ISCs from both Id2KO and WT embryos revealed no significant differences in the expression of ñstemnessò genes, including *Lgr5*, *Ascl2* and *Tcf4*. In total around 600 genes were differently expressed in middle and posterior parts of *Id2*-mutant ISCs (log2FC Ó 0.5, FDR < 0.01). Among the mostly changed genes are *Atoh1*, regulating a secretory lineage choice in TA cells, as well as ISC markers *Lrig1* and *Olfm4*.

Altogether, here I confirm that in the absence of *Id2* gene activity, Lgr5GFP+ cells appear at E9.5, and contribute to adult ISCs *in vivo*. The transcriptional profile of ISCs is affected by *Id2* loss. Precociously specified Lgr5GFP+ cells cause impaired cell differentiation and tumor development already at neonatal stage.

6. Discussion.

6.1. First Lgr5+ ISC progenitors appear at E13.5 within a developing mouse gut epithelium.

Numerous studies on the small intestinal epithelium have elucidated the key transcriptional factors and chromatin modifiers, regulating identity of adult ISCs (Korinek, 1998; Tian, 2015; Chiacchiera, 2016). Wnt signaling activity plays an essential role in maintenance of gut epithelial homeostasis, since it regulates a master switch between proliferation and differentiation, establishing a proper crypt-villi axis in gut epithelium. However, the entire process, controlling emergence of so-called adult state, with functionally specified ISCs, from its fetal progenitors during gut development remained uncovered. Current results on transcriptional networks, required for establishing Lgr5+ progenitors of ISCs in embryonic epithelium, are limited, instigating some confusion and controversy in the field of developmental biology. Thus, the role of Wnt/ϐ-catenin activity in a proper specification of embryonic Lgr5+ intestinal cells is poorly understood. *Lgr5*-expressing cells have been detected at E15.5 stage in intervillus region and reside exclusively in a forming crypt compartment ï an eventual place of Lgr5+ adult ISCs (Garcia et al., 2009); (Kim, 2012); (Kinzel et al., 2014). Fig.5C). This hypothesis is strengthened by co-expression of other ISC markers, such as *CD44* (Kim et al., 2007), *Axin2* (Garcia et al., 2009) and *Olfm4* (Kinzel, 2014) in intervillus pockets. This model indicated the appearance of embryonic precursors of adult ISCs late during embryogenesis. However, according to the recent studies from Shyer and colleagues (Shyer, 2015), *Lgr5*-expressing cells are found throughout the epithelium already in the embryonic day 12.5 (E12.5) small intestine, just prior to villus formation. Over the following days of development, *Lgr5* expression, as well as *CD44*, is lost in the forming villus tip and is progressively restricted to the space between villi as they form. Authors suggest the opposite mechanism of Wnt activity in crypt progenitors where subadjacent mesenchyme drives villus clusters gene expression (*Bmp4, Pdgfa*), thus repressing ubiquitous expression of *Lgr5* gene in villi.

In the present study, I characterize the process of the embryonic small intestine development by using mouse animal model. I aimed to resolve very important questions related to whether predefined stem cell progenitors exist in the fetal intestinal epithelium and await a specification stimulus or whether all epithelial cells that proliferate are equipotent. Our findings established the essential role of canonical Wnt activation for a proper maturation of ISCs both *in vitro* and *in vivo*.

Lgr5 gene transcriptional activity is supposed to be specific to the most primitive cell type committed to an ISC lineage (Cao, 2013). In this regard, most of the current studies on ISCs are conducted by using Lgr5-CreRT-eGFP mouse strain (Barker, 2007), where *Lgr5* gene transcription could be examined by GFP cassette expression, as well as by Tamoxifen inducible Cre-recombinase activity. These limitations are due to the lack of specific antibodies against *Lgr5* gene product. On the other side, although multiple markers for ISC populations has been proposed, many of them do not

have a direct evidence for stemness as shown by lineage tracing or transplantation experiments (Barker, 2012).

Our RNA *in situ* analysis against *Lgr5* mRNA molecules, strengthened with FACS-based quantification of Lgr5GFP+ cells, demonstrate the presence of Lgr5+ cells subset within E13.5 intestinal gut epithelium of *Lgr5*$^{eGFP\text{-}CreRT2}$ knock-in mouse embryo. Immunostaining against GFP confirmed that Lgr5+ population is emerging as a minor cell population from posterior part of the growing gut. During the embryonic development, the amount of *Lgr5*-expressing cells is increasing gradually, whereas the highest number of Lgr5GFP+ cells was found at E15.5 ï the time point of active epithelial reorganization into differentiated villi and intervilli. Furthermore, I examined the capacity of E13.5 Lgr5-expressing cells to give rise to ISCs by cell fate mapping experiment. Thus, here I show for the first time that a subset of embryonic Lgr5+ cells contributes to adult ISCs. RNA-sequencing on a very low amount of Lgr5GFP+ embryonic cells (500 cells per replicate) enabled us to explore further the transcriptional status of ISCs progenitors when compared to the rest *Lgr5*-negative cells within E13.5 epithelium. Bioinformatical analysis revealed that Lgr5+ cells are expressing many Wnt/ß-catenin signaling target genes, implying that activation of Wnt pathway takes place in a cell-specific manner. Moreover, this population expresses the genes, controlling cell cycle progression and proliferation. Notably, the rest intestinal epithelium is rather Wnt signaling negative, as it is enriched for Wnt antagonist *Sfrp5*, as well for the markers of intestinal differentiation, such as *Fabp1/Fabp2*, *Anpep1* and *Slc2a3*.

In this study, it was important to characterize embryonic intestinal cells on a genome-wide transcriptional level, because amount of Lgr5 mRNA and protein are usually low and the transgenic mice may not represent 100% of a desired cell population. I have examined the expression level of other stem cell markers expression (*CD44*, *Ascl2*, *Olfm4*), in conjunction with *Lgr5* to substantiate their biological relevance to early Wnt signalling response.

Our comprehensive analysis of E13.5 gut epithelium resolves a very important controversy, existing over appearance of adult ISCs progenies *in vivo*. Previous models hypothesized that the whole embryonic intestinal epithelium is composed of Wnt-responsive Lgr5+ cells and their amount is decreasing at E15.5 by getting restricted to the intervillus compartment (Shyer, 2015). By combining many experimental approaches, including cell fate mapping, *in situ* hybridization, FACS analysis and *ex vivo* cell culture, I demonstrate here that the first Lgr5+ISC progenitors emerge at E13.5 as a minor subset of cells, expressing Wnt signalling target genes. Yet, these genes are expressed on a low level in comparison to adult state.

6.2. The embryonic intestinal cells do not fully resemble adult ISCs.

The embryonic epithelium undergoes dramatic changes to maturate into the functional small intestine. Thus, many embryonic epithelial genes, such as *Shh*, *Id2*, *Tcf7l1*, become silent after neonatal stage and cell-specific differentiation markers could be easily recognized (see chapter 5.2.2). On the other hand, a newborn mouse is subjected to a new environment, including nutrition, microbes and changed hormonal status. Obviously, adult Lgr5+ cells should have a high self-renewing and differentiation capacity to maintain the small intestine due to its constant exposure to biological and mechanical insults. But to claim it we are challenged to the methodological issue on how to compare the functional relevance of ISCs to embryonic progenitors. In 2009, Sato and colleagues reported a successful method, devised for growing the long-term three-dimensional culture of adult intestinal epithelium as organoids (Sato et al., 2009). Thus, establishing a method, required for growing embryonic Lgr5+ cells in culture conditions, was an important step for my research. When I started my PhD project, only organoids, derived either from the adult gut (Sato, 2009), or from human iPSCs (Spence et al., 2011) were described. By adapting these culture conditions for mouse embryonic material, I established the method to maintain primary isolated cells *ex vivo*. This protocol, describing the isolation of living embryonic intestinal cells, FACS sorting and seeding the cells in ibidi chambers, became a widely used technique not only in our lab, but also for our collaborators. However, at this time two other research groups (Fordham et al., 2013); (Mustata et al., 2013) independently reported the similar protocol.

Our data on establishing the conditions for growing E13.5 Lgr5+ cells *ex vivo* was very essential to support the idea that embryonic progenitors of ISCs do not fully represent their adult state. Moreover, our findings are supporting the published report of Mustata et.al (2013), where embryonic intestinal cells< E14.0 fail to form crypt-like organoids. Indeed, E13.5 Lgr5+ cells grown in adult ISCs growth conditions (R-Spo, EGF, Noggin), do not have a high capacity to generate organoids, that are harbouring ISCs *ex vivo* (Fig. 21C). The embryonic intestinal epithelium is highly proliferative and gives rise to undifferentiated spheroids that subsequently maturate into Lgr5+ ISCs *in vivo* (Fordham, 2013). Furthermore, I have compared the properties of cellular composition of spheroid-derived organoids (Fig. 20B). Histological examination of organoids showed the presence of all four intestinal cell types: lysozyme-positive Paneth cells, chromogranin A-positive enteroendocrine cells, alkaline phosphatase-positive enterocytes as well as PAS-stained Goblet cells (Fig.20B, lowest panel). However, spheroid-derived organoids do not contain Paneth cells (Fig.20B, upper panel). I assume that most likely, these structures represent the stepwise maturation of embryonic intestinal epithelium, taking place *in vivo*. This statement is based on the fact that Goblet and enterocytes are present already at E15.5 in new-formed villi, whereas Paneth cells appear only 3 weeks later, at stage P7-14, when crypt compartment with adult ISCs is established.

Altogether, our data provide a valuable information regarding the functional properties of early embryonic gut material for further stem cell investigations, such as cell lineage choice, cell ageing and tissue transplantation issues.

6.3. Embryonic intestinal cells, heterozygous for *Id2* gene, have a high proliferation and contribute to adult ISCs pool *in vivo.*

Our results, demonstrating that embryonic Lgr5-negative cells proliferate and give rise to both organoids and spheroids more efficiently then Lgr5+ population, were rather unexpected. This phenomenon is very important, since it shows the functional differences between adult ISCs and their embryonic progenitors. Notably, the cell culture conditions and growth factors with which we test the properties of E13.5 Lgr5+ cells may be not optimal to represent the proper capacities of the isolated population. We canôt exclude the necessity of signalling factors provided by sub-epithelial tissues either. In fact, our 3D *ex vivo* system lack the mesenchymal, stromal, immune and neural cells that contribute to the functional gut *in vivo.*

To examine further if Lgr5+ progenitorsô specification takes place earlier in a certain embryonic cell population or not pre-determined and forced by independent molecular signalling from surrounding mesenchyme, I decided to analyze the dynamics of cell population(s) within the actively growing epithelium at E11.5. Importantly, the addressed question required to work on animal level because the cellular complexity cannot be fully recapitulated *ex vivo.* For this approach, we have designed an experimental strategy, where all intestinal epithelial cells would be labelled and manipulated *in vivo*. *Id2* gene, encoding **i**nhibitor of **d**ifferentiation, is a target of Wnt/BMP signaling and regulates cell growth, cell fate determination and differentiation in stem cells and their progenitors during development and adult life. In mouse, *Id2* is highly expressed in the small intestine starting from E9.5-10.5, this gene product is abundant in both, epithelium and mesenchyme (Fig.22A), while we did not detect *Id2* expression in adult intestine (Fig.22 B,C). Based on our previous *in situ* and RNA-seq data, *Id2* knock-in inducible reporter mouse (Rawlins, 2009), available for crosses, have been selected. When bred to $Rosa^{tdTomato/eGFP}$ reporter mouse, resulted $Id2^{Cre}Rosa^{tdTomato/eGFP}$ embryos after Tamoxifen administration would lose their red cassette (*tdTomato*) in all embryonic intestinal cells and become GFP^{+} forever. We suggested to identify a cell population, that divides the fastest (if so - gaining GFP expression first) within the growing intestinal epithelium, thus having a potential to become Lgr5+ progenitor population.

Despite our expectations, the labelling efficiency of $Id2^{Cre/+}Rosa^{tdTomato/eGFP}$ embryos, injected with Tamoxifen at E11.5 and analyzed the next day after Cre recombinase induction, was very low (3,3% instead of expected >90%). Analysis of labelled cellsô ratio after 2,4, 5 and 7 days gave a gradual increase in their number, but never reached 80%. Of note, while the lineage tracing is powerful for studying stem cells in adult epithelia (Kretzschmar, 2012), its application for embryonic studies is limited due to side effects caused by Tamoxifen administration (such as spontaneous

abortions in pregnant mice or hemorrhage and toxicity for embryos). In addition, the field uses different doses of tamoxifen, which can affect labelling efficiency and read-out.

Considering the possibility in varying labelling efficiency that is evident not only between different mouse models, harboring a similar gene promoter, but also within a given strain (Rios, 2016), I have tested other mouse reporter systems, *Rosa*$^{Stop/tdTomato}$ and *Rosa*$^{Stop/LacZ}$. The experiments with lineage tracing of *Id2*^{Cre} expressing cells gave a very interesting and important phenomenon: *Id2* gene heterozygosity (specifically for Id2$^{Cre+\ high}$ cells) seemed to play a role in an increased cell proliferation and contribution to ISCs lineage *in vivo* (Fig. 24C-I).

6.4. Lgr5+ cells at E13.5 do not origin exclusively from Id2^{high} cell population.

Our data suggested a possible role of Id2$^{Cre+\ high}$ cells in establishing Lgr5+ progenitors (Fig. 27A), since the number of Lgr5+ cells have been significantly increased at E13.5 and E15.5 in *Id2*$^{Cre/+}$*Lgr5*$^{CreRT-GFP}$ embryos. I wanted to understand if all Lgr5+ progenitors are generated by a pool of Id2$^{Cre+high}$ population. The molecular identity of two populations: Id2$^{Cre/+}$Lgr5$^{CreRT-GFP}$, traced from E11.5, and not labelled Lgr5$^{CreRT-GFP}$ populations as if they belong to distinct cell types, was assessed by RNA-sequencing. An experiment with triple heterozygous cross using *Id2*^{CreRT}, *Lgr5*$^{CreRT-GFP}$ and *Rosa*$^{Stop/tdTomato}$ mice was designed. We followed the cell fate of E11.5 Id2$^{Cre/+}$ cells by tdTomato label, induced by Tamoxifen treatment, whereas *Lgr5*$^{CreRT-GFP}$ knock-in cassette would start to be expressed only at E13.5 (Fig. 26B-E). Co-localization of green *Lgr5*-expressing cells with labelled Id2^{Tomato} cells (giving an orange signal on FACS) would demonstrate that Lgr5+ progenies originate from Id2$^{CreRT+\ high}$ population *in vivo*.

Lgr5$^{CreRT-GFP/}$*Id2*^{Cre}/*Rosa*$^{Stop/tdTomato}$ embryo, injected with Tam at E11.5 and analyzed at E13.5, shows that approximately 10% of all *Id2*$^{Cre+}$/*Rosa*^{tdTomato} gave rise to Lgr5+ progenies (Figure 26C, see Q1 and Q2 quadrants). In our experiment only 25-30% of Lgr5^{EGFP+} cells originate from Id2 $^{highCre+}$ population (Fig. 26C, Q2- Q3). When the embryos were analysed prior to villi-intervilli specification at E15.5, I saw that the amount of red labelled *Lgr5*$^{CreRT-GFP}$ cells increased twice (25%), showing that those cells continue to proliferate and contribute to future ISCs pool. Our results of RNA-seq revealed no significant DE genes, identified between Lgr5+ and Id2$^{+/-}$ Lgr5^{GFP} cell populations either.

Summarizing, the results of Lgr5+ cells tracing demonstrate that most likely the specification of Lgr5+ cells does not take place in a specific cell population and rather is not pre-determined. In support to this idea, lineage tracing of other stem cell marker-specific populations, like *Axin2*, *Foxa2* and *CD133* (shown by our groupmembers), gave very similar results. Moreover, it seems, that regardless of what cell population gave rise to Lgr5+ cells, at E13.5 Lgr5+ cells have an identical transcriptional profile, responsive to Wnt-signaling. Apparently, determination of Lgr5+ cells occurs

in any cell before E11.5 and may be regulated by mesenchymal signaling crosstalk or dictated by position of a cell.

6.5. Deciphering the molecular mechanism, which establishes the Lgr5+ progenitor population within E13.5 gut.

6.5.1. Id2KO intestinal epithelium has an increased number of Lgr5+ cells.

Lgr5$^{GFP/+}$ mice crossed with *Id2*$^{CreRT/+}$ background displayed an increased number of Lgr5GFP+ cells and their high proliferation capacities, implying that *Id2* gene itself may act upstream of Wnt signaling and play role in Lgr5+ cells formation. Moreover, Russel and colleagues (2004) showed that loss of *Id2* (Id2KO) in the mouse intestinal epithelium prevents exit from cell cycle and proper differentiation of enterocyte precursor cells during embryogenesis. *Id2-null* intestinal epithelial progenitors have a hyperproliferative state at E18.5 and fail to undergo terminal differentiation. An impaired differentiation leads to tumor progression in postnatal life (Russell et al., 2004). We therefore reasoned that this dramatic phenotype could be explained by an abnormal number of ISCs progenitors, formed during the small intestine development.

FACS analysis of E11.5 Id2KOLgr5^{GFP} embryos showed the precocious appearance of Lgr5+ cell population within the developing gut epithelium (30% of total epithelial cells), whereas wild-type control (Id2$^{+/+}$Lgr5^{GFP}) remains GFP-negative until E13.5. Moreover, at E9.5, as soon as the embryonic gut tube closed, Lgr5+ cells are already present in *Id2*-null mice (Fig. 29A-B). Immunostaining against GFP showed that these cells are occupying the posterior part of the intestinal epithelium, as shown on E9.5 and E11.5 sections (Fig. 29A, C). Thus, *Id2* gene dysfunction affects early activation of Wnt target - *Lgr5* gene expression. To examine further if precociously formed Lgr5+ cells resemble molecular characteristics of ISCs progenitors at E13.5 in a wild-type state, I have performed RNA-sequencing of Id2KO cells at E11.5.

When we compared Lgr5KO cells to control EpCam WT, more than 1000 differentially expressed genes (p-value<0,01) were found (Fig. 31A). Bioinformatical analysis revealed that indeed *Id2* loss has an effect on upregulation of Wnt-responsive target genes, such as *Lgr5* gene itself, *Tnfrsf19, Smoc2.* Interestingly, Id2KO Lgr5+ cells are expressing adult ISC markers *Lrig1* and *Prom1*, absent in E13.5 WT Lgr5+ cells. Notably, *Prom1*-expressing cells in adult crypts are more susceptible to tumor transformation. (Zhu L, 2009). We assume that *Id2* is gatekeeping early maturation of the intestinal epithelium.

6.5.2. Blocking of Wnt secretion attenuates transcription of early activated Wnt-responsive genes *in vivo*.

Among other DE genes, which are were not detected in control WT Lgr5+ cells, we have found ligands *Wnt6* and *Wnt 11.* We hypothesized that these ligands can mediate an early activated Wnt signaling response, caused by *Id2* deletion. It has been demonstrated before that both ligands are normally provided by Paneth cells in adult crypts (Sato, 2011; Farin, 2012; Durand, 2012). Moreover, Wnt6 and Wnt 11 have been identified as potential signaling molecules in intestinal cancers (Dimitriadis A, 2001; Ouko, 2006). Wnt11-secreting cells medium stimulates proliferation and migration of IEC6 intestinal epithelial cells in non-canonical Wnt signaling pathway (Ouko, 2006), whereas Wnt6 stimulates *ex vivo* growth of intestinal organoids (Farin, 2012).

I aimed further to understand the role of Wnt ligands in precocious specification of Lgr5+ ISC progenitors at E9.5. Thus, blocking of Wnt secreted molecules by Wnt C59 compound (Proffit, 2013) in a developing intestinal epithelium (E9.5 + E10.5) prevents increased number of Lgr5+ cells at E11.5. Changes in genes expression of Wnt C59-treated samples, as well as in a negative control, were analyzed by qRT-PCR. Our data confirm that Wnt signaling target genes, such as *Lgr5*, *Smoc2*, *Wnt6*, specific for E11.5 Id2KO gut, are absent upon Wnt inhibition *in vivo*.

The Spence group has investigated the similar question regarding the role of Wnt signaling during mammalian gut development (Chin, 2016). *Wnt11* ligand has been identified as one of four upregulated genes, present in E13.5/E15.5 wild-type intestine. Notably, in their experiment the whole gut structure has been analyzed, without purification of mesenchyme- or epithelial-derived cells. This is a very interesting finding, since our RNA-seq data for E13.5 WT cells lack mesenchymal tissue. I suggest that Wnt6 and Wnt11 genes activation, taking place in wild-type mesenchyme, may in fact participate in embryonic gut development. Our data show that in Id2KO embryos the expression of Wnt6 ligand is specific for epithelial cells, whereas the upregulation of Wnt11 is observed in both intestinal mesenchyme and epithelium.

Chin et al. (2016) also inhibited Wnt secretion separately in epithelial and mesenchymal cells by using *Wntless-floxed* mouse model. Interestingly, their data show that blocking Wnt ligand secretion at E13.5 from the mesenchyme or the epithelium doesnôt change proliferation. In contrast, Wnt ligands secreted from the mesenchyme at E15.5 are required for Wnt/ß-catenin target gene expression and proliferation in the epithelium.

Independently, I have conducted the similar experiment with Wnt C59 compound by treating Id2KOLgr5^{GFP} and Id2WTLgr5^{GFP} embryos at later stages, E13.4+E14.5+E15.25. The embryos were collected at E15.5 and the small intestines were subjected to further FACS analysis, immunostaining

and RT-PCR analysis. Upon Wnt C-59 treatment, a significant loss of Lgr5GFP+ cells was observed also in WT embryos ï up to 6-fold decrease (Fig. 39D) in comparison to control vehicle-treated samples, as it was shown by FACS (Fig. 39B) and anti-GFP immunostaining (Fig. 39C). Interestingly, Id2KO embryos were affected less ï up to 3-fold downregulation of Lgr5GFP+ cells for posterior small intestine (Fig. 40A,B), yet the intensity of GFP signal has been reduced for both villi and intervilli regions (from 10^4 to 10^3 shown by FACS, also Fig. 40B). These results indicate that development of wild-type embryonic epithelium is also Wnt-signaling dependent. Most probably, in *Id2*-null mice Wnt C59-mediated blocking of Wnt ligands after E13.5 is late, because the cells are affected by other downstream activated mechanisms.

Altogether our data demonstrate that secreted Wnt molecules are playing essential role in establishing Wnt signaling response. Our results confirm that blocking of Wnt pathway decreases Lgr5+ cells number at E15.5 (Chin, 2016). Importantly, our approach with Wnt C59 treatment has been shown to be more efficient (Nigmatullina, 2017), then using *Wntless-floxed* mouse model. Yet the molecular source, providing Wnt ligands during the embryonic gut development has to be identified.

Interestingly, the niche, maintaining Wnt ligands in the adult small intestine, is poorly understood as well. Paneth cells are believed to provide Wnt ligands to neighboring Lgr5+ cells, however, ISCs could function even after complete loss of Paneth cells (Durand et al., 2012; Kim 2012). Recent data from Stzepourginski et al., (2017) and Horigouchi et al,. (2017) report that mesenchymal cells, localized around crypts, might maintain ISCs by secreting Wnt2b and Angiopoietin like protein (*Angptl2*). These results indicate that the proper development and functioning of ISCs is highly dependent on epithelial-mesenchymal signals crosstalk.

6.5.3. *Id2* deficiency causes increased number of abnormally specified Lgr5+ cells during villi-intervilli formation.

To evaluate further the functional consequences of early Wnt signaling activation in intestinal epithelium development, I analyzed embryos at E15.5 ï the stage when villus formation occurs. The amount of $Lgr5^{GFP+}$ cells at E15.5 in $Lgr5^{eGFP\text{-}CreRT}$ (WT) mouse embryos has been measured and compared to *Id2*-mutant $Lgr5^{eGFP\text{-}CreRT}$ samples. Intestinal epithelium was analyzed separately for anterior and posterior parts, since the signaling molecules and organoids forming capacity were demonstrated to be different for these regions (de Santa Barbara, 2003). Accordingly, here I showed that at E15.5 WT embryos have up to 15% of Lgr5GFP+ cells in anterior intestine and much more ï 40% - in posterior part (Fig. 33B, 34C).

In the Id2KO intestine, during active proliferation of epithelial cells prior to villi formation, $Lgr5^+$ cells occupy around 60% of anterior and up to 90% of all posterior cells (Fig. 33C, 34C). As confirmed by immunosfluorescent staining, Lgr5 GFP+ cells are evenly distributed within the

posterior gut, occupying both villi and intevilli regions (Fig. 34B). However, a highest GFP signal was detected in intervillus pockets.

To characterize consequences of such a dramatic upregulation of Lgr5 stem cell marker in E15.5 intestinal epithelium, qRT-PCR analysis of E15.5 $Lgr5^{GFP+}$ cells from both Id2 WT and Id2 KO embryos, as well as control $EpCam^{+}Lgr5^{GFP-}$ cells has been performed. Many genes, such as *Lgr5* gene itself, *Smoc2*, *Lrig1* were upregulated maximum by 2-4 times in a posterior gut, whereas anterior cells didnôt show dramatic differences in their genes expression. We have tested other targets from our E11.5 list with differentially expressed genes list, including *Snai*2, *Wnt*11, *Wnt*6, *R-spo*1, *R-spo*3 and *Id*1-*Id*3. However, these genes were not upregulated significantly, implying that upon *Id2* loss redundant mechanisms partially rescue the dramatic effect, demonstrated in early embryonic gut development. Most probably, any unrelated ISCs genes activity in villi is blocked by compensatory signals, coming from surrounding mesenchyme with BMP clusters. In fact, qPCR results of E17.5 Id2KO Lgr5GFP+ cells donôt show any significant differences in their genes, when compared to WT cells.

Despite this compensatory effect, the genes, responsible for cell cycle control, such as *Ccnb1* and *Ccnd2*, were highly upregulated in *Id2* mutant epithelial cells (Nigmatullina, 2017). Thus, our data have elucidated the abnormalities, caused by deregulated cell cycle, as has been described by Russel et al (2004).

6.5.4. E15.5 Id2KO epithelial cells form tumor-like spheroids *ex vivo*.

The clonogenic potential of Id2KO epithelial cells has been tested *ex vivo*. In this approach, I separated the small intestine into 2 parts ï anterior and posterior. As reported earlier for newborn mice intestine (Fordham, 2013), posterior cells give rise to organoids, whereas anterior cells form predominantly spheroids.

As expected, WT epithelial cells from posterior gut generated only organoids (Fig. 36C, 36D). When I examined posterior *Id2*-deficient samples, I observed a significant advantage in their growth, proliferation and differentiation in comparison to WT cells (Fig. 36B, D, E). These *Id2* KO posterior cells grow more efficiently, as demonstrated by 2-fold increase in number for organoids and 24-fold - for undifferentiated spheroids (n>20, Fig. 36E).

To characterize further the identity of Id2KO-derived cells, grown *ex vivo* for 1 week, I have collected organoids and spheroids from Id2-deficient posterior part. Surprisingly, I have detected an enormous upregulation of markers for epithelial-mesenchymal transition (EMT), as well as cancer markers *Trop2* and *Cnx43* (Fig. 37). It has been reported earlier that *Cnx43* and *Trop2* are markers of embryonic undifferentiated cells in spheroids (Mustata, 2013), never found in organoids. Indeed, in our experiment all WT organoids are negative for these genes. However, organoids and spheroids, formed by Id2KO cells have increased level of *Cnx43* and *Trop2*. ISC signature genes, such as *Lgr5,*

Smoc2 and *Axin2* were upregulated in Id2KO organoids and spheroids. *Lrig1*, identified as a DE gene in our E11.5 Id2KO RNA-seg is also increased exclusively in Id2KO derived structures.

Notably, both Id2KO-derived embryonic spheroids and organoids required R-spondin 1 for their growth and survival, whereas WT spheroids proliferate without Wnt supplements. Summarizing, Id2KO epithelial cells in cell culture form tumor-like structures. However, by histochemical analysis of Id2KO embryos at E15.5 I didnôt observe any significant abnormalities in gut development, as confirmed by qPCR data of isolated intestinal cells (chapter 6.5.3). Neither cell proliferation nor differentiation was affected *in vivo* (Fig.35C, F). I assume that redundant mechanisms, driven by mesenchyme, are compensating loss of *Id2* functions in embryo. Since *ex vivo* system is missing sub-epithelial mesenchyme, Id2KO cells gain molecular properties of cancer cells.

6.5.5. *Id2* KO embryos small intestine homeostasis after neonatal stage.

Our comprehensive analysis of E15.5 Id2KO epithelium indicates that Id2 is involved in the spatial restriction of Lgr5+ cells by inhibiting Wnt/ß-catenin signalling. Upon *Id2* loss, Lgr5+ progenitors are precociously born and represents up to 90% of total posterior gut epithelium. Here I examined intestinal morphology of newborn and adult Id2KO mice. According to Russel, 2004, *Id2*-mutant mouse at E18.5 have intestinal polyps, in which secretory Goblet cells are either overrepresented or completely absent. However, our detailed analysis of Id2KO sections showed reduced amount of secretory Goblet cells throughout the whole intestinal epithelium. Furthermore, cell proliferation assay with EdU-injected embryos allowed to visualize the regions with actively proliferating cells. As expected, in WT embryo proliferative cells are localized in intervillus compartment (Fig. 41A), whereas Id2KO-specific adenoma has a high proliferation in both villi-intervilli regions (Fig. 41B). Those abnormally dividing cells within mutant embryonic gut caused improperly differentiated structures, such as: cells hyperplasia, merged villi, or merged crypt compartments (Fig 42B), or villi with keratinized intervillus epithelium (Fig. 42D) in comparison to healthy wilt-type state (Fig. 42A). In general, newborn Id2KO mouse small intestine has less differentiated villi formed. I hypothesize that abnormally appeared Lgr5 stem cells actively divide and establish crypt-like hyperplastic regions within the embryonic gut (Fig. 41B). Consistent with our qPCR data analysis, performed on E15.5 Id2KO embryo samples, enormous upregulation of a cancer marker - nuclear Trop2, is detected *in vivo* at stages E18.5-P0 (Fig. 42E, F). Therefore, Id2 KO neonate mice develop tumor so early, already at neonatal stages, since *Id2* gene, suppressor of early Wnt activation in gut, is not expressed. *Id2* gene loss causes abnormal tissue differentiation, accompanied by nuclear Trop2 accumulation. Our hypothesis was further confirmed by Id2KO Lgr5 cells lineage tracing (chapter 6.5.6).

Despite of the significant abnormalities in embryonic development, adult intestine of Id2KO mice does not show expected severe cancer progression (Fig. 42H). However, further immuno-histochemical studies (IHC) showed differentiation abnormalities not only in those polyps, but

throughout the whole epithelium. Thus, PAS staining of *Id2* mutant small intestine demonstrated significantly reduced number of secretory lineage cells ï Goblets in villi and Paneth cells in crypts. When stained with DAPI and ß-catenin, *Id2*-deficient epithelium could be recognized by unusual cells shape in ISCs crypt compartment (Fig. 43A,B,E,F). Thus, PAS and anti-Lysozyme stainings showed that Id2KO small intestine has less Paneth cells (instead of 5 - only 1 or 2), constantly degranulated from lysozyme (Fig.42F, 43C, G).

It will be important to address the role of *Id2* gene in functioning of Paneth cells. Previous studies have showed that *Id2* is expressed in intestinal intraepithelial lymphocytes and plays an essential role in the intestinal mucosal barrier (Kim, 2004). Our finding shows that *Id2* mutant mice have a constant Paneth cell degranulation, which affects the defense against pathogens in the intestinal epithelium.

In summary, adult Id2 KO mouse has less abnormality in the small intestine in comparison to neonates. This could be explained by compensatory programs occurring after crypt formation and Paneth cells development on a second week after birth. The other reason could be that after E15.5 when villi-intervilli differentiated, Lgr5-gene expression in villi is inhibited by molecular signals coming from mesenchymal niche. In general, we canœt exclude the role of surrounding mesenchymal cell-to cell interactions that could provide Wnt ligands/antagonists and other essential signals for a proper gut homeostasis.

6.5.6. Precociously specified Lgr5+ cells become adult ISCs in *Id2* mutant mice.

Molecular properties of embryonic intestinal epithelium of *Id2*-null mice prompted us to test the capacity of precociously specified Lgr5GFP+ cells to contribute to ISCs in adult state. Here I have designed an approach, which allows to follow specifically the cell fate of early-activated Id2KO Lgr5+ cells within the intestinal gut epithelium and distinguish contribution of these cells into adult Lgr5+ ISCs *in vivo*.

The tamoxifen-induced lineage tracing, performed on $Id2^{Cre/Cre}$ $Lgr5^{GFP\text{-}Cre}$ embryos would result in unspecific labeling of both *Id2-Cre* and *Lgr5GFP-Cre* expressing cells. Thus, $Id2^{GFP}$ knock-in mouse was used for generating $Id2^{GFP/GFP}$ (Id2KO) genotype. Importantly, *Id2* gene is silent in adult state and Lgr5GFP+ cells could be visualized on $Id2^{GFP/GFP}$ genetical background as a green population. Therefore, tamoxifen induction at E11.5 of $Id2^{GFP/GFP}Lgr5^{Cre\ GFP}Rosa^{tdTomato}$ embryo specifically labelled only precocious Id2KO *Lgr5Cre*-expressing cells. Our data demonstrate that Id2KO Lgr5+cells, appeared at E11.5, gave rise to ISCs in adult mouse with a cohesive ribbon of labelled differentiated cells (Fig. 45C). Importantly, control animals $Id2^{GFP/GFP}Rosa^{tdTomato}$ (Fig. 45A) and $Lgr5^{Cre\text{-}GFP}Rosa^{tdTomato}$ (Fig. 45C) embryos were not labelled upon Tam administration.

Further FACS quantification of E11.5 Tam labelled embryos revealed that adult Id2KO posterior intestine contains 3-fold increased amount of Lgr5GFP+ cells (Fig. 46B). Our data indicate that loss of *Id2* results in expansion of Lgr5+ cells in adult mice. Notably, in a posterior Id2KO epithelium up to 50% of all ISCs are derived from E11.5 precociously activated Lgr5+ cells. Bioinformatical analysis of Lgr5GFP+ISCs from both Id2KO and WT embryos revealed no significant differences in the expression of ñstemnessò genes, including *Lgr5, Ascl2* and *Tcf4*. Nevertheless, in total around 600 genes were differently expressed in middle and posterior parts of *Id2*-mutant ISCs (log2FC Ó 0.5, FDR < 0.01). Among the mostly changed genes are *Atoh1*, regulating a secretory lineage choice in TA cells, as well as ISC markers *Lrig1*, *Axin2* and *Olfm4.* These findings reveal significant changes in transcriptional profile of Id2KO-derived ISCs in comparison to Lgr5+ ISCs in control wild-type animals.

Summarizing, in the present study I have identified that Id2 controls Lgr5+ ISC progenitorsô specification in the embryonic gut epithelium. In wild-type embryo, Lgr5+ intestinal progenitors are formed at E13.5 and become restricted to the intervillus region at E15.5, residing in the crypt compartment in adult state (Fig.45, upper panel). Upon loss of *Id2*, Lgr5+ intestinal progenitor cells appear at E9.5 and their amount increases dramatically after E11.5. *Id2* mutant Lgr5+ cells occupy both villi and intervilli at E15.5, which leads to ectopic neoplastic transformations of the gut and impaired differentiation of intestinal secretory cells (Fig.45, lower panel). In conclusion, *Id2* has been identified as a main regulator, restricting transcription of Wnt signalling genes, such as *Lgr5, Tnfrsf19,*

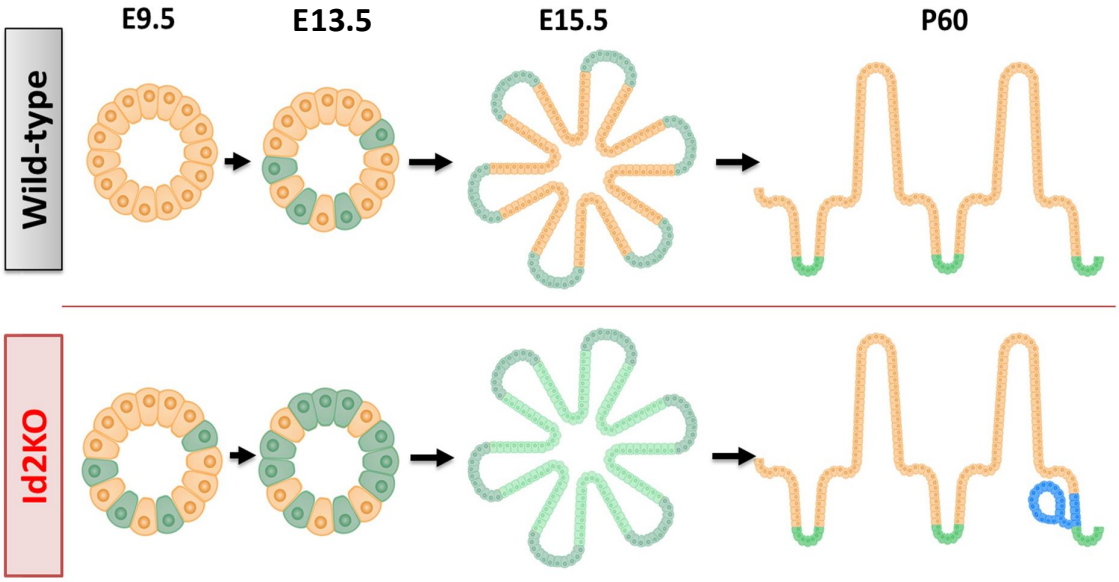

Figure 45. The role of Id2 in the small intestine development. In wild-type embryo, Lgr5+ ISC progenitors (green) appear at E13.5 as a minor cell population and reside in the crypts in adult state (P60). In *Id2*-deficient embryonic epithelium, Lgr5+ progenitors are formed at E9.5, they represent up to 90% of the posterior epithelial cells at E15.5. In adult mice, *Id2* loss causes ectopic neoplastic transformation (blue) of the small intestine. Detailed description- in chapter 6.5.6.

Smoc2, Wnt6 and *Wnt11. Id2*-deficient epithelium cells express genes, implicated in cell cycle control as well as molecular markers of cancer progression. Now, it will be important to understand the molecular partners of Id2, triggering precocious activation of Lgr5+ progenitors program. This knowledge will provide the mechanisms into the process of embryonic stem cell commitment and potential therapeutic strategies for gastrointestinal disorders.

7. Methods.

7.1. Mice.

All animal procedures were performed in compliance with the guidelines of the European Union and were approved by the ethics committee of Rheinland-Pfalz, Germany. Mice were maintained and crossed at the Translational Animal Research Center (TARC) in Mainz. CD1 mice (obtained from Charles River Laboratories) were used for heterozygous crosses with $Lgr5^{GFP}$, $Id2^{Cre}$, $Rosa^{tdTomato}$ mice or used alone as a wild-type control in histology, microscopy and FACS-sorting.

Studies on *Id2* gene functions were performed on embryos generated by heterozygous $Id2^{Cre/+}$ male and female breeding. To generate $Id2^{Cre/Cre}$ (KO) $Lgr5^{GFP\text{-}CreRT}$ embryos, $Id2^{Cre/+}$ mice were crossed with $Id2^{Cre/+}Lgr5^{GFP\text{-}CreRT}$ mouse background. The day of identification of a vaginal plug was considered as embryonic day 0.5 (E0.5). The animals were sacrificed by CO_2 asphyxiation followed by cervical dislocation.

7.2. *In vivo* mouse treatment procedures.

7.2.1. Tamoxifen induction.

For lineage tracing experiments, Tamoxifen (Sigma) in concentration 10mg/mL was dissolved in peanut oil (Sigma) by 15 min sonication and used in all experiments as 0,1 mg/g of body weight. Tamoxifen in a volume of 300 εL/mouse was given by oral gavage. As tamoxifen injection can compromise the ability of pregnant mice to have natural birth, pups were delivered by cesarean section at E19.5ï E20. For a long lineage tracing experiment, following adult P60 stage, newborn mice were fed by adoptive lactating CD1 females.

7.2.2. Wnt C-59 experiment.

Wnt C-59 (Tocris) was prepared as a mixture of 0,5% methylcellulose/PBS, supplemented with 5% DMSO and 0,01% Tween-20. Wnt C-59 was administered at 5 µg/g of body weight. In this study vehicle was always volume-matched mixture of 0,5% methylcellulose/PBS, supplemented with 5% DMSO and 0,01% Tween-20.

7.2.3. EdU injection.

Pregnant females at E15.5 or newborn mice at P1 were intraperitoneally injected with EdU (Abcam) in concentration 25µg/g of body weight. After 30 minutes following EdU administration mice were sacrificed and the small intestines were dissected for further cell proliferation analysis by

FACS (chapter 7.8.) or immunostaining (chapter 7.12). EdU+ cells were identified by using Click-iT EdU Cell Proliferation Assay (ThermoFisher). The protocol is described in chapter 5.5.2.

7.3. Genotyping PCR.

Embryonic tissue pieces or tail biopsies of adult mice were used for genotyping. Tissue samples were lysed by Protein Kinase K (PK, 300 µg/ml) in a tail buffer for 3 hours (or overnight) at 55°C with shaking at 800 rpm. Digestion process was stopped by heating-inactivation for 15 min at 95°C. 1µL of prepared DNA was used for each PCR tube. Routine genotyping PCR was performed with self-prepared DNA Taq polymerase from bacterial lysate, while some experiments required a clean commercial enzyme - OneTaq polymerase (Neb). All PCR primers were designed using online primer tool: https://www.ncbi.nlm.nih.gov/tools/primer-blast/.

7.3.1. Genotyping primers.

Primer	5' => 3' sequence
For-Lgr5-EGFP-WT com	CTG CTC TCT GCT CCC AGT CT
Rev-Lgr5-EGFP	GAA CTT CAG GGT CAG CTT GC
Rev-Lgr5-EGFP-WT	ATA CCC CAT CCC TTT TGA GC
Id2 WT For	CTTCCTCCTACGAG AGCAT
Id2 Com	CTCACCTGCAAGGACAGGAT
Id2 mut For	GCTCCTGGACAGGAATCAAG
GFP_Fwr	AGGACGACGGCAACTACAAG
GFP_Rev	GCCCGGGATTCTCTTCTACG
dsRed_fwr	GCAGGACGGCACCTTCATCT
dsRed-rev	AGTCCACGTAGTGGTTGCCG
Rosa26 for	AAAGTCGCTCTGAGTTGTTAT
CreERT rev	CCTGATCCTGGCAATTTCG
CreERT2 for	CGACCAGGTTCGTTCACTCA
Cre ERT2 rev	TCAGCTACACCAGAGACGGA
RosaLacZ mut rev	GCGAAGAGTTTGTCCTCAACC
RosaLacZ com for	AAAGTCGCTCTGAGTTGTTAT
For-Tomato-WT	CTCTGCTGCCTCCTGGCTTCT
Rev-Tomato-WT	CGAGGCGGATCACAAGCAATA
Rev-Tomato-Mut	TCAATGGGCGGGGGTCGTT

7.3.2. PCR reaction composition.

Reagent	**stock**	**one tube, µL**
10X Standard Taq Reaction Buffer (NEB)	10X	1.5
dNPT's	10mM	0.3
Primer Frw	10µM	1
Primer Rev	10µM	1
DNA	tail	1
Taq Pol home made	lysate	0.1
H2O		10.1

7.3.3. PCR-program.

Step	**temperature**	**duration**
Initial Denaturation	95°C	3 minutes
35 Cycles	95°C X°C 72°C	30 seconds 30 seconds 1 minute/kb
Final Extension	72°C	3 minutes
Hold	4°C	

Amplified PCR products were detected and analyzed by 1-2% agarose gel electrophoresis.

7.4. ß-galactosidase (LacZ) staining protocol.

For tissue sections the embryos were fixed with 4% PFA for 30 min at RT, cryo-protected in 30% sucrose (in 1X PBS) overnight at 4°C and frozen in O.C.T. at -80°C. 10µm cryosections were obtained using Leica CM3050 cryostat system and immediately adhered to SuperfrostÊ Ultra Plus glass slides (Thermo ScientificÊ). Frozen sections, placed in glass jars, were fixed in 1% PFA for 5 min, washed from the fixative for 3 times with 1X PBS and incubated in the darkness in standard ß-gal staining solution (see the table below) overnight at RT. Stained sections were washed, dehydrated and mounted using Immu-Mount (Thermo ScientificÊ).

For the whole mount LacZ staining, the intestines of *Lgr5*$^{GFP\text{-}CreRT}$/*Rosa*^{LacZ} or *Id2*^{Cre}/*Rosa*^{LacZ} adult mice from lineage tracing experiments were dissected out. The organs were washed in 1X PBS, fixed with 0,5% glutaraldehyde/PBS for 20 min at RT, washed 3 times in 1X PBS and incubated in a rinse buffer (see the table below) for 30 min. The small intestine was subsequently stained in the same ß-gal staining substrate in darkness at RT until blue color developed. The stained samples were post-fixed in 4% PFA/PBS at 4°C.

Rinse buffer

Reagent	Final concentration
Sodium phosphate dibasic (0.5 M; pH 7.0ï 7.5)	0,1M
Sodium phosphate monobasic	5 mM

(0.5 m; pH 7.0ï 7.5)	
MgCl2 · 6H2O (1 M)	2mM
Sodium deoxycholate	0.01%
NP-40	0.02%

β-gal staining solution

Reagent	Final concentration
Potassium ferricyanide	5 mM
Potassium ferrocyanide	5 mM
X-gal solution	1 mg/mL

7.5. RNA *in situ* hybridization.

7.5.1. ISH RNA probes preparation.

ISH RNA probes (antisense strand) representing 400-600 bp fragments were produced under standard PCR conditions using Taq-Polymerase and cDNA specific primers, as described in chapter 7.3.1. Gel-purified PCR products were ligated into the pGEM®-T vector (Promega) by manufacturerôs protocol with blue/white clone selection after transformation. Plasmids were isolated by the miniprep method and correct insertion of the probe sequence was confirmed by sequencing. DIG-labeled, single-stranded RNA probes of defined length were generated by *in vitro* transcription using DIG RNA Labeling Mix (Roche). DIG-11-UTP was incorporated by SP6/T7 promotors of linearized transcription vector.

7.5.2. ISH RNA *in situ* hybridization on slides.

10 µm paraffin sections were pre-melted at 58 °C for 3 h and deparaffinized through rehydration: 2x 5 min Xylol => 2x 5 min EtOH 100% => 2 min EtOH 70% => 2 min EtOH 50% => 2 min EtOH 30% =>5 min 1X PBS.

Slides were fixed *in* 4% FA in PBS for 15 min and the fixative was removed by washings in 1x PBS. Bleaching of slides:15 min in 6% H2O2 followed by serial washings in 1X PBS. Then I added 20µg/ml of Proteinase K (Sigma) for 10 min digestion. Slides were additionally fixed for 15 min in 4% FA in PBS and washed in 1xPBS several times. Acetylation of slides was performed in 100 mM Tris-Cl, pH 7.5 with 10 min incubation in 0.25% Acetic Anhydride, followed by 2 times washing in 2x SSC buffer, pH 5.0. The samples were dehydrated by serial incubations: 2 min EtOH 30% => 2 min EtOH 50% => 2 min EtOH 70% => 2x 5 min EtOH 100%. Slides dried on air for 30 min.

Hybridization:

1. 1 ul of RNA was used per 1 ml of hybridization buffer.
2. RNA amount was adjasted with H20 till 10-20 ul. RNA probes were denaturated at 80C for 5 min on PCR machine and added to the hybridization buffer.
3. 100 ul of the hybridization solution was added per slide and covered by cover slip.
4. Slides were kept in the humid chamber in dark at 63C overnight.

The next day slides were washed from unbound probe by serial washings in SSC buffer.

1x 15 min 5x SSC in 50% Formamide at 60C with rocking
2x 15 min 2x SSC in 50% Formamide at 60C with rocking
2x 15 min 1x SSC at 60C with rocking
1x 30 min 0.2x SSC at 60C with rocking

Samples were washed 2 times in TBS, blocked for 1h with a blocking solution and then incubated with anti-DIG antibody 1/1000 (in Blocking solution) at 4C in humid chamber overnight. The next day slides were washed 6 times x 30 min in TBSx at RT and for 2 times x 10 min in NTMT medium.

Staining: 1 ul/ml of NBT (Roche) + 3.5 ul/ml of BCIP (Roche) in NTMT buffer in dark humid chamber at RT till the color developed.

Solutions:

10xPBS: (for 1 L)	80 g NaCl, 2 g KCl, 14.4 g Na_2HPO_4, 2.4 g KH_2PO_4
20xSSC pH 4.5-5.0: (for 1L)	175,3 g NaCl, 88,2 g NaCitrate adjust with citric acid till correct pH
Hybridization buffer:	5xSSC, 50% Formamide, 10% Dextran sulfate, 1X Denhardt, 100ug/ml Heparin, 100ug/ml tRNA (boiled at 95C for 5min), 5mM EDTA adjust with citric acid till pH 4.5-5.0
TBS:	2mM KCl, 150 mM NaCl, 100mM Tris-Cl pH 7.5
TBSX:	2mM KCl 150 mM NaCl, 100mM Tris-Cl pH 7.5, 0,1% Triton X-100

Blocking solution:	1% Boehringer blocking Reagent, 10% goat serum in TBSX
NTMT:	50mM $MgCl_2$, 100 mM NaCl, 100mM Tris-Cl pH 9.0-9.5, 0.1% Tween-20

RNA *in situ* probes	5ô => 3ô sequence
Id2 fwr	CTCTCCCAATCTTTTGCAGGC
Id2 rev	GCACTGGTTGTCTGAAATAAAGCA
Shh Frw	CCTCTCCTGCTATG CTCCTG
Shh rev	TGTGTGG CACGCTTTATTTC

7.6. 3D *ex vivo* cell culture.

FACS-isolated embryonic intestinal cells were cultured according to Sato et al. (2009) protocol for adult ISCs. Briefly, 250/500/1000 cells were sorted in Eppendorf tubes, containing 15 µL of intestinal medium (see the table below). The cells were immediately collected by centrifugation at 3000 rpm for 3 min at RT. Pelleted cells were mixed with 25 µL of ice-thawed Matrigel (Corning), plated as a drop on 8-well chambers (ibidi) and incubated at 37C in CO2-incubator for 10 min. After polymerization of Matrigel, cells were covered with 300 µL of intestinal medium and incubated at 37C in CO2-incubator. The medium was exchanged every 2 days. Colonies formed after approximately 5 days in culture.

Intestinal medium (with growth factors)

Component	Final concentration
Advanced DMEM/F12 (Invitrogen)	50/50
B-27® Supplement (50X, Thermo Fisher Scientific)	1X
Penicillin-streptomycin cocktail (100X, Thermo Fisher Scientific)	1X
MEM Non-Essential Amino Acid Solution (100X, Sigma)	
L-glutamine (200mM, Sigma)	2mM
HEPES (Sigma)	15mM
Y-27632 inhibitor (1M, Tocris)	10µM
R-spondin-1 (25 µg, R&D systems)	500 ng/mL

Noggin (10 µg, R&D systems)	100 ng/mL
EGF (10 µg, R&D systems)	100 ng/mL

7.7. Tissue preparation.

Tissues or whole embryos were fixed for 20 min for OCT and overnight for paraffin embedding, respectively. For paraffin, tissue was rinsed with PBS, dehydrated in serial ethanol rinses (3 min in 50% EtOH; 3 min in 70% EtOH; 2 x 5 min in 100% EtOH and 2x 5min in xylol and infused with liquid paraffin. For OCT, samples were washed in 1X PBS, incubated overnight in 30% sucrose/PBS and embedded in OCT. Paraffin blocks were sectioned at 7µm for IHC or 10µm for RNA in situ hybridization by using Leica RM2255 microtome. 10µm cryosections were obtained using Leica CM3050 cryostat system and immediately adhered to SuperfrostÊ Ultra Plus glass slides (Thermo ScientificÊ). Frozen sections, placed in glass jars, were fixed in 1% PFA for 5 min, washed from the fixative for 3 times with 1X PBS and stored at -20C.

7.8. Immunostainings.

Slides preparation: Standard immunofluorescence staining was performed on 10-µm frozen sections and immuno-histochemistry on 7-µm paraffin sections.

Paraffin sections were deparaffinized in xylol (2x 5min), rehydrated by serial ethanol rinses (2 x 5 min in 100% EtOH, 3 min in 70% EtOH, 3 min in 50% EtOH and 5 min in ddH2O. To unmask epitopes, slides were boiled for 50 min in 10 mM sodium citrate (pH 6.0), washed in H2O and incubated in 3% H_2O_2 for 15 min to quench endogenous peroxidases. After several washes in 1X PBS, slides were ready to use for antibody staining. Cryosections were fixed for 20 min in 4% paraformaldehyde, washed in 1X PBS and preceded for antibody staining.

Immunofluorescent staining: Paraffin and cryosections were blocked by goat or donkey serum solution (5% serum, 0.1% Tween-20 and 1X PBS) for 1h at RT in a humid chamber. Primary antibodies (see table below) were diluted in a blocking buffer and incubated overnight at 4C. Alexa Fluor488-, 568- or 688-conjugated secondary antibodies (Invitrogen, 1:300) with DAPI (1:1000) were diluted in 1X PBS +0,1%Tween-20. Slides were mounted with Immo-mount medium (Thermo Fisher Scientific).

7.9. Immunohistochemistry.

7.9.1. PAS staining.

Cryosections were equilibrated to RT and fixed with 4% PFA/FA (Sigma) in PBS for 10 min. After 2 times washing for 5 min in 1xPBS and H2O, the slides were immersed in Periodic Acid Solution (Sigma) for 5 minutes at room temperature. Rinsed in dH20 for several times, the slides were immediately put in Schiffôs Reagent (Sigma) for 15 minutes at

room temperature (18ï 26°C) and 7. The colour was developed by washing slides in running tap water for 5 minutes. Dehydrated slides were mounted in Roti®-Mount medium (Roth).

7.9.2. H&E staining.

Paraffin slides were deparaffinize through 2 changes of xylene x 10 minutes each. The slides were prepared for further staining by step-wise rehydration: 2 changes of 100% EtOH, 5 minutes each=> 95% alcohol for 2 minutes => 70% alcohol for 2 minutes => Washings in distilled water. The samples were stained in Mayer hematoxylin solution (Sigma) for 8 minutes and wash in warm running tap water for 5 minutes. The slides were rinsed in distilled water followed by 10 short dips in 95% EtOH. Counterstaining was perfomed in eosin solution (Sigma) for 1 min => Dehydration through 95% EtOH, 2 changes of 100% alcohol x 5 minutes each. The slides were cleared in 2 changes of xylene, 5 minutes each and mounted with xylene based Roti®-Mount medium (Roth).

7.11. Antibodies.

Name	Supplier	Dilution
Polyclonal Rabbit Anti-Human Lysozyme A0099	Dako Deutschland	1:200 IF, IHC
beta-Catenin (D10A8) XP® Rabbit 8480 S	New England BioLabs GmbH	1:50 IF, IHC
mouse Villin (C-19) sc-7672	Santa Cruz Biotechnology	1:200 IF
goat Lrig (P-16) sc-50076	Santa Cruz Biotechnology	1:500
goat EpCAM (A-20) SC-23788	Santa Cruz Biotechnology	1:200 IF
goat Trop2 (C-12) SC-103908	Santa Cruz Biotechnology	1:200 IF, IHC
mouse Anti-ß-Catenin C7207	Sigma-Aldrich Chemie GmbH	1:100 IF, IHC
Rat CD326 EpCam PerCP eFluor710	eBioscience	1:200 FACS
Rat CD326 EpCam APC 1:200	eBioscience	1:200 FACS
Rat CD24 PE-Cy7	Sigma-Aldrich Chemie GmbH	1:200 FACS
Rat CD31 PE	BD Pharmingen	1:400 FACS
Rat CD45 PE	BD Pharmingen	1:400 FACS
Rabbit anti-GFP	LifeTechnologies	1:3000 IF
UEA1 -TRITC	Sigma-Aldrich Chemie GmbH	1:200 FACS, 1:1000 IF
Biotin-SP AffiniPure F(ab') Fragment Donkey Anti-Rabbit IgG	Dianova GmbH	1:3000 IHC
Biotin-SP AffiniPure F(ab')2 Fragment Donkey Anti-Mouse IgG	Dianova GmbH	1:3000 IHC
Biotin-SP AffiniPure F(ab')2 Fragment Donkey Anti-Goat IgG	Dianova GmbH	1:3000 IHC
Peroxidase AffiniPure F(ab')2 Fragment Donkey Anti-Goat IgG (H+L)	Dianova GmbH	1:3000 IHC
Peroxidase AffiniPure F(ab')2 Fragment Donkey Anti-Rabbit IgG (H+L)	Dianova GmbH	1:3000 IHC
anti-DIG	Roche	1:1000 RNA in situ

Goat anti-Rabbit Alexa568 secondary antibody	LifeTechnologies	1:300 IF
Goat anti-mouse Alexa488 secondary antibody	LifeTechnologies	1:300 IF
Donkey anti-Rabbit Alexa688 secondary antibody	LifeTechnologies	1:300 IF

7.12. Intestinal cells isolation using FACS sorting.

7.12.1. Isolation of embryonic epithelial cells and sorting.

Embryos were dissected out at indicated stages, the small intestine were isolated and cut in pieces of 2 mm. The samples were digested for 10 min with 0.15mg/ml collagenase (Sigma) in PBS at 37℃ with shaking at 800 rpm. To obtain a single cell suspension the cells were collected by centrifugation at 200g for 3 min, washed twice and resuspended in PBS supplemented with 2% FSC of goat serum. Cells were stained with *APC*- or *PerCP-eFluor® 710*ï conjugated anti-EpCam 1:200 (eBioscience) antibody for 15 min at room temperature. Living cells were gated by DAPI signal exclusion. Embryonic intestinal epithelial cells were isolated as $EpCam^{+}$ population. ($EpCam^{+}GFP^{+}$ - for Lgr5eGFP+ cells population) FACS sorting and analysis was performed using BD FACS Aria III SORP cell sorter with 100 ε M nozzle, BD Fortessa and FlowJo software.

7.12.2. Isolation of adult ISCs and sorting.

Small intestines were dissected from adult (2 months old) animals, cut in small pieces and placed into 50 ml conical tubes. The samples were washed 3 times for 10 min in PBS/EDTA on a rocking plate at room temperature. Villi were mechanically removed by gentle shaking 3 times and vigorous pipetting using a 10 ml pipette. Crypts collected by centrifugation at 200g for 3 min, washed twice with PBS and incubated for 5 with 0.15 mg/ml collagenase (Sigma) and 0.1 mg/ml DNase I (Qiagen) at 37°C on a rocking plate. Single cell suspensions were washed twice and re-suspended in PBS supplemented with 2% FCS/goat serum. Cells were stained with PE-conjugated anti-CD45 at 1:400 (BD Biosciences) and anti-CD31 at 1:400 (BD Biosciences) antibody for 30 min at room temperature. Living cells were gated by DAPI dye exclusion. ISCs were isolated as $EpCam^{+}$Lgr5-$GFP^{high}CD31^{-}CD45^{-}$. Fluorescence-activated cell sorting analysis was performed using BD FACS Aria III SORP cell sorter 100 ε M nozzle and FlowJo software.

7.13. Chemical compounds screening.

For the morphological screen, E15.5 intestinal cells were plated in Matrigel and the normal growth medium was added for first 5 days. After formation of spheroids/organoids at day 5, the chemical compounds have been added in the indicated final concentrations: ICG-001 (Tocris) - 10μM;

XAV 939 (Tocris)- 1µM; TWS119 (Tocris)- 5µM; DAPT (Sigma)-1µM; TAPI-1 (Sigma)-10 µM. Stock concentrations were prepared in DMSO, as well as a vehicle control.

7.14 Preparation of embryonic cells for RNA-sequencing.

cDNA libraried have been prepared with SMART-Seq v4 Ultra Low Input RNA Kit for Sequencing (Clontech) according to manufacturerô protocol. The detailed procedure of samples preparation is described in chapter 5.2.2.

7.15. Reverse Transcription Polymerase Chain Reaction Experiments.

7.15.1. qRT-PCR on embryonic intestinal cells, isolated from mouse embryos.

Sorted cells were collected in 19:1 mixture of Dilution Buffer (Clontech) and RNAse inhibitor, and RNA was extracted by using Smarter UltraLow RNA kit v4, as described in chapter 5.2.2. qRTï PCR was performed on total cDNA libraries in amount of 10 ng. The cell fractions, listed in the table below, were subjected to analysis in 3 replicates each time:

Stage	Id2 KO samples	Control samples
E11.5	Id2KO EpCam^{+} Lgr5^{GFP-}; Id2KO EpCam^{+}Lgr5^{GFP}	Id2WT EpCam^{+}
E13.5	Id2KO EpCam^{+} Lgr5^{GFP-}; Id2KO EpCam^{+}Lgr5^{GFP+}	Id2WT EpCam^{+} Lgr5^{GFP-}; Id2WT EpCam+Lgr5^{GFP+}
E15.5	Id2KO EpCam^{+} Lgr5^{GFP-}; Id2KO EpCam^{+}Lgr5^{GFP+}	Id2WT EpCam^{+} Lgr5^{GFP-}; Id2WT EpCam+Lgr5^{GFP+}

7.15.2. qRT-PCR on E15.5 cells, isolated from 3D *ex vivo* cell culture.

E15.5 cells, grown in Matrigel-based cell medium, were collected after 7 days of culturing. Spheroids and organoids, formed from Id2 WT and Id2 KO cells, were manually picked up under the bright-field microscope by using a pipette with cut tip (for 200 µL). Collected samples were cleared from debris by 2 times washing in 1X PBS and centrifugation at 3000 rpm x 3 min. The cells from organoids/spheroids were homogenized by TRIzol (Invitrogen) before RNA isolation. Total RNA was extracted using RNAeasy Micro kit (Qiagen) and treated with DNAse (Promega). cDNA was synthesized with an Invitrogen Superscript III kit.

All used primers are listed in the table below. Relative gene expression was measured using SYBR green master mix kit (Applied Biosystems) with ViiATM 7 cycler (Applied Biosystems). Calculations were performed with qpqCT method by normalization to *EpCam* or *Tbp1* genes expression (E15.5).

Primer	5' =>3' sequence
EpCam qPCR F-1	CGAAGAACCGACAAGGACAC

EpCam qPCR R-1	GATGGTCGTAGGGGCTTTCT
Lgr5 qPCR Frw	CTACTCGAAGACTTACCCAGT
Lgr5 qPCR Rev	GCATTGGGGTGAATGATAG
Lin7a-1 qPCR Fr	AGCAGCAGCAGTTGCTCATT
Lin7a-1 qPCR Rev	ATTTGTGACTGGCGGATGAT
Osr2 qPCR Fr	GACGAGAGGCCATACACCTG
Osr2 qPCR Rev	AGGGCTTTTCTTTGGAATGG
Tfpi2 qPCR Fr	AGGCCTGGTCTGTGTAGCAG
Tfpi2 qPCR Rev	GGACTGGAGCAAAATGATGG
Kcne3 qPCR Fr	GTGGGACATCCACGAAGAGA
Kcne3 qPCR Rev	TCCCGTTGGAAGTCTCCATA
St8sia3 qPCR Fr	TAAAGGTCCAGTTGGCTTGG
St8sia3 qPCR Rev	CGTTTGGGTGACAGGTGTTT
Slc2a3 qPCR Fr	CATCTCCATTGTCCTCCAGC
Slc2a3 qPCR Rev	CAATCGTGGCATAGATCGGT
Axin2 qPCR Fr	ACAGGAGGATGCTGAAGGCT
Axin2 qPCR Rev	ATTCGTCACTCGCCTTCTTG
Smoc2_qPCR Fr	AGGACCTTCCTGTCCCGAT
Smoc2_qPCR Rev	CTTCCTCTCAGCCACACACC
Trop2 qPCR Frw	GAACGCGTCGCAGAAGGGC
Trop2 qPCR Rev	CGGCGGCCCATGAACAGTGA
Cnx43 qPCR Fw	TGGGGGAAAGGCGTGAGGGA
Cnx43 qPCR Rev	ACCCATGTCTGGGCACCTCTCTT
Sfrp5 qPCR F	CTGGACAACGACCTCTGCAT
Sfrp5 qPCR R	CATCTGTTCCATGAGGCCAT
Tbp1 qPCR Fw	TGTACCGCAGCTTCAAAATATTGTAT
Tbp1 qPCR Rev	AAATCAACGCAGTTGTCCGTG

7.16. Statistical Evaluation.

Statistical analyses were performed with GraphPad Prism. All experimental data are expressed as mean ± SEM. The significance of differences between groups was determined by paired or unpaired t- test analysis.

8. Literature.

- BARKER, N. 2014. Adult intestinal stem cells: critical drivers of epithelial homeostasis and regeneration. *Nat Rev Mol Cell Biol,* 15**,** 19-33.
- BARKER, N., VAN ES, J. H., KUIPERS, J., KUJALA, P., VAN DEN BORN, M., COZIJNSEN, M., HAEGEBARTH, A., KORVING, J., BEGTHEL, H., PETERS, P. J. & CLEVERS, H. 2007. Identification of stem cells in small intestine and colon by marker gene Lgr5. *Nature,* 449**,** 1003-7.
- BARKER, N., VAN OUDENAARDEN, A. & CLEVERS, H. 2012. Identifying the stem cell of the intestinal crypt: strategies and pitfalls. *Cell Stem Cell,* 11**,** 452-60.
- BATTS, L. E., POLK, D. B., DUBOIS, R. N. & KULESSA, H. 2006. Bmp signaling is required for intestinal growth and morphogenesis. *Dev Dyn,* 235**,** 1563-70.
- BLANPAIN, C., HORSLEY, V., FUCHS, E. 2007. Epithelial Stem Cells: Turning over New Leaves. *Cell. ,* 128**,** 445-458.
- BLANPAIN, C. & SIMONS, B. D. 2013. Unravelling stem cell dynamics by lineage tracing. *Nat Rev Mol Cell Biol,* 14**,** 489-502.
- CHIN, A. M., TSAI, Y. H., FINKBEINER, S. R., NAGY, M. S., WALKER, E. M., ETHEN, N. J., WILLIAMS, B. O., BATTLE, M. A. & SPENCE, J. R. 2016. A Dynamic WNT/beta-CATENIN Signaling Environment Leads to WNT-Independent and WNT-Dependent Proliferation of Embryonic Intestinal Progenitor Cells. *Stem Cell Reports,* 7**,** 826-839.
- CLEVERS, H. 2013. The intestinal crypt, a prototype stem cell compartment. *Cell,* 154**,** 274-84.
- CROSNIER, C., STAMATAKI, D. & LEWIS, J. 2006. Organizing cell renewal in the intestine: stem cells, signals and combinatorial control. *Nat Rev Genet,* 7**,** 349-59.
- DE SANTA BARBARA, P., VAN DEN BRINK, G.R., ROBERTS, D.J. 2003. Development and differentiation of the intestinal epithelium. *Cellular and Molecular Life Sciences,* 60(7)**,** 1322-1332.
- DONATI, G. & WATT, F. M. 2015. Stem cell heterogeneity and plasticity in epithelia. *Cell Stem Cell,* 16**,** 465-76.
- DURAND, A., DONAHUE, B., PEIGNON, G., LETOURNEUR, F., CAGNARD, N., SLOMIANNY, C., PERRET, C., SHROYER, N. F. & ROMAGNOLO, B. 2012. Functional intestinal stem cells after Paneth cell ablation induced by the loss of transcription factor Math1 (Atoh1). *Proc Natl Acad Sci U S A,* 109**,** 8965-70.
- FATEHULLAH, A., TAN, S. H. & BARKER, N. 2016. Organoids as an in vitro model of human development and disease. *Nat Cell Biol,* 18**,** 246-54.
- FEVR, T., ROBINE, S.LOUVARD, D.HUELSKEN, J. 2007. Wnt/beta-catenin is essential for intestinal homeostasis and maintenance of intestinal stem cells. *Mol Cell Biol,* 27**,** 7551-9.
- FORDHAM, R. P., YUI, S., HANNAN, N. R., SOENDERGAARD, C., MADGWICK, A., SCHWEIGER, P. J., NIELSEN, O. H., VALLIER, L., PEDERSEN, R. A., NAKAMURA, T., WATANABE, M. & JENSEN, K. B. 2013. Transplantation of expanded fetal intestinal progenitors contributes to colon regeneration after injury. *Cell Stem Cell,* 13**,** 734-44.
- GARCIA, M. I., GHIANI, M., LEFORT, A., LIBERT, F., STROLLO, S. & VASSART, G. 2009. LGR5 deficiency deregulates Wnt signaling and leads to precocious Paneth cell differentiation in the fetal intestine. *Dev Biol,* 331**,** 58-67.
- GERBE, F., VAN ES, J.H., MAKRINI, L., BRULIN B, MELLITZER G, ROBINE S, ROMAGNOLO B, SHROYER NF,BOURGAUX JF, PIGNODEL C, CLEVERS H, JAY. P. 2011. Distinct ATOH1 and Neurog3 requirements define tuft cells as a new secretory cell type in the intestinal epithelium. *J Cell Biol,* 192**,** 767-780.
- GRIGORIEFF, A., ET AL. 2005. Wnt signaling in intestinal epithlium. from development to cancer. *Genome Res,* 12**,** 47-56.

- GRODEN, J., THLIVERIS, A., SAMOWITZ, W., CARLSON, M., GELBERT, L., ALBERTSEN, H., JOSLYN, G., STEVENS J, SPIRIO L, ROBERTSON, M., ET AL. 1991. Identification and characterization of the familial adenomatous polyposis coli gene. *Cell. Aug 9,* 66**,** 589-600.
- GUIU, J. & JENSEN, K. B. 2015. From Definitive Endoderm to Gut-a Process of Growth and Maturation. *Stem Cells Dev,* 24**,** 1972-83.
- HARAMIS, A. P., BEGTHEL, H., VAN DEN BORN, M., VAN ES J, JONKHEER S, OFFERHAUS GJ, CLEVERS H. 2004 De novo crypt formation and juvenile polyposis on BMP inhibition in mouse intestine. *Science,* Mar 12;303**,** 1684-6.
- HE, X. C., ZHANG, J., TONG, W. G., TAWFIK, O., ROSS, J., SCOVILLE, D. H., TIAN, Q., ZENG, X., HE, X., WIEDEMANN, L. M., MISHINA, Y. & LI, L. 2004. BMP signaling inhibits intestinal stem cell self-renewal through suppression of Wnt-beta-catenin signaling. *Nat Genet,* 36**,** 1117-21.
- HOWE, J. R., ROTH, S., RINGOLD, J.C., SUMMERS, R.W., JÄRVINEN HJ, SISTONEN P, TOMLINSON IP, HOULSTON RS, BEVAN S, MITROS FA, STONE EM, AALTONEN LA. 1998. Mutations in the SMAD4/DPC4 gene in juvenile polyposis. *Science,* May 15;280**,** 1086-8.
- IRELAND, H., KEMP, R., HOUGHTON, C., HOWARD, L., CLARKE, A. R., SANSOM, O. J. & WINTON, D. J. 2004. Inducible cre-mediated control of gene expression in the murine gastrointestinal tract: effect of loss of β-catenin. *Gastroenterology,* 126**,** 1236-1246.
- JENSEN, J., PEDERSEN, E.E., GALANTE, P., HALD, J., HELLER RS, ISHIBASHI M, KAGEYAMA R, GUILLEMOT F, SERUP P, MADSEN OD. 2000 Control of endodermal endocrine development by Hes-1 *Nat Genet. ,* Jan;24**,** 36-44.
- JEON, M. K., KLAUS, C., KAEMMERER, E. & GASSLER, N. 2013. Intestinal barrier: Molecular pathways and modifiers. *World J Gastrointest Pathophysiol,* 4**,** 94-9.
- KARLSSON, L., LINDAHL. P., HEATH, J., BETSHOLTZ, C. 2000. Abnormal gastrointestinal development in PDGF-A and PDGFR-α deficient mice implicates a novel mesenchymal structure with putative instructive properties in villus morphogenesis. *Development* 127**,** 3457-3466.
- KIM, B. M., MAO, J., TAKETO, M. M. & SHIVDASANI, R. A. 2007. Phases of canonical Wnt signaling during the development of mouse intestinal epithelium. *Gastroenterology,* 133**,** 529-38.
- KIM, T. H., ESCUDERO, S., SHIVDASANI, R.A. 2012 Intact function of Lgr5 receptor-expressing intestinal stem cells in the absence of Paneth cells. *Proc Natl Acad Sci U S A. Mar 6;109(10)* 3932-7.
- KIM, T. H., KIM, B. M., MAO, J., ROWAN, S. & SHIVDASANI, R. A. 2011. Endodermal Hedgehog signals modulate Notch pathway activity in the developing digestive tract mesenchyme. *Development,* 138**,** 3225-33.
- KIM, T. H., LI, F., FERREIRO-NEIRA, I., HO, L. L., LUYTEN, A., NALAPAREDDY, K., LONG, H., VERZI, M. & SHIVDASANI, R. A. 2014. Broadly permissive intestinal chromatin underlies lateral inhibition and cell plasticity. *Nature,* 506**,** 511-5.
- KINZEL, B., PIKIOLEK, M., ORSINI, V., SPRUNGER, J., ISKEN, A., ZIETZLING, S., DESPLANCHES, M., DUBOST, V., BREUSTEDT, D., VALDEZ, R., LIU, D., THEIL, D., MULLER, M., DIETRICH, B., BOUWMEESTER, T., RUFFNER, H. & TCHORZ, J. S. 2014. Functional roles of Lgr4 and Lgr5 in embryonic gut, kidney and skin development in mice. *Dev Biol,* 390**,** 181-90.
- KINZLER, K. W., NILBERT, M.C., VOGELSTEIN, B., BRYAN TM, LEVY DB, SMITH KJ, PREISINGER AC, HAMILTON SR, HEDGE P, MARKHAM A, ET AL. 1991 Identification of a gene located at chromosome 5q21 that is mutated in colorectal cancers. *Science,* Mar 15;251**,** 1366-70.
- KORINEK, V., BARKER, N., PETRA MOERER1, ELLY VAN DONSELAAR3, GERWIN HULS1, PETER J. PETERS, CLEVERS, H. 1998. Depletion of epithelial stem-cell compartments in the small intestine of mice lacking Tcf-4. *Nature genetics,* 19.
- KRETZSCHMAR, K. & CLEVERS, H. 2016. Organoids: Modeling Development and the Stem Cell Niche in a Dish. *Dev Cell,* 38**,** 590-600.
- KRETZSCHMAR, K. & WATT, F. M. 2012. Lineage tracing. *Cell,* 148**,** 33-45.

- KUHNERT, F., DAVIS CR, WANG HT, CHU P, LEE M, YUAN J, NUSSE R, KUO CJ. 2004. Essential requirement for Wnt signaling in proliferation of adult small intestine and colon revealed by adenoviral expression of Dickkopf-1. . *Proc Natl Acad Sci U S A.* **,** 266-71.
- LE GUEN, L., MARCHAL, S., FAURE, S. & DE SANTA BARBARA, P. 2015. Mesenchymal-epithelial interactions during digestive tract development and epithelial stem cell regeneration. *Cell Mol Life Sci,* 72**,** 3883-96.
- LEOW, C. C., ROMERO, M.S., ROSS, S., POLAKIS P, GAO, W.Q. 2004. Hath1, down-regulated in colon adenocarcinomas, inhibits proliferation and tumorigenesis of colon cancer cells. . *Cancer Res.,* 64**,** 6050-6057.
- MADISON, B. B., BRAUNSTEIN, K., KUIZON E, PORTMAN K, QIAO XT, GUMUCIO DL. 2005. Epithelial hedgehog signals pattern the intestinal crypt-villus axis. *Development,* Jan;132(2):**,** 279-89.
- MAO, J., KIM, B. M., RAJURKAR, M., SHIVDASANI, R. A. & MCMAHON, A. P. 2010. Hedgehog signaling controls mesenchymal growth in the developing mammalian digestive tract. *Development,* 137**,** 1721-9.
- MILANO, J., MCKAY, J., DAGENAIS, C., FOSTER-BROWN, L., POGNAN, F., GADIENT, R., JACOBS, R. T., ZACCO, A., GREENBERG, B. & CIACCIO, P. J. 2004. Modulation of notch processing by gamma-secretase inhibitors causes intestinal goblet cell metaplasia and induction of genes known to specify gut secretory lineage differentiation. *Toxicol Sci,* 82**,** 341-58.
- MONTGOMERY, R. K., CARLONE, D. L., RICHMOND, C. A., FARILLA, L., KRANENDONK, M. E., HENDERSON, D. E., BAFFOUR-AWUAH, N. Y., AMBRUZS, D. M., FOGLI, L. K., ALGRA, S. & BREAULT, D. T. 2011. Mouse telomerase reverse transcriptase (mTert) expression marks slowly cycling intestinal stem cells. *Proc Natl Acad Sci U S A,* 108**,** 179-84.
- MUNCAN, V., SANSOM, O. J. TERTOOLEN, L.PHESSE, T. J.BEGTHEL, H.SANCHO, E.COLE, A. M.GREGORIEFF, A.DE ALBORAN, I. M., CLEVERS, H.CLARKE, A. R. 2006. Rapid loss of intestinal crypts upon conditional deletion of the Wnt/Tcf-4 target gene c-Myc. *Mol Cell Biol,* 26**,** 8418-26.
- MUNOZ, J., STANGE, D. E., SCHEPERS, A. G., VAN DE WETERING, M., KOO, B. K., ITZKOVITZ, S., VOLCKMANN, R., KUNG, K. S., KOSTER, J., RADULESCU, S., MYANT, K., VERSTEEG, R., SANSOM, O. J., VAN ES, J. H., BARKER, N., VAN OUDENAARDEN, A., MOHAMMED, S., HECK, A. J. & CLEVERS, H. 2012. The Lgr5 intestinal stem cell signature: robust expression of proposed quiescent '+4' cell markers. *EMBO J,* 31**,** 3079-91.
- MUSTATA, R. C., VASILE, G., FERNANDEZ-VALLONE, V., STROLLO, S., LEFORT, A., LIBERT, F., MONTEYNE, D., PEREZ-MORGA, D., VASSART, G. & GARCIA, M. I. 2013. Identification of Lgr5-independent spheroid-generating progenitors of the mouse fetal intestinal epithelium. *Cell Rep,* 5**,** 421-32.
- NOWAK, J. A., POLAK, L., PASOLLI, H. A. & FUCHS, E. 2008. Hair follicle stem cells are specified and function in early skin morphogenesis. *Cell Stem Cell,* 3**,** 33-43.
- NUSSE, R. & VARMUS, H. 2012. Three decades of Wnts: a personal perspective on how a scientific field developed. *EMBO J,* 31**,** 2670-84.
- PELLEGRINET, L., RODILLA, V., LIU, Z., CHEN, S., KOCH, U., ESPINOSA, L., KAESTNER, K. H., KOPAN, R., LEWIS, J. & RADTKE, F. 2011. Dll1- and dll4-mediated notch signaling are required for homeostasis of intestinal stem cells. *Gastroenterology,* 140**,** 1230-1240 e1-7.
- PINTO, D., GREGORIEFF, A., BEGTHEL, H., CLEVERS. H. 2003a. Canonical Wnt signals are essential for homeostasis of the intestinal epithelium. *Genes Dev. ,* Jul 15;17**,** 1709-13.
- PINTO, D., GREGORIEFF, A., BEGTHEL, H., CLEVERS, H. 2003b. Canonical Wnt signals are essential for homeostasis of the intestinal epithelium. *Genes &Dev. ,* 12**,** 47-56.
- POTTEN, C. S., BOOTH C, TUDOR GL, BOOTH D, BRADY G, HURLEY P, ASHTON G, CLARKE R, SAKAKIBARA S, OKANO H. 2003 Identification of a putative intestinal stem cell and early lineage marker; musashi-1. *Differentiation,* Jan;71**,** 28-41.
- POWELL, A. E., WANG, Y., LI, Y., POULIN, E. J., MEANS, A. L., WASHINGTON, M. K., HIGGINBOTHAM, J. N., JUCHHEIM, A., PRASAD, N., LEVY, S. E., GUO, Y., SHYR, Y., ARONOW,

B. J., HAIGIS, K. M., FRANKLIN, J. L. & COFFEY, R. J. 2012. The pan-ErbB negative regulator Lrig1 is an intestinal stem cell marker that functions as a tumor suppressor. *Cell,* 149**,** 146-58.

- POWELL, S. M., ZILZ, N., BEAZER-BARCLAY, Y., BRYAN, T.M., HAMILTON, .SR., THIBODEAU SN, VOGELSTEIN B, KINZLER, K.W. 1992. APC mutations occur early during colorectal tumorigenesis. *Nature,* Sep 17;359**,** 235-7.
- RAMALHO-SANTOS, M., MELTON, D.A., MCMAHON, A.P. 2000. Hedgehog signals regulate multiple aspects of gastrointestinal development. *Development. ,* Jun;127**,** 2763-72.
- RAWLINS, E. L., CLARK, C. P., XUE, Y. & HOGAN, B. L. 2009. The Id2+ distal tip lung epithelium contains individual multipotent embryonic progenitor cells. *Development,* 136**,** 3741-5.
- RENZ, H. B., P. HORNEF, M. 2011. The impact of perinatal immune development on mucosal homeostasis and chronic inflammation. *Nat Rev Immunol,* 12**,** 9-23.
- RICCIO, O., VAN GIJN, M. E., BEZDEK, A. C., PELLEGRINET, L., VAN ES, J. H., ZIMBER-STROBL, U., STROBL, L. J., HONJO, T., CLEVERS, H. & RADTKE, F. 2008. Loss of intestinal crypt progenitor cells owing to inactivation of both Notch1 and Notch2 is accompanied by derepression of CDK inhibitors p27Kip1 and p57Kip2. *EMBO Rep,* 9**,** 377-83.
- RUSSELL, R. G., LASORELLA, A., DETTIN, L. E. & IAVARONE, A. 2004. Id2 drives differentiation and suppresses tumor formation in the intestinal epithelium. *Cancer Research,* 64**,** 7220-7225.
- SANGIORGI, E. & CAPECCHI, M. R. 2008. Bmi1 is expressed in vivo in intestinal stem cells. *Nat Genet,* 40**,** 915-20.
- SANSOM, O. J., REED, K.R., HAYES, A.J., IRELAND, H., BRINKMANN H, NEWTON IP, BATLLE E, SIMON-ASSMANN P, CLEVERS H, NATHKE IS, CLARKE AR, WINTON DJ. 2004. Loss of Apc in vivo immediately perturbs Wnt signaling, differentiation, and migration. *Genes Dev.***,** 1385-90.
- SATO, T. & CLEVERS, H. 2013. Primary mouse small intestinal epithelial cell cultures. *Methods Mol Biol,* 945**,** 319-28.
- SATO, T., VRIES, R. G., SNIPPERT, H. J., VAN DE WETERING, M., BARKER, N., STANGE, D. E., VAN ES, J. H., ABO, A., KUJALA, P., PETERS, P. J. & CLEVERS, H. 2009. Single Lgr5 stem cells build crypt-villus structures in vitro without a mesenchymal niche. *Nature,* 459**,** 262-5.
- SCHUIJERS, J., JUNKER, J. P., MOKRY, M., HATZIS, P., KOO, B. K., SASSELLI, V., VAN DER FLIER, L. G., CUPPEN, E., VAN OUDENAARDEN, A. & CLEVERS, H. 2015. Ascl2 acts as an R-spondin/Wnt-responsive switch to control stemness in intestinal crypts. *Cell Stem Cell,* 16**,** 158-70.
- SHYER, A. E., HUYCKE, T. R., LEE, C., MAHADEVAN, L. & TABIN, C. J. 2015. Bending gradients: how the intestinal stem cell gets its home. *Cell,* 161**,** 569-80.
- SNIPPERT, H. J., VAN ES, J. H., VAN DEN BORN, M., BEGTHEL, H., STANGE, D. E., BARKER, N. & CLEVERS, H. 2009. Prominin-1/CD133 marks stem cells and early progenitors in mouse small intestine. *Gastroenterology,* 136**,** 2187-2194 e1.
- SPENCE, J. R., MAYHEW, C. N., RANKIN, S. A., KUHAR, M. F., VALLANCE, J. E., TOLLE, K., HOSKINS, E. E., KALINICHENKO, V. V., WELLS, S. I., ZORN, A. M., SHROYER, N. F. & WELLS, J. M. 2011. Directed differentiation of human pluripotent stem cells into intestinal tissue in vitro. *Nature,* 470**,** 105-9.
- STZEPOURGINSKI, I., NIGRO, G., JACOB, J. M., DULAUROY, S., SANSONETTI, P. J., EBERL, G. & PEDUTO, L. 2017. CD34+ mesenchymal cells are a major component of the intestinal stem cells niche at homeostasis and after injury. *Proc Natl Acad Sci U S A*.
- SU, L. K., KINZLER, K.W., VOGELSTEIN, B., PREISINGER, A.C., MOSER AR, LUONGO C, GOULD KA, DOVE, W.F. 1992 Multiple intestinal neoplasia caused by a mutation in the murine homolog of the APC gene. *Science,* May 1;256**,** 668-70.
- TAKEDA, N., JAIN, R., LEBOEUF, M. R., WANG, Q., LU, M. M. & EPSTEIN, J. A. 2011. Interconversion between intestinal stem cell populations in distinct niches. *Science,* 334**,** 1420-4.

- TETTEH, P. W., BASAK, O., FARIN, H. F., WIEBRANDS, K., KRETZSCHMAR, K., BEGTHEL, H., VAN DEN BORN, M., KORVING, J., DE SAUVAGE, F., VAN ES, J. H., VAN OUDENAARDEN, A. & CLEVERS, H. 2016. Replacement of Lost Lgr5-Positive Stem Cells through Plasticity of Their Enterocyte-Lineage Daughters. *Cell Stem Cell,* 18**,** 203-13.
- TIAN, H., BIEHS, B., CHIU, C., SIEBEL, C. W., WU, Y., COSTA, M., DE SAUVAGE, F. J. & KLEIN, O. D. 2015. Opposing activities of Notch and Wnt signaling regulate intestinal stem cells and gut homeostasis. *Cell Rep,* 11**,** 33-42.
- TIAN, H., BIEHS, B., WARMING, S., LEONG, K. G., RANGELL, L., KLEIN, O. D. & DE SAUVAGE, F. J. 2011. A reserve stem cell population in small intestine renders Lgr5-positive cells dispensable. *Nature,* 478**,** 255-9.
- UMAR, S. 2010. Intestinal stem cells. *Curr Gastroenterol Rep,* 12**,** 340-8.
- VAN DE WETERING, M., SANCHO, E., VERWEIJ C, DE LAU W, OVING I, HURLSTONE A, VAN DER HORN K, BATLLE E, COUDREUSE D, HARAMIS AP, TJON-PON-FONG M, MOERER P, VAN DEN BORN M, SOETE G, PALS S, EILERS M, MEDEMA R, CLEVERS H. 2002. The beta-catenin/TCF-4 complex imposes a crypt progenitor phenotype on colorectal cancer cells. *Cell,* 111**,** 241–250.
- VAN DER FLIER, L. G., VAN GIJN, M. E., HATZIS, P., KUJALA, P., HAEGEBARTH, A., STANGE, D. E., BEGTHEL, H., VAN DEN BORN, M., GURYEV, V., OVING, I., VAN ES, J. H., BARKER, N., PETERS, P. J., VAN DE WETERING, M. & CLEVERS, H. 2009. Transcription factor achaete scute-like 2 controls intestinal stem cell fate. *Cell,* 136**,** 903-12.
- VAN ES, J. H., DE GEEST, N., VAN DE BORN, M., CLEVERS, H. & HASSAN, B. A. 2010. Intestinal stem cells lacking the Math1 tumour suppressor are refractory to Notch inhibitors. *Nat Commun,* 1**,** 18.
- VAN ES, J. H., SATO, T., VAN DE WETERING, M., LYUBIMOVA, A., NEE, A. N., GREGORIEFF, A., SASAKI, N., ZEINSTRA, L., VAN DEN BORN, M., KORVING, J., MARTENS, A. C., BARKER, N., VAN OUDENAARDEN, A. & CLEVERS, H. 2012. Dll1+ secretory progenitor cells revert to stem cells upon crypt damage. *Nat Cell Biol,* 14**,** 1099-104.
- VAN ES, J. H., VAN GIJN ME, RICCIO O, VAN DEN BORN M, VOOIJS M, BEGTHEL H, COZIJNSEN M, ROBINE S, WINTON DJ, RADTKE F, CLEVERS H. 2005. Notch/gamma-secretase inhibition turns proliferative cells in intestinal crypts and adenomas into goblet cells. *Nature. ,* Jun 16;435**,** 959-63.
- VAN NOORT, M., MEELDIJK, J., VAN DER ZEE, R., DESTREE, O., CLEVERS, H. 2002. Wnt signaling controls the phosphorylation status of beta-catenin. *J Biol Chem,* 277**,** 17901-5.
- VANDUSSEN, K. L., CARULLI, A.J., KEELEY, T.M, ET AL. 2012. Notch signaling modulates proliferation and differentiation of intestinal crypt base columnar stem cells. . *Development* 139**,** 488-497.
- VANDUSSEN, K. L. & SAMUELSON, L. C. 2010. Mouse atonal homolog 1 directs intestinal progenitors to secretory cell rather than absorptive cell fate. *Dev Biol,* 346**,** 215-23.
- WALTON, K. D., WHIDDEN, M., KOLTERUD, A., SHOFFNER, S. K., CZERWINSKI, M. J., KUSHWAHA, J., PARMAR, N., CHANDHRASEKHAR, D., FREDDO, A. M., SCHNELL, S. & GUMUCIO, D. L. 2016. Villification in the mouse: Bmp signals control intestinal villus patterning. *Development,* 143**,** 427-36.
- WELLS, J. M., SPENCE, J. R. 2014. How to make an intestine. *Development,* 141**,** 752-60.
- WU, Y., CAIN-HOM, C., CHOY, L., HAGENBEEK, T. J., DE LEON, G. P., CHEN, Y., FINKLE, D., VENOOK, R., WU, X., RIDGWAY, J., SCHAHIN-REED, D., DOW, G. J., SHELTON, A., STAWICKI, S., WATTS, R. J., ZHANG, J., CHOY, R., HOWARD, P., KADYK, L., YAN, M., ZHA, J., CALLAHAN, C. A., HYMOWITZ, S. G. & SIEBEL, C. W. 2010. Therapeutic antibody targeting of individual Notch receptors. *Nature,* 464**,** 1052-7.
- YANG, Q., BERMINGHAM, N.A., FINEGOLD, M.J., ZOGHBI, H.Y. 2001. Requirement of Math1 for secretory cell lineage commitment in the mouse intestine. *Science,* 294**,** 2155-2158. .

9. Acknowledgments.

I would like to acknowledge all people, who have helped me and encouraged to get where I am in now.